UNIVERSITY OF SOUTHAMPTON

FACULTY OF MEDICINE

School of Medicine

The role of microRNAs in human Rhinovirus replication and implications in asthma

by

Victor Paky Bondanese

Thesis for the degree of Doctor of Philosophy

September 2011

UNIVERSITY OF SOUTHAMPTON

ABSTRACT

FACULTY OF MEDICINE
SCHOOL OF MEDICINE

Doctor of Philosophy

THE ROLE OF MICRORNAS IN HUMAN RHINOVIRUS REPLICATION AND IMPLICATIONS IN ASTHMA.

by Victor Paky Bondanese

MicroRNAs are small non-coding RNA molecules that have attracted much attention for their role as post-transcriptional regulators of gene expression. In addition to repressing translation from target mRNAs, they have also been shown to participate in the innate immunity response against a number of viruses. The main hypothesis of this thesis is that microRNAs are able to regulate Human Rhinovirus (HRV) replication. Although HRV is responsible for the common cold in healthy people, it is also one of the major causes of asthma exacerbations which can be life threatening and represent an unmet clinical need.

To test whether microRNAs are used by cells against the virus, HRV replication was followed in cells with either normal or reduced levels of microRNAs. Reducing the amount of mature microRNAs proved to be challenging and required the prolonged silencing of *DICER1*, one of the genes necessary for microRNA biogenesis. This increased the replication of HRV-1B in BEAS-2B cells, a human bronchial epithelial cell line. Moreover, using the same cell line, it was also possible to show that microRNAs interact directly with HRV-1B genomic RNA. In fact, the latter co-immunoprecipitated with Ago2 which is one of the proteins that microRNAs need to associate with in order to exert their effects.

These results supported the hypothesis that HRV is regulated by microRNAs in bronchial epithelial cells (BECs). Since asthmatic BECs have been shown to allow greater replication of HRVs, it is possible that antiviral microRNAs contribute to this difference. This implies that the microRNA expression is different between healthy and asthmatic BECs. Using RT-qPCR microRNA arrays, we identified microRNAs which were under-expressed in asthmatic BECs. Among those, eight were predicted by bioinformatic analysis to target both HRV-1B and HRV-16. Five of those microRNAs were confirmed to be under-expressed in asthmatic BECs using a larger sample set (n=13 healthy; n=15 asthmatic). We used BEAS-2B cells again to test whether lack of those microRNAs can favour HRV replication. The results showed that silencing either miR-155 or miR-128 allowed higher replication of HRV-1B.

Interestingly, all the five microRNAs identified above (under-expressed in asthmatic BECs and predicted to target both HRV-1B and -16) are predicted or have already been shown to target components of TGF-β and IL-13 signalling pathways. Focusing on miR-155 for technical reasons, our results suggest that the microRNAs identified by our arrays are able to regulate the TGF-β and IL-13 response of human BECs. This is very exciting as both cytokines are known to be involved in the pathology of asthma. Moreover, it has been suggested that TGF-β also has a role in asthma exacerbations thanks to its ability to dampen the innate immune response.

In conclusion, the results presented here suggest that lack of a pool of microRNAs may contribute to the asthmatic phenotype and to virus-induced asthma exacerbations. Such microRNAs indeed, have the potential to influence cellular pathways related to remodelling and inflammation. Moreover, they can also influence HRV replication both directly and indirectly through regulation of the TGF-β pathway and therefore they constitute interesting therapeutic targets.

Table of contents

List of figures

List of tables

DECLARATION OF AUTHORSHIP

I, Victor Paky Bondanese

declare that the thesis entitled

The role of microRNAs in human Rhinovirus replication and implications in asthma

and the work presented in the thesis are both my own, and have been generated by me as the result of my own original research. I confirm that:

- this work was done wholly or mainly while in candidature for a research degree at this University;
- where any part of this thesis has previously been submitted for a degree or any other qualification at this University or any other institution, this has been clearly stated;
- where I have consulted the published work of others, this is always clearly attributed;
- where I have quoted from the work of others, the source is always given. With the exception of such quotations, this thesis is entirely my own work;
- I have acknowledged all main sources of help;
- where the thesis is based on work done by myself jointly with others, I have made clear exactly what was done by others and what I have contributed myself;
- none of this work has been published before submission.

Signed: ……..

Date:…….

Acknowledgements

I'd like to thank my supervisors Dr. Tilman Sanchez-Elsner and Prof. Donna Davies for their invaluable guidance during these four years that I've spent at the University of Southampton. I am grateful to them, because without I wouldn't have been able to take on the challenge of this PhD at all. In particular Prof. Davies managed to secure the funds that I have lived on during the past four years. As a consequence I really want to thank the Roger Brooke charity and the AAIR charity for actually putting in the bulk of these funds. I also owe a big thank you to Frank Anderson for being my personal hero in making sure all these good intentions turned actually into numbers in my bank account.

As I've heard from Heleen once, no PhD runs smoothly and without problems, and mine is no exception. I am deeply grateful to have had Tilman, who supported me in many ways, not only as my main supervisor. With his ability to read me wisely, he laughed at me when I needed to be spurred, asked more from me, or sometimes less, listened to my moaning and managed to make me come back on track. I could not have had a better supervisor. I was also blessed to cross my road with Fethi Louafi. He was the most inspiring colleague I've actually worked with so far. It was so uplifting to share my work-related (and personal) blessings and curses with him. His fizzy spirit and fresh look at things will always inspire me and remind me to look somewhere else with hope, when the room I am in looks "a wee bit" too dark.

I also thank my good luck for my good friend Eirini, with whom so much time I have spent talking about pretty much anything, good or bad that happened in our lives. I wish you all the luck and happiness you deserve my friend.

Well, as you can imagine there have been grey days, but I am sure I would have had many more without the best duet I've ever met "in vivo". Salah and Joe, I owe you many cramps behind my ears for the too much laughing. I enjoy your ways of having the longest arguments one can think of, just for the sake of it. I think you're a blessing to anyone who knows the both of you. Knowing only one would certainly be just a pain, but together you guys are a great gift! (just joking, thanks for turning every day into a happy one).

I was very lucky to be working on level E where we seem to attract only nice, friendly people. From the "historic" ones like Michelle, Yuk, Karen (whose amazing baking skills make often a great surprise in the morning!) Rebecca, Sioban and Jimmy, to the latest signing Bea, Alex and Annie.

The Junk RNA group has been a great group to spend these past three years in and I really want to thank all the members. I've certainly learnt something from each one of you, since the early days when it was only Tilman, Rocio and me and when every morning had a good reason for a

meeting. The impressive expansion that this group had in the last year or so brought in very interesting people such as Fethi and Mirella, with whom I've daily shared "gioie e dolori" with our co-IP experiments. There have been days that it seemed only she could understand me in the lab. I thank also Hitasha for the many interesting conversations we have and for her genuine excitement that I find so contagious. Ana, Markus and Andy are the latest additions but already feel like indispensible parts of the group. I wish you all good luck with your adventures and I thank you for making our workplace a nice place to be in. I also want to thank everybody in the Brooke lab in particular Camelia for having got me started with the virus work. I am very grateful to Nicole, who not only provided me with many invaluable samples, but also had the patience to deal with me and my questions especially when I was starting.
Thanks to all the other friends I'm lucky to have, and also the "lost" ones.

I dedicate this thesis to my family. Mom and dad, thank you very much for trusting and supporting me. Since the first years at university to the day I told you the crazy plan to go to the UK and… well that was it, not much of a plan eh? Thanks mom for always encouraging and supporting me at every step. Dad, you were so right. I'll never forget what you told me when I was taking my first flight to London, thanks for your inspirational words, as unexpected as strong and supporting. The determination and stubbornness you taught me, well… they make a big part not only of this project, but also of my adult life. I owe you so much of what I am. Thanks to my brothers, Vincenzo and Yuruari, for not getting mad at me for all the times I've forgotten their birthdays… one day I'll make a party just for us three! Thank you for being my family, to be always there for me. I also want to thank my uncle Ermanno and aunt Lois for helping me at the beginning of this period and always checking on me thereafter, you've been so lovely to offer me a safe net when I most needed it and I'll never forget it.

Finally, this would have not been written at all if it wasn't for you Heleen. Thank you for being my angel (and for making sure I wouldn't starve). You are the most genuine person I've ever met and I'm honoured I can call you amore mio.

Abbreviations

Names of genes / proteins

Throughout this entire thesis the official gene symbols have been used, unless otherwise stated. In general, when referring to either the gene or mRNA all capital letters and italics were used. When referring to protein, only the first letter was in capital letter and not italics style was used. For example:

SMAD2 → gene or mRNA

Smad2 → protein

Abbreviations

3' UTR:	3' untranslated region
ADAM33:	A Disintegrin And Metalloproteinase domain-containing protein 33
BECs:	Bronchoepithelial cells
BHR:	Bronchial Hyperresponsiveness
Cat.n:	Catalogue number
cDNA:	complementary DNA
DNA:	Deoxyribonucleic acid
ECM:	Extracellular matix
EGF:	Epidermal growth factor
EGFR:	Epidermal growth factor receptor
FBS:	Foetal bovine serum
Fc:	Crystallizable fragment of an immunoglobulin
FCεRI:	High affinity IgE receptor I (FC immunoglobulin epsilon receptor I)
GM-CSF:	Granulocyte Macrophage Colony Stimulating Factor
HCV:	Hepatitis C virus
HIV:	Human Immunodeficiency Virus
Hours pi:	Hours post-infection
Hours pt:	Hours post-transfection
HRV:	Human Rhinovirus
HSV-1:	Herpes Simplex Virus 1
ICAM-1:	InterCellular Adhesion Molecule 1
IFN:	Interferon
IFNR:	Interferon receptor
IFN-β:	Interferon beta
IFN-γ:	Interferon gamma

IFN-λ:	Interferon lambda
IgE:	Immunoglobulin E (epsilon)
IgG:	Immunoglobulin G (gamma)
IL13RA1:	Interleukin 13 Receptor alpha 1 (gene or mRNA)
IL13Rα1:	Interleukin 13 Receptor alpha 1 (protein)
IL-4, -12, -13:	Interleukin 4, 12, 13
IL-4:	Interleukin 4
IL4R:	IL-4 receptor
IL4Rα:	IL-4 receptor alpha
IP-10:	Interferon gamma inducible 10kD protein, or CXCL10: chemokine (C-X-C motif) ligand 10
IRF3:	Interferon regulatory factor 3
JAK:	Janus kinase
LAP:	Latency Associated Peptide
LAT:	Latency Associated Transcript
LPS:	Lipopolysaccharide
MDA5:	Melanoma differentiation-associated gene 5
miR:	microRNA
miRISC:	microRNA-induced silencing complex
miRNA:	microRNA
MOI:	Multiplicity of Infection
mRNA:	messenger RNA
NF-kB:	Nuclear Factor kappa B
o.p.m.:	Oscillations per minute
ORF:	Open Reading Frame
ORMDL3:	ORM1-like 3
PAMP:	Pathogen Associated Molecular Pattern
PBMC-MΦ:	Peripheral Blood Mononuclear Cell derived Macrophages
PBS:	Phosphate-buffered saline
PCR:	Polymerase Chain Reaction
PFV-1:	Primate Foamy Virus type 1
PMA:	Phorbol 12-myristate 13-acetate
PRRs:	Pathogen Recognition Receptors
p-SMAD:	phosphorylated SMAD
p-STAT:	phosphorylated STAT
PU.1:	Alternative symbol for the gene SPI1 (transcription factor)

qPCR:	Quantitative PCR
RANTES:	Regulated upon Activation, Normal T-cell Expressed, and Secreted or CCL5: Chemokine (C-C motif) ligand 5
RF:	Replicative form
RIG-I:	Retinoic acid-inducible gene I
RISC:	RNA-induced silencing complex
RLHs:	RIG-I-like helicases
RNA:	Ribonucleic acid
RNP:	Ribonucleoprotein (RNA complexed with proteins)
rpm:	rotations per minute
RT:	Reverse Transcription
RT-qPCR:	Reverse transcription followed by qPCR
SOCS1:	Suppressor of cytokine signaling 1
SPI1:	Spleen focus forming virus (SFFV) proviral integration oncogene
STAT:	Signal Transducer and Activator of Transcriprion
SV-40:	Simian virus 40
SV-5:	Simian virus 5
TGF-β:	Transforming Growth Factor beta
TGFBR1:	Transforming Growth Factor beta receptor 1
TGFBR2:	Transforming Growth Factor beta receptor 2
Th:	T helper
THP1MΦ:	THP-1 derived Macrophages
TLR:	Toll-like receptor
TNF-α:	Tumor Necrosis Factor alpha
TSLP:	Thymic stromal lymphopoietin
TYK:	Tyrosin kinase
VCAM-1:	Vascular Cell Adhesion Molecule 1
VSV:	Vescicular Stomatitis Virus
xg:	number of g (number of times higher than gravity acceleration; also known as "relative centrifugal force")

Chapter 1

INTRODUCTION

1.1 Asthma

1.1.1 General disease overview

With an estimated 300 million subjects affected, asthma is one of the most prevalent health problems worldwide with significant social and economic costs.
It is a chronic respiratory condition that burdens the asthmatic patient with recurrent episodes of reduced respiratory function, caused by airflow obstruction that is generally reversible. Stimuli able to cause these acute episodes (also referred to as asthma exacerbations) include "stress" (Wright et al. 1998), exercise, cold air, aero-allergens and viral infections (Wark & Gibson 2006). The intensity of such attacks can vary, ranging from moderate and described as wheezing, chest tightness, shortness of breath, to very serious and life-threatening. In fact 250,000 asthma-related deaths are reported to occur every year worldwide (GINA 2010).

Asthma is a complex disease, highly heterogeneous in the details of its triggers and manifestation. However, in medical practice it is described as a "chronic inflammatory disorder of the airways in which many cells play a role" (GINA 2010). The chronic inflammation of the lung is associated with what is referred to as bronchial hyperresponsiveness (BHR) and airway remodelling. In fact a thicker and hyper-reactive layer of smooth muscles makes the airways "twitchy". Moreover, oedema of the mucosa, mucus overproduction and thickening of the airway walls contribute to airflow obstruction (Holgate 2010a).

It is widely accepted that there is a major hereditary component, but this is clearly a complex genetic contribution, and environmental factors can have a large influence in the onset of the disease (Cookson 2002). Studies aiming at identifying asthma related genes, pointed sometimes at genes whose products are known to play a role in the pathology of asthma (eg Th2 cytokines, TGF-β, IgE receptor), and sometimes to unexpected ones whose products' role or function are not fully characterised yet (eg *ADAM33*, *ORMDL3*) (Holgate 2010b, Moffatt et al. 2007).

1.1.2 Chronic inflammation.

Allergy, a disorder of the immune system where immune cells are hyper-sensitive to foreign molecules, is very commonly associated with asthma. Immunoglobulin E (IgE) antibodies are at the basis of allergic reactions. In fact, on the one hand they specifically bind the allergen, while on the other hand they are bound by receptors (FCεRI) at the surface of mast cells and basophils. In a subject with atopic asthma then, allergen binding induces mast cells and basophils to release large amounts of several cytokines, amongst which histamine and

cysteinyl leukotrienes. These trigger asthma exacerbations by stimulating airway smooth muscle contraction, increasing vascular permeability and further leukocyte chemotaxis (Montuschi & Peters-Golden 2010, Ogawa & Calhoun 2006).
However, not all atopic people develop asthma and at the same time asthma is not exclusively allergic (Pearce et al. 1999). Nevertheless, a very similar pattern of chronic inflammation is also a striking characteristic of non-allergic forms of the disease (GINA 2010, Humbert et al. 1999, Turato et al. 2008) and recognition of its importance has been crucial for asthma treatment. Indeed, there is no cure for asthma, and the management of this disease aims at maintaining its clinical manifestations under control. This is achieved by reducing the chronic inflammation using anti-inflammatory medications, and reversing the bronchoconstriction using bronchodilators (Bernstein 2008, GINA 2010).

In summary, the airways of asthmatic subjects are in a chronic inflammatory state, with many activated immune cells and a predominant Th2 cytokine profile, even in the absence of allergy and increased levels of IgE.
Th2 cytokines establish a self-sustaining pro-inflammatory environment. By inducing the release of several other chemokines (ie RANTES and eotaxin) and over-expression of endothelial adhesion proteins (in particular ICAM-1 and VCAM-1) they promote recruitment and activation of many infiltrating immune cells in the airways, typically mast cells, basophils, eosinophils and neutrophils. The activity of all these cell types, in the context of the chronic inflammation, is responsible for the asthmatic symptoms.

1.1.3 IL-4 and IL-13

Il-4 and IL-13 are central Th2 cytokines and have important roles in asthma (Holgate 2008, Neurath et al. 2002). They are pleiotropic cytokines with largely overlapping effects (Jiang et al. 2000). In fact, among other effects, both IL-4 and IL-13, promote B cell growth and induce IgE class switch, promote eosinophilia by inducing eotaxin, and induce the hypersecretion of mucus in the lung.
While IL-4 is the Th2 driving cytokine, IL-13 does not activate human T cells.
However, IL-13 inhibits the production of IFN-γ and IL-12, which are Th1 driving cytokines. Therefore, it supports IL-4 in repressing the development of Th1 cells while favouring the establishment of a pro-Th2 microenvironment.

IL-4 can signal through two receptors, namely IL4R type I and II, while IL-13 uses only type II (Hershey 2003, Jiang et al. 2000). Hematopoietic cells typically express type I receptor, composed of IL4Rα and the common gamma (γc) chain, a receptor subunit used also by other

cytokines, such as IL-2, IL-7, IL-9 and IL-15. Type II receptor is instead composed of IL4Rα and IL13Rα1, and it is most often found on non-hematopoietic cells, while it is not expressed in human T cells, explaining their lack of responsiveness to IL-13.

Ligand binding activates the associated tyrosine kinases, which belong to the Janus kinase (JAK) family. Most often, IL4Rα has been shown to associate with JAK1, while γc and IL13Rα1 associate with JAK3 and TYK2 respectively (Jiang et al. 2000).

IL4Rα is the main signalling subunit. It is in fact associated with signal transducer and activator of transcription (STAT) 6, which is responsible for most effects of both cytokines. Members of the STAT family are all characterized by a similar pattern of action: upon phosphorylation by a JAK kinase, they dissociate from the receptor to form homo- and hetero-dimers with other STAT proteins. This complex then exerts its transcriptional activity in the nucleus, where it influences the expression of target genes (see fig. 1-1).

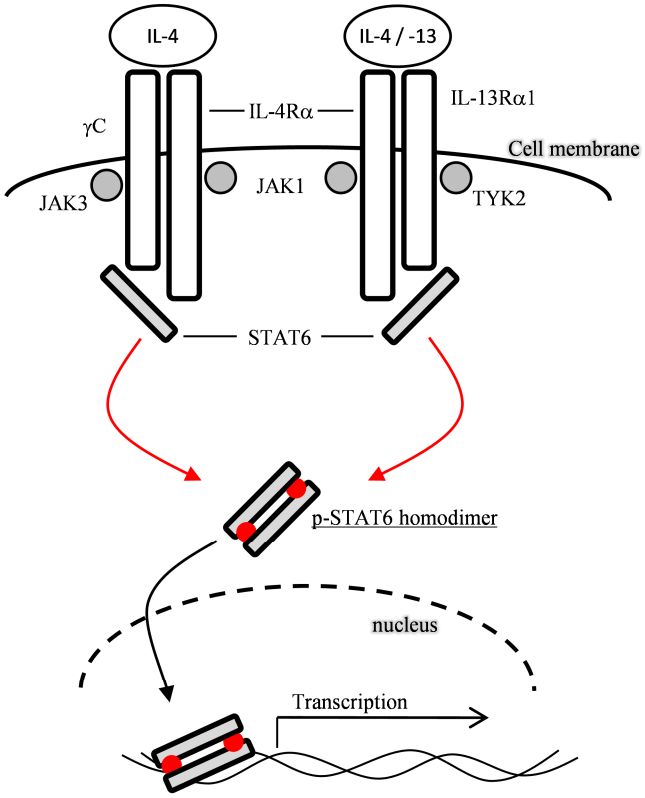

fig. 1-1. Schematic of IL-13 and IL-4 pathway.
Following cytokine binding, the receptor becomes activated and this culminates in the activation of tyrosine kinases associated to the receptor subunits. Such kinases phosphorylate STAT6 that is now able to dissociate from the receptor and form homo-dimers (with other p-STAT6 molecules). The dimers have transcriptional activity. In fact they translocate into the nucleus where they regulate the expression of target genes.

1.1.4 Airway remodelling.

Airway obstruction in asthma can be totally or only partially reversible, being caused by a combination of physiological and structural factors that altogether contribute to airway narrowing. In fact, besides spasm of bronchial smooth muscles, that can be therapeutically relaxed and therefore quickly reversed, chronic inflammation of the airways also brings oedema of the mucosa and increased production of mucus. On top of this, thickening of the airway walls is promoted, with increased production of extracellular matrix (ECM), differentiation of myofibroblasts, increased airway smooth muscle cells and angiogenesis, processes that altogether are referred to as airway remodelling (Fahy 2001, Hashimoto et al. 2005). These are persistent features that cannot be quickly reversed and therefore contribute to impair lung function.

Airway remodelling and airway inflammation in asthma are intertwined; which occurs first is not known. For a long time remodelling has been considered as a consequence of recurrent tissue damage caused by the chronic inflammation. However, recent studies on very young asthmatic children, have established that airway remodelling is well already on its way at very early stages. Indeed, epithelial damage and in particular thickening of the basal membrane are very common in asthmatic lungs, even in the absence of other signs of inflammation (Baraldo et al. 2011, Barbato et al. 2006, Kim et al. 2007, Malmstrom et al. 2011, Saglani et al. 2005, Saglani et al. 2007). In addition more recently, it has been shown that TGF-β and signs of airway remodelling are induced in asthmatics by bronchoconstriction alone (Grainge et al. 2011). These striking observations challenged the traditional views, about airway remodelling being a consequence of long-lasting disease (Holgate et al. 2009, Knight et al. 2004).

1.1.5 Epithelial-mesenchymal communication in asthma.

It is clear that lung epithelium is damaged in asthmatics (Holgate 2007). In normal conditions, epithelial damage is repaired very quickly in order to preserve function of the epithelium. Epithelial cells adjacent the area of interest, de-differentiate and migrate onto the site of damage. Here, they proliferate covering the damaged area and finally re-differentiate back into the original epithelial phenotype, restoring the healthy lining surface (Erjefält & Persson 1997).

In asthma, instead the epithelium enters a state of “frustrated repair” and stress, where signals of repair (Puddicombe et al. 2000) are not finalised, the epithelium is not repaired and as a matter of fact cell junctions, that ensure the correct epithelial barrier function, are compromised

(Swindle et al. 2009, Xiao et al. 2011). This aberrant wound healing scenario is initiated by several stimuli typically associated with asthma exacerbations, such as allergens, pollutants, irritants and viral infections, but it is then supported by an inherent deficiency of asthmatic epithelial cells to repair. Instead, they chronically express not only pro-fibrotic enzymes (Stevens et al. 2008), and growth factors such as TGF-β, that stimulate airway remodelling, but also pro-inflammatory factors such as GM-CSF and TSLP (Burgess 2009). All this contributed to the idea, first elaborated by Holgate et al., that in asthma, the epithelium has a major role in both chronic inflammation and airway remodelling. In fact, the asthmatic epithelium engages aberrant interactions (often referred to as the epithelial-mesenchymal trophic unit) with both underlying structural cells, such as fibroblasts and smooth muscle cells, and immune cells (Holgate et al. 2000).

A scrupulous description of the molecular details at the basis of this model is beyond the focus of this thesis, but such model emphasises that it is becoming increasingly evident that the airway epithelium in asthma does not just suffer from the chronic inflammation, but certainly contributes actively to, if not initiates, the pathology.

1.1.6 Transforming growth factor beta (TGF-β)

TGF-β is one important player in the aberrant wound healing scenario just described. This growth factor has profound effects on both airways' structural and immune cells. Indeed, TGF-β has been proven to participate both directly and indirectly to the recruitment of inflammatory cells relevant to asthma, such as mast cells (Gruber et al. 1994), eosinophils (Luttmann et al. 1998) and neutrophils (Thelen et al. 1995). TGF-β has dramatic effects on airway remodelling. In fact, it induces proliferation of fibroblasts, their differentiation into myofibroblasts, and the proliferation and survival of smooth muscle cells. It stimulates the accumulation of ECM and promotes angiogenesis by inducing expression of VEGF (Burgess 2009).

TGF-β undergoes a complex post-translational maturation before becoming active. It is in fact secreted in an inactive form. The inactive form is bound by components of the ECM, where it is stored and from where it can be released by different proteases such as thrombin, neutrophil elastase or mast cell chymase (Taipale et al. 1992, Taipale et al. 1995). This provides an additional level of regulation of its activity. In fact, final maturation requires removal of the so called latency associated peptide (LAP) by proteases such as plasmin, sialidase or neuraminidase, generating the biologically active molecule. The latter is constituted of two peptides joined by a disulphide bond and it is now able to interact with its receptor. Also LAP removal occurs extracellularly. In vivo this means that LAP removal occurs in the contect of the

extracellular matrix (ECM), where many proteolytic enzymes contribute to regulate both the availability and the final maturation of TGF-β (Khalil 1999).

Three isoforms belong to the TGF-β subfamily, numbered from 1 to 3, and TGF-β1 is the prototype member. These isoforms show largely overlapping cellular effects *in vitro*. However, *in vivo* their functions are not redundant, particularly in development. This may be the result of a combination of differences in their pattern of expression and regulation, besides the use of specific receptor subunits. TβRI and TβRII are the best characterised receptor subunits with serine/threonine kinase activity. Mature TGF-β binds first to a TβRII homodimer. TβRI homodimer then joins in, forming the active receptor. TGF-β has been shown to signal mainly through the SMAD pathway, where the active receptor phosphorylates Smad2 and/or Smad3 (p-Smad2/3). The latter can then dissociate from the receptor subunits and form heterometric complexes with Smad4 (see fig. 1-2). This complex can finally translocate into the nucleus and modulate gene expression (Shi & Massagué 2003).

TGF-β is expressed ubiquitously, also in the healthy lung, but its abundance is certainly higher in asthmatic lungs, especially after allergen challenge or bronchoconstriction (Grainge et al. 2011). Many reports pinpointed that the isoform TGF-β2 is the one to be upregulated in asthma. However, which cells are responsible for this increased production is still a matter of debate and research. In fact, both immune and structural cells that are increased and activated in asthma, such as neutrophils, eosinophils, macrophages, fibroblasts and smooth muscle cells have all been shown to express it. Also, mechanical stress mimicking bronchoconstriction has been shown to upregulate release of TGF-β2 from bronchial epithelial cells (BECs) *ex vivo* (Tschumperlin et al. 2003). This type of analysis is complicated by the fact that TGF-β is stored in the ECM in an inactive form, offering additional opportunities to modulate its activity. In any case, whatever the main source, the TGF-β pathway is over-activated in asthma. Indeed, higher levels of p-Smads are found in the epithelium of asthmatics as compared to healthy subjects (Sagara et al. 2002) and asthmatic attacks further increase them (Torrego et al. 2007).

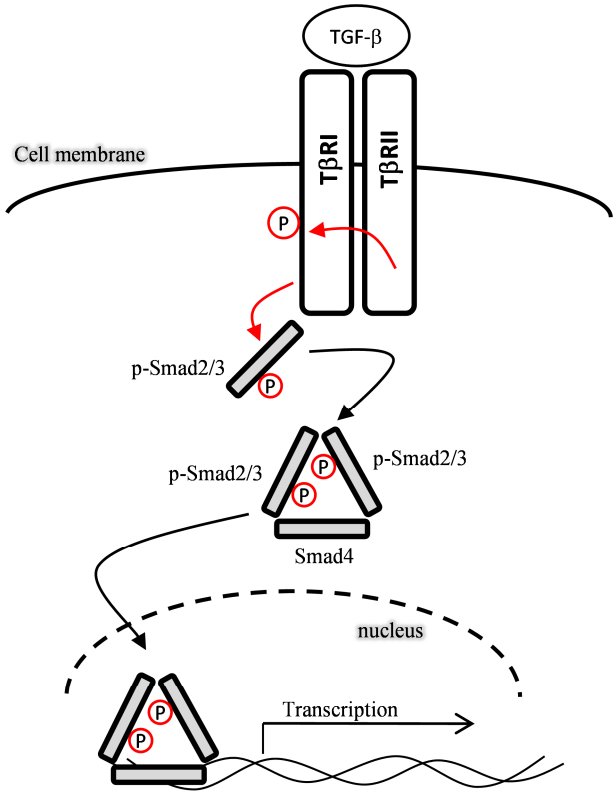

fig. 1-2. Schematic of TGF-β SMAD-dependent pathway.
The receptor subunits possess a (intracellular) C-terminal serine/threonine kinase domain. They have been shown to be homodimers therefore the mature receptor is actually a hetero-tetramer. However, this has been simplified in this schematic. Mature TGF-β binds first to TβRII. The latter is contitutively active and phosphorylates TβRI when it joins in, forming the active receptor. Therefore TβRI phosphorylates the receptor-associated Smad (Smad2 or 3). These can now associate with Smad4 (also referred to as co-SMAD) forming a complex with transcriptional activity which can therefore enter the nucleus and regulate expression of target genes.

1.2 Human Rhinovirus infections in asthma.

Asthma exacerbations are severe attacks with worsening of the symptoms, and represent a major problem in the management of the disease. Corticosteroids or other anti-inflammatory treatments in fact are only marginally effective, and patients require additional medication and emergency care (Grünberg et al. 2001, Hansbro et al. 2008).

Viral respiratory tract infections are the major cause of asthma exacerbations, and in particular human rhinovirus (HRV) has been found to be the most common virus (Johnston 2005). It has long been documented that severe asthma exacerbations peak in spring and fall, in close coincidence with patterns of HRV spread in the community (Johnston et al. 1996). Interestingly, in addition to the well recognized role of HRV in asthma exacerbations, recent studies suggest that HRV may be one of the main causative agents of asthma itself, certainly in the context of a predisposing genetic background. In fact, repeated infections with this virus in the first years of life are very strongly associated with developing asthma later on (Dharmage et al. 2009, Heymann et al. 2004).

1.2.1 HRV targets bronchial epithelial cells (BECs) and it replicates more in asthmatics.

Compared with healthy subjects, asthmatics do not contract colds more often or have more severe colds in terms of upper airways symptoms. Instead, they suffer from more severe and longer lasting symptoms of the lower respiratory tract, which culminate in severe asthma exacerbations (Corne et al. 2002, Gern 2003, Skoner et al. 1996). For a long time it was commonly accepted that Rhinovirus infections were limited to the upper airways. However, this has been proven not to be true and that actually the virus spreads in the lower airways (Gern et al. 1997). Here, the bronchial epithelium is the main target of HRV (Friedlander & Busse 2005, Hayden 2004, Laza-Stanca et al. 2006, Mosser et al. 2002). It is likely that the virus then causes asthma exacerbations through a combination of cellular damage and cytokine induction (Wark & Gibson 2006). In fact, bronchial epithelial cells (BECs) infected by HRV express several pro-inflammatory cytokines, such as IP-10, RANTES, IL-6, IL-8, TNF-α, and this is enhanced in the context of the asthmatic chronic inflammation (Kallal & Lukacs 2008, Papadopoulos et al. 2000, Wark et al. 2007). In fact, alveolar macrophages and epithelial cells from asthmatics have been shown to be deficient in producing IFN-β and λ after viral infection (Contoli et al. 2006). As a consequence, viral replication in asthmatic BECs is favoured, increasing cytokine release and cytotoxic cell death (Wark et al. 2005).

This deficiency seems to be restricted to these cell types. Asthmatic and healthy fibroblasts, for instance, have been shown not to differ in this regard (Bedke et al. 2009). Although therapeutic

use of IFN-β seems viable given that downstream signalling pathways are intact in BECs (Wark et al. 2005), the reasons behind the epithelial deficiency in IFN production have not been fully clarified yet. Indeed, the picture is complicated by the fact that many factors important in asthma such as TNF-α (Subauste et al. 1995), EGF (Subauste & Proud 2001), TGF-β (Thomas et al. 2009), IL-13 (Lachowicz-Scroggins et al. 2010), have all been shown to promote HRV replication. In particular, TGF-β is also able to reduce IFN production. Therefore, further studies are required to unravel the reasons behind the asthmatic defect.

All this is pointing at the epithelium as the "culprit", and that intrinsic properties of the asthmatic epithelium are responsible for the pathology. Identifying the reasons behind these characteristics of the epithelium is not straightforward, and no definitive explanation has yet been proposed.
Therefore, there is the need to investigate further HRV replication in bronchial epithelial cells, and the mechanisms these cells use in defence.

1.2.2 Replication of HRV.

HRV is a small non-enveloped virus belonging to the family Picornaviridae, and it is one of the major causative agents of common cold in humans. The genome is composed of a single stranded (ss) RNA molecule of positive polarity (see fig. 1-3). This means that the genomic RNA also functions as template for translation. In fact, viral translation starts immediately after entry, producing both structural and non-structural proteins. The latter then allow replication of the viral RNA that is eventually assembled into viral capsids and released by cell lysis.
Cellular receptors for HRV are the intercellular adhesion molecule 1 (ICAM-1) for the major subgroup (to which HRV-16 belongs) and the low-density lipoprotein receptor (LDLR) for the minor subgroup (such as HRV-1B).
Once viral RNA has entered the host cell, the internal ribosome entry site (IRES) at the 5' untranslated region (5' UTR), allows translation of the single open reading frame (ORF) that encodes all viral proteins. Although a single polypeptide is initially synthesised, it cleaves itself, eventually producing different separate proteins. Viral proteases are responsible for this maturation process. They are also able to cut host cell proteins. One of the latter proteins is poly(rC) binding protein-2 (PCBP2) and its cleavage has been proposed to participate to the switch between viral translation and replication. Full length PCBP2 is in fact necessary for viral IRES-dependent translation and can also participate in viral transcription. Cleaved protein instead can participate only in the second process (Perera et al. 2007). This serves viral needs

very well. Initially the few molecules of genomic RNA that entered the cell are used to produce viral proteins. Later on, once enough proteins have been accumulated, more genomic RNA is needed. This switch is then facilitated by viral proteases cutting PCBP2. By doing so, since the cleaved form of PCBP2 can no longer sustain translation, they inhibit translation and favour viral RNA transcription. The latter is performed by viral RNA-dependent polymerases that use genomic RNA as a template. The first event for viral replication is synthesis of the minus strand. It requires that the (+) viral RNA forms a looped structure, with proteins bridging the opposite ends, which very interestingly resembles the initiation of translation from cellular mRNAs (Herold & Andino 2001). The double stranded RNA molecule (dsRNA) that is therefore generated, constitutes the replicative form (RF) so called because it allows synthesis of more genomic RNA (Xiang et al. 1997). The latter can then be used to produce more viral proteins, more RFs or be assembled in viral capsids forming viral progeny (see fig. 1-7 A).

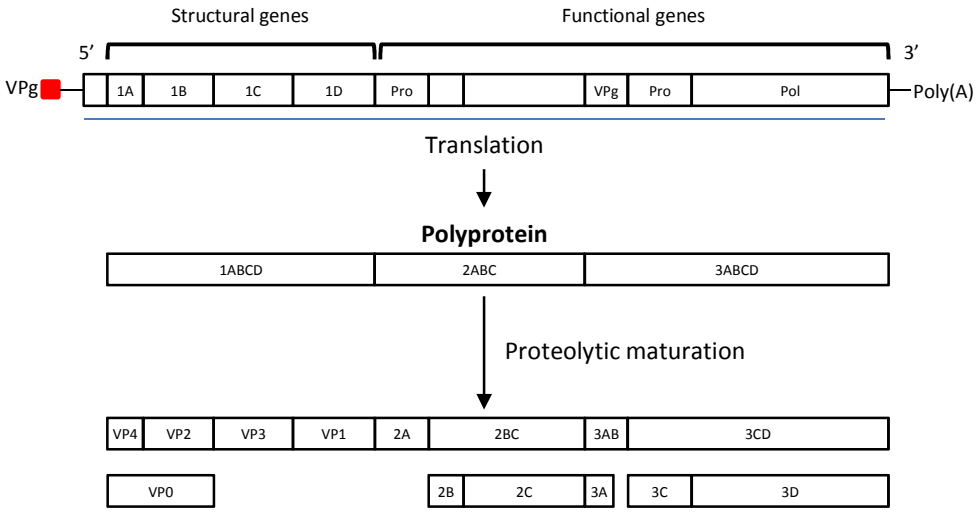

fig. 1-3. Schematic representation of the organization of HRV genome.
The polypeptide that is at first synthesised undergoes spontaneous self-cleavage. After this, the viral proteases generated act on the rest of the polyprotein, giving rise to the several independent proteins iindicated.

1.3 Innate immunity against viruses.

Vertebrates have developed several mechanisms in order to preserve their own health. Innate immunity against pathogens is possible thanks to cellular pathogen-recognition receptors (PRRs). Viral RNA molecules are recognized in mammalian cells, mainly by two classes of sensors: toll-like receptors (TLRs) and retinoic acid-inducible gene I (RIG-I)-like helicases (RLHs) (Mogensen & Paludan 2001, Yoneyama & Fujita 2007). In particular, replication of HRV in bronchial epithelial cells has been shown to activate pathways dependent on PRRs that recognise dsRNA, namely TLR3 and melanoma differentiation-associated gene 5 (MDA5) a member of the RLH family (Chen et al. 2006, Hewson et al. 2005, Wang et al. 2009). In fact, as mentioned above, large quantities of dsRNA accumulate during replication of the virus, and UV-irradiated virus, which is replication-deficient, does not activate such pathways. In addition, a recent investigation showed that in primary human BECs also RIG-I, the other RLH, is required for the antiviral response. TLR3 seems to be leading the response, while expression of the other two RLHs is strongly induced soon after infection (Slater et al. 2010).
Upon ligand binding, these PRRs start a signalling cascade that activates key transcription factors, NF-kB and IRF3 (see fig. 1-4) resulting in the induction of several pro-inflammatory cytokines (e.g. IL-8, TNF-α, IL-6) and IFNs (type I and III in BECs) (Onoguchi et al. 2007, Stark et al. 1998, Takeuchi & Akira 2007).

IFNs have been known for a very long time to be important in the antiviral innate immune response. They signal through Jak-STAT pathways, eliciting a series of host cell responses that aim to prevent pathogen replication, and limit its spreading to neighbouring cells. Among the best characterised antiviral proteins, induced by IFNs there are (Donnelly & Kotenko 2010, Stark et al. 1998):

- dsRNA-dependent protein kinase (PKR), whose main effect is a general inhibition of protein synthesis; it is also able to bind dsRNA and induce expression of IFNs
- 2',5'-oligoadenylate synthetase 2-5 (OAS) which products activate RNAse L that cleaves ssRNAs
- Mx GTPase proteins that inhibit viral RNA replication.

Every action has a reaction, and viruses develop mechanisms to counter attack the innate immune system. This is very common and it is believed to confirm the importance of the mechanism counterattacked. Some viruses act at the first steps of the host response. For instance, NS1 of influenza virus (García-Sastre et al. 1998) and σ-3 of reovirus (Miller & Samuel 1992) bind dsRNA competing with the PRRs and reducing their activation. Other viruses affect downstream components, for example the protease NS3-4A from HCV (Li et al.

2005) cleaves MAVS blocking RLH signalling, while protein V of SV5 blocks IFN signalling by targeting STAT1 for degradation (Didcock et al. 1999).

Although the effectors just mentioned are well characterised, recently it has become increasingly evident that microRNAs are also part of the antiviral innate immune system. Because microRNAs are at the focus of this thesis, a more detailed description of their biology will follow.

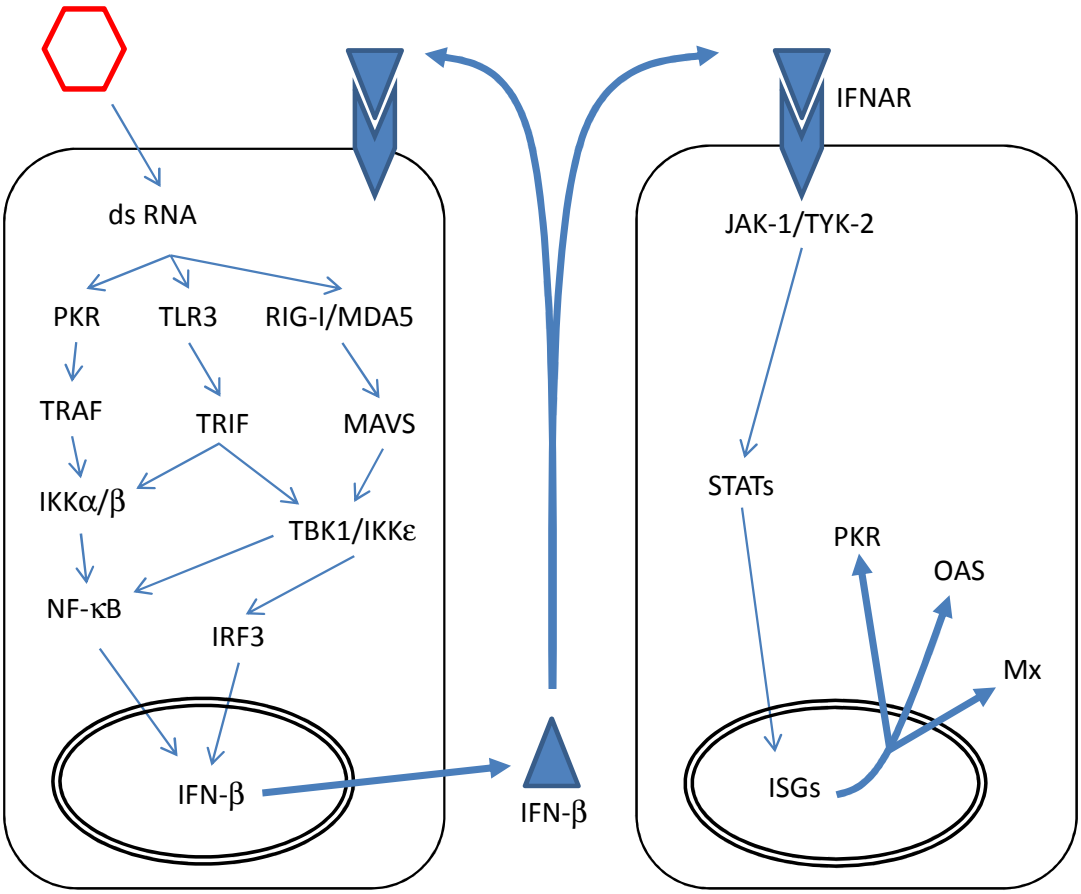

fig. 1-4. IFN induction and effector pathways.
During viral replication dsRNA molecules are formed which are bound by intracellular receptors such as TRL3, RIG-I and MDA-5. These initiate a signalling cascade that culminates in the activation of IRF-3 and NF-kB that enter the nucleus where they activate expression of IFN-β and pro-inflammatory cytokines. IFN-β is secreted extracellularly and acts both on the infected and neighbouring cells. IFN-β binds the type I IFN receptor (IFNAR) that phosphorylates STAT1 and STAT2. P-STATs bind together and in the nucleus induce the expression of interferon-stimulated genes (ISGs) such as the antiviral effectors mentioned in the text (PKR, Mx proteins and OAS).

1.4 MicroRNAs.

1.4.1 General overview.

MicroRNAs (or miRs) are small (20-26 nucelotides) non-coding single stranded RNAs which regulate gene expression at the post-transcriptional level. MicroRNAs are involved in many different biological processes such as development, cellular differentiation and maturation, apoptosis (Pedersen et al. 2007).

MicroRNAs are synthesised in the nucleus as a long primary transcript, referred to as pri-microRNA. The latter is cleaved by a nuclear complex containing the protein Drosha and referred to as a microprocessor (Gregory et al. 2004, Lee et al. 2003). The shorter RNA molecule so obtained has a typical hairpin-loop secondary structure, and constitutes the microRNA precursor (pre-microRNA). This is transferred into the cytoplasm through involvement of a nuclear exporting protein, exportin-5 (Yi et al. 2003). Here, the pre-miR is bound by a complex that cleaves it further, and yields the mature microRNA. Such a cytoplasmic complex contains Dicer, the enzyme that actually cuts the pre-microRNA. A mature microRNA is not simply released in the cytoplasm. Instead, it associates with other proteins, forming a ribonucleoproteic (RNP) complex known as micro-RNA-induced-silencing complex (miRISC). The latter is what effectively regulates gene expression. Dicer is also involved in "handing" the mature microRNA to proteins of the miRISC (see fig. 1-6). These include at least one member of the Argonaute (Ago) family. Ago proteins have been shown to be necessary and sufficient for microRNA activity (Rivas et al. 2005). Humans express four different Ago proteins, numbered from 1 to 4 and Ago2 is the only one that has been shown to have hydrolytic properties (Meister et al. 2004).

Mature microRNAs modulate the stability and the rate of translation of their target mRNAs, which they bind thanks to base-pair complementarity. An interesting feature is that microRNAs do not need to bind with their full sequence in order to exert their effects. Although every base pairing contributes towards stability of the duplex, the most important nucleotides are between position 2 to 8 (from the 5' end of the miR). This is called the "seed" region of a microRNA. Typically, a microRNA binds to its target sequence (on the target mRNA) by forming base pairs at its seed region, and then with a few more nucleotides at its 3' end. Therefore, a bulge in the middle of the microRNA:mRNA duplex is quite characteristic of mammalian microRNAs (fig. 1-5). However, the whole microRNA sequence can also base pair with the target. This is most common in plants, and it is also the case with artificial siRNAs. Only microRNAs that make a perfect match with their target sequence and are complexed with Ago2 induce direct cleavage of target mRNAs at the target sequence. In general, once they bind to a target mRNA, microRNAs can cause translational inhibition, induce degradation of, or directly cut the target. It has been

shown that microRNAs can indeed interfere with translation at the initiation or elongation steps, or promote cleavage of the newly synthesised protein. Other very common actions of microRNAs are recruitment of de-capping or de-adenylating enzymes (fig. 1-6). Cap and polyA are very important elements of mRNAs, and their removal will eventually lead to mRNA degradation. Thus, although most microRNAs bind with imperfect matches (not allowing a direct cut of the target by Ago2), it is increasingly being accepted that their predominant effect is mRNA degradation (Esslinger & Förstemann 2009, Guo et al. 2010, Huntzinger & Izaurralde 2011). All these activities are actually carried out by proteins of the miRISC. In fact, Ago proteins tethered to mRNAs thanks to a microRNA-independent mechanism can still regulate translation (Pillai et al. 2004).

Not requiring a perfect match for their activity, microRNAs with the same sequence can interact with many different mRNAs. This means that the expression of different genes can be modulated by microRNA molecules with the same sequence, in other words by the same microRNA (Filipowicz et al. 2008). This however entails that it is not straightforward to predict which genes can be regulated by a specific microRNA and for this purpose complex algorithms have been developed.

1.4.2 Prediction of microRNA targets.

More than 900 human microRNAs have been characterized to date. In order to predict microRNA targets, several algorithms have been developed, and are continuously updated, based on details gathered from experimentally validated examples. The aspects considered are the complementarity between microRNA and target, the stability of the duplex formed, the conservation of the target sequence across different species (Maziere & Enright 2007), and site accessibility (Kertesz et al. 2007).

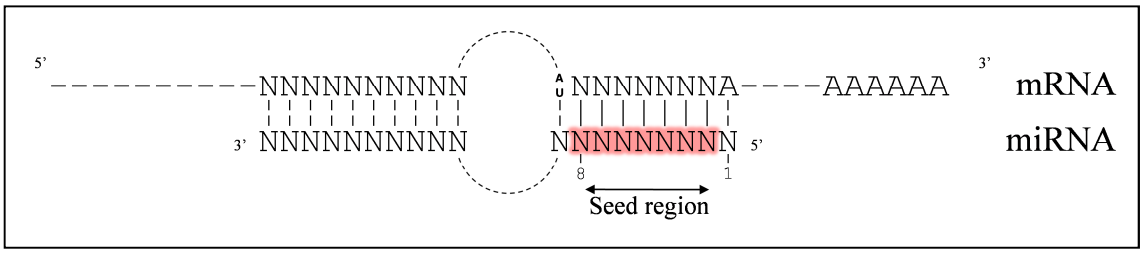

fig. 1-5. Schematic of microRNA:mRNA duplex.
MicroRNAs (miRNAs) interact with their mRNA targets by base pairing. In animals, generally this interaction does not involve the whole microRNA sequence. The most important portion of the microRNA is between nucleotides 2 to 8. This region is referred to as the "seed" region. Prediction programs detect miR targets by looking for complementarity with mainly the seed region of a microRNA. Generally, at least 6 nucleotides belonging to the seed are needed in order for the base pairing to be considered strong enough. In addition, an A residue on the mRNA (corresponding to position 1 of the miRNA) and an A or U at position 9 improve the site efficiency even if they do not base pair with miRNA nucleotides. Finally, some degree of complementarity is often present at the 3' portion of the microRNA. Therefore a bulge is typical of most microRNA:mRNA interactions.

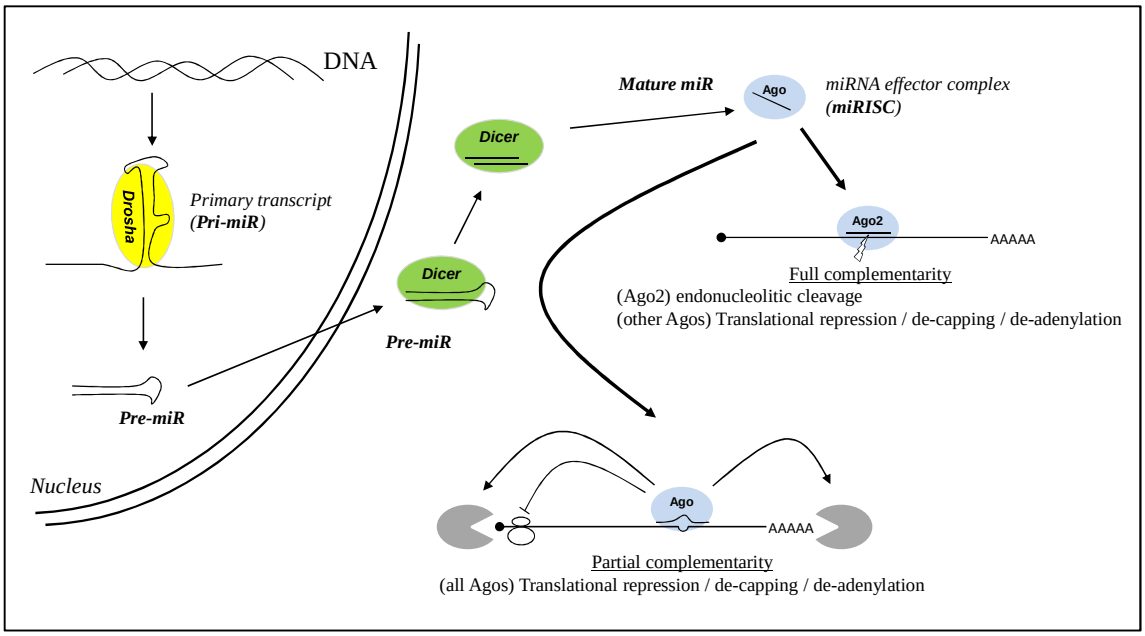

fig. 1-6. Schematic representation of microRNA biogenesis.
Mature microRNAs associate with proteins forming a complex referred to as microRNA-induced Silencing Complex (miRISC). Essential components of miRISCs are Ago proteins, which are able to affect translation of the microRNA target. In humans there are four Ago proteins. All associate with microRNAs. However, only Ago2 is able to catalyze the cleavage of the target when there is perfect complementarity between microRNA and target sequence. When instead the complementarity is not perfect and/or the other Ago proteins are involved, the miRISC either exerts translational repression or impairs the stability of the target (de-adenilation or de-capping of mRNAs).

1.4.3 MicroRNAs in immunity.

Being part of the mechanisms that cells use in order to regulate and fine tune gene expression, it is not surprising that microRNAs are widely involved in many different biological processes such as development, cellular differentiation and maturation or apoptosis. For the same reasons, their deregulation perturbs gene expression, causing several pathologies and their involvement in cancer highlights their importance for normal cell function (Garzon et al. 2009).
A few examples will follow regarding innate immunity and lung.

For instance, in macrophages, three microRNAs have been shown to participate in pathways already mentioned. LPS, a TLR4 ligand, causes up-regulation of miR-155 (O'Connell et al. 2007) but down-regulation of miR-125b in murine macrophages (Tili et al. 2007). As expected by their opposite regulation by LPS, the two microRNAs have opposite effects on the expression of TNF-α, which is released after LPS treatment. MiR-155 expression has been shown to increase TNF-α production, while miR-125 expression caused its reduction (Tili et al. 2007). In fact, often microRNAs are used by cells to reinforce or further regulate their responses, and this often involves targeting of signalling molecules. For instance miR-146a/b contributes to the normal inflammatory response, most probably by preventing excessive inflammation. The microRNA indeed, targets IRAK1, 2 and TRAF6, signalling proteins downstream of PRRs (Taganov et al. 2006). In addition, miR-155 has a central role during dendritic cell maturation. It causes down-regulation of a transcription factor (PU.1) that drives changes associated with cell activation (Martinez-Nunez et al. 2009).

The expression of microRNAs is highly regulated during lung development (Williams et al. 2007), both in human and in mouse, suggesting an important role during this process (Tomankova et al. 2010). Deletion of several microRNAs is lethal, and miR-155 deficient mice showed impaired immune responses in addition to lungs with evident airway remodelling (Rodriguez et al. 2007).
MicroRNAs have also been proposed to contribute to idiopathic pulmonary fibrosis (IPF). Members of the Let-7 family favour epithelial-mesenchymal transition in lung epithelial cells, while miR-155 and miR-29 have pro-fibrotic effects in fibroblasts (Pandit et al. 2011).
Most of what has been done regarding asthma, involves mouse models of allergen induced disease. miR-126 and miR-21 have been shown to be up-regulated after allergen exposure favouring Th2 cytokine release (Mattes et al. 2009). MiR-21 was also shown to be up-regulated by IL-13 and to contribute to establishing a Th2 cytokine profile by targeting IL-12 (Lu et al. 2009). IL-13 is also able to down-regulate miR-133a in mouse bronchial smooth muscle cells, and this in turn causes increased expressed of RhoA, a protein implicated in airway hyperresponsiveness (Chiba et al. 2009).

Recently, a microRNA array has been performed with lung biopsies from both asthmatic patients and healthy people, showing no difference (Williams et al. 2009). However, biopsies include all the different cell types in the airway wall, from infiltrating leukocytes to smooth muscle cells. The same authors in fact, propose that microRNA expression shows strong cell type-specific differences, but they did not use primary human samples to analyse this further. Therefore, this matter still requires further investigation.

1.4.4 MicroRNAs and viruses.

Intriguingly, in organisms that lack the IFN system, such as plants and invertebrates, microRNAs and microRNA-related pathways (in general referred to as RNA interference) constitute the main antiviral system.

In these organisms, dsRNA molecules formed during viral replication, are bound and processed by Dicer proteins. This generates siRNA molecules, specific against the virus (Ding et al. 2004, Saumet & Lecellier 2006). From the structural point of view, there is no difference between microRNAs and siRNAs. The only difference is in their origin: endogenous for microRNAs, exogenous for siRNAs. As a matter of fact, both associate with effector Ago proteins and, depending on their degree of sequence homology, both have the same effects on target RNAs. Hence, these siRNAs produced by Dicer during viral infection, allow host cells to degrade the genome of the invading virus. Moreover, spreading of the infection is efficiently prevented, because many more copies of these antiviral siRNAs are rapidly synthesised inside the infected cells, and distributed to the other cells of the organism. Besides this, plants adopt also their own microRNAs in order to fight back viral infections and changing the amount of such microRNAs affects viral replication (du Lu et al. 2008).

The importance of this microRNA-based immunity is strengthened by the fact that many viruses have evolved specific counter defences. In fact, they express viral suppressors of RNA silencing (VSRs) that disrupt microRNA activity. In fact, most VSRs are proteins that inhibit RNA silencing by competing with Dicer for the precursor dsRNAs and pre-miRs, and also the mature microRNA can be sequestered by VSRs (Li & Ding 2006).

It is not surprising that VSRs are very common in plant and invertebrate viruses, considering the extraordinary role that RNA silencing plays in their antiviral defence.

Viruses and cellular RNA interference pathways are deeply intertwined also in mammals, although they have evolved the IFN system which, as earlier described, can be elicited by viral dsRNAs. It has been proposed that the IFN system has been evolved as an alternative to the dsRNA-induced RNA silencing. However, microRNAs seem to have kept antiviral functions also in mammals. Both viruses and host cells in fact, express microRNAs that play a role during viral infection. Viruses can be specifically and directly targeted by either artificial siRNAs or

cellular microRNAs, hampering viral replication. Moreover, mammalian viruses encode VSRs, reinforcing further the idea that microRNAs have antiviral roles in higher vertebrates (Li & Ding 2006). For instance, ADV (Adenovirus) expresses VA1, a non-coding RNA that specifically blocks microRNA biogenesis by binding both Dicer and exportin-5, both molecules important for microRNA biogenesis (Lu & Cullen 2004). DICER-deficient murine macrophages have been shown to be more permissive to VSV (Vescicular Stomatitis Virus) than wild type, albeit they showed no difference in type I IFN production (Otsuka et al. 2007). Dicer expression has also been shown to hamper replication of influenza A (Matskevich & Moelling 2007). Cellular microRNAs have been shown to have direct antiviral activity against retroviruses such as HIV (Triboulet et al. 2007) and PFV-1 (Lecellier et al. 2005). In response, both viruses express VSRs, Tat and Tas, respectively. HCV exemplifies how microRNAs can influence viral tissue tropism and work either in favour or against viruses. In fact, miR-122, a liver-specific micro-RNA was able to facilitate HCV replication (Jopling et al. 2005). Intriguingly, IFN-β has been shown to down-regulate miR-122, and up-regulate the expression of a series of micro-RNAs with sequence-specific anti-HCV activity (Pedersen et al. 2007).

Viruses also make use of microRNAs both from viral or host cell origin, targeting cellular genes but also viral genes. For instance, SV-40 (Simian virus 40) encodes and expresses a microRNA that targets one of its genes, the large T antigen. This does not reduce viral production but reduces the activity of cytotoxic T cells against infected cells (Sullivan et al. 2005). HSV-1 (Herpex Simplex Virus-1) expresses instead a microRNA (named miR-LAT) during the latency period that by targeting the TGF-β pathway has anti-apoptotic effects (Gupta et al. 2006). VSV instead, uses a cellular microRNA to its own advantage. In fact, it up-regulates miR-146a which, as already mentioned, attenuates PRRs signalling. Therefore by up-regulating miR-146a, VSV reduces the host's antiviral immunity (Hou et al. 2009).

The idea that microRNAs contribute to shape tissue tropism of viruses is increasingly being accepted. MicroRNAs can influence in which tissues and cells viruses are able to replicate. For instance, the case of miR-122 and HCV together with a few investigations based on ectopic expression of microRNAs confirms this (Brown et al. 2006, Kelly et al. 2008, Perez et al. 2009). As a consequence of microRNAs being an important arm of the innate immunity, it is expected that changes in microRNA expression have the potential to influence viral replication in natural occurring infections.

Considering the many examples of antiviral microRNAs reported so far, it is conceivable that also HRV is susceptible to regulation by microRNAs. If this were true then, it would be possible that the lung of asthmatics, and in particular the bronchial epithelium, presents a pathological microRNA profile that helps rhinovirus to replicate more. This possibility has not yet been investigated.

Although it has been shown that artificial siRNAs were able to inhibit HRV-16 replication (Phipps et al. 2004) in a plaque forming assay (employing HeLa cells), the involvement of microRNAs in cellular responses to HRV infection has not been investigated yet.

In conclusion, differences in microRNA expression could contribute to the aberrant characteristics of the asthmatic epithelium that seem to be responsible for both the pathophysiology of asthma and the response to respiratory viruses.

1.5 Hypothesis

We hypothesised that:

1) microRNAs are able to regulate HRV replication in bronchial epithelial cells, via either direct (see fig. 1-7 B) or indirect mechanisms.
2) microRNAs are differently expressed in asthmatic bronchial epithelial cells compared to healthy cells, contributing to asthmatic hallmarks of this cell type.

This project aims to address a role for microRNAs in the cellular antiviral innate response, focusing on HRV infection of bronchial epithelial cells. In particular, the project aims to address a role for anti-HRV microRNAs, in the different outcome of HRV infection of cells from asthmatic and healthy subjects.

The objectives are to:

1) Identify cell models in which HRV replicate differently.
2) Show that HRV replicates more efficiently when microRNAs are less abundant.
3) Apply these findings to human BECs, the model that would provide the link to asthma exacerbations.
4) Identify which microRNAs are differentially expressed in asthmatic and healthy HBECs, and to show that changes in such microRNAs are able to affect properties of asthmatic BECs and modulate HRV replication.

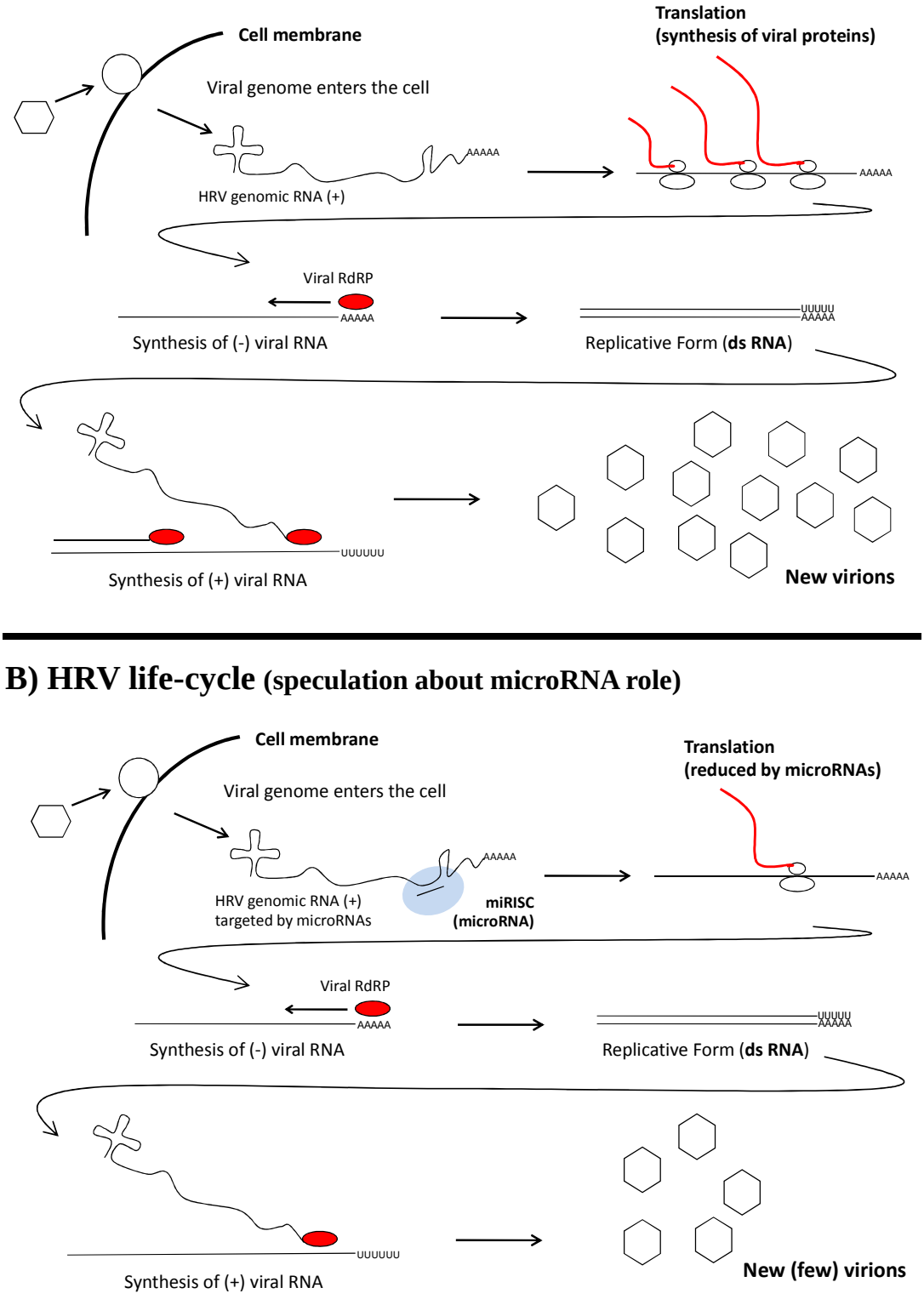

fig. 1-7. HRV RNA replication, and speculation about antiviral microRNAs.
Schematic representation of (**A**) HRV life cycle and (**B**) the hypothesis that microRNAs, binding to the (+) HRV RNA, would hamper production of viral proteins and hence the production of new genomic RNA.

Chapter 2

MATERIALS AND METHODS.

2.1 List of Reagents

Antibody anti-Ago2, clone 11A9 (rat IgG2a) available from Ascenion (Rudel et al. 2008).
Antibody normal rat IgG cat.n: sc-2026, Santa Cruz biotechnology, inc.
Anti-miR™ miRNA Inhibitors - hsa-miR-106b, cat.n: AM10067, Ambion
Anti-miR™ miRNA Inhibitors - hsa-miR-128, cat.n: AM11746, Ambion
Anti-miR™ miRNA Inhibitors - hsa-miR-155, cat.n: AM12601, Ambion
Anti-miR™ miRNA Inhibitors - hsa-miR-18a, cat.n: AM12973, Ambion
Anti-miR™ miRNA Inhibitors - hsa-miR-19b, cat.n: AM10629, Ambion
Anti-miR™ miRNA Inhibitors - Negative Control cat.n: 1, cat.n: AM17010, Ambion
BSA (Bovine Serum Albumin), nuclease free, cat.n: B9001S, New England Biolabs inc. (NEB)
Complete Protease Inhibitor Cocktail Tablets, cat.n: 0469312400, Roche
Doxycycline hyclate ≥98% (TLC) cat.n: D9891-5G, Fluka, Sigma
EDTA Disodium Salt, cat.n: D/0700/53 C30, Thermo Fisher Scientific Inc
FBS (Fetal Bovine Serum) heat inactivated, cat. N: 10108-165, GIBCO, Invitrogen
Glycogen 20mg, cat.n: 10901393001, Roche
High Capacity cDNA Reverse Transcription Kit, cat.n: 4374967, Applied Biosystems
MEM with Glutamax I, cat.n: 41090-028, GIBCO, Invitrogen
MgCl2 (Magnesium chloride hexahydrate) cat.n: M2393, Sigma
NaCl for molecular biology, cat.n: 71376-1KG, Sigma
NaHCO3 (Sodium bicarbonate) solution 7.5%, cat.n: S8761, Sigma
Non Essential Aminoacids Solution 10 mM (100X) liquid, cat.n: 11140-050, GIBCO, Invitrogen
Oligofectamine Transfection Reagent, cat.n: 12252-011, Invitrogen
PBS tablets, cat.n: 18912-014, GIBCO, Invitrogen
Pen/Strep 100x (Penicillin-Streptomycin, liquid), cat.n: 15070-063, GIBCO, Invitrogen
Protein G Sepharose 4 Fast Flow, cat.n: 17-0618-01, GE Healthcare
Proteinase K from Tritirachium album, cat.n: P2308-10MG, Sigma
QIAquick Gel Extraction Kit, cat.n: 28704, Qiagen
Recombinant human IL-13, cat.n: 213-IL-005, R&D Systems
Recombinant human TGF-b1 cat.n: 100-21, PeproTech Ltd.
Restriction enzymes used were purchased from New England Biolabs (NEB)
RPMI Medium 1640 with GlutaMAX™-I, cat.n: 72400-054, GIBCO, Invitrogen
Sodium dodecyl sulphate (SDS) cat.n: S/5200/53 C107, Thermo Fisher Scientific Inc
sspDNA (sonicated salmon sperm DNA) “DNA, MB grade” cat. N: 11 467 140 001, Roche
SuperFect Transfection Reagent, cat.n: 301305, Qiagen
TaqMan Universal PCR Master Mix, No AmpErase UNG, cat.n: 4364341, Applied Biosystems

TRI Reagent Solution, cat.n: AM9738, Applied Biosystems

Tris hydrochloride solution (Tris HCl, 1M pH 7.5) cat.n: BPE1757-500, Thermo Fisher Scientific Inc

Tryptose phosphate broth solution, cat.no: T8159, Sigma

Water, Ultrapure DNAse/RNAse-Free distilled water, cat.n: 10977035, Invitrogen

2.2 Cell culture (growth media).

All cells were cultured at 37°C in a humified 5% CO_2 incubator.

HeLa cells at high passage number (>50) were cultured in:

Dulbecco's Modified Eagles Medium (DMEM, Gibco), supplemented with 10% (v/v) heat inactivated foetal bovine serum (FBS), 50 IU/ml penicillin, 50 mg/ml streptomycin, 2 mM L-glutamine.

HeLa cells at low passage number (<50) were cultured in:

MEM with Glutamax I (GIBCO) supplemented with 10% (v/v) heat inactivated foetal bovine serum (FBS), 50 IU/ml penicillin, 50 mg/ml streptomycin.

THP-1 and BEAS-2B cells were cultured in:

RPMI medium with Glutamax I (GIBCO) supplemented with 10% FBS.

2.3 Generation of THP-1-derived macrophages (THP1MΦ).

4 x 10^5 THP-1 cells/ml/well were seeded in 12-well plates, in differentiation medium: RPMI with Glutamax I, supplemented with 5% FBS and 200nM Phorbol 12-myristate 13-acetate (PMA). 24 hours later, the medium was replaced with growth medium: RPMI medium with Glutamax I (GIBCO) supplemented with 5% FBS. The THP1MΦ so obtained were finally infected with HRV-1B 24 hours later (48 hours after seeding in differentiation medium).

2.4 Culture of primary human bronchial epithelial cells (BECs)

BECs culturing medium: Bronchial Epithelial Medium BEGM®.

It is prepared by adding the following components to 500 ml of BEBM Basal medium (Cambrex cat.n. CC-3171): 0.5 ml Hydrocortisone, 0.5 ml Retinoic acid, 2 ml Bovine pituitary extract, 0.5 ml human recombinant epidermal growth factor, 0.5ml Epinephrine, 0.5 ml

Transferrin, 0.5 ml Gentamycin sulfate amphotericin-B, 0.5 ml TrIIodothyronine (T3), and 0.5 ml Insulin.

BECs starvation medium: BEBM basal medium (Cambrex cat.n. CC-3171) supplemented with 0.1% (w/v) Bovine Serum Albumin (Sigma cat.n. A3059), 1% (v/v) ITS (Sigma cat.n. I3146)

Primary human BECs were obtained and plated out by trained researchers and technicians from the Brooke Laboratories, following a well-established protocol, briefly described here. Bronchial brushings from asthmatic patients and healthy volunteers were placed in 5 ml sterile PBS. In sterile conditions, 5 ml RPMI 1640 supplemented with 2 mM L-Glutamine, 25000 units Penicillin G Sodium and 25 mg Streptomycin sulphate, and 20% Fetal Bovine serum were added. The cells shed in the medium were then centrifuged for 5 minutes, at room temperature at 167 x g. The cell pellet was then resuspended in 3 ml of BEGM®. Cells were passed through a Disposable Needle (0.6x25 23G NHS supplies cat.n. FTR266) with a disposable 5ml syringe (NHS supplies cat.n. FWC306) and dispensed in equal aliquots into T25 tissue culture flasks, precoated with Collagen I at 0.029 mg/ml for 30 minutes. Cells were incubated at 37^0C, 5% CO_2 for about 1 week until confluent, when they were passaged into collagen-coated T75 flasks and cultured until confluent. Finally, the cells were passaged again (p2=second passage) and seeded into collagen-coated 24-well plates at a cell density $0.2x10^5$ cells per well.

Healthy

Patient ID	Age	Sex	% predicted FEV_1	PC_{20} (mg/ml)	fig. 4-6 and fig. 4-7	fig. 4-1	fig. 4-2
DS44	24	M	103	17	V		V
DS50	27	F	-	17	V		V
DS59	21	F	117	>8		V	V
DS63	24	M	83	-		V	V
DS87	20	F	101	>8		V	V
Syn A64	20	F	96	-	V		V
Syn A65	20	M	98	-	V		V
Syn A70	22	F	119	-	V		V
Syn A73	20	M	102	-	V		V
Syn A74	33	M	105	-	V		V
Syn A77	27	M	110	-	V		V
Syn A79	22	F	126.7	-	V	V	V
Syn A92	21	F	90	-	V		V
Average	**23.3**		**104.2**				

Asthmatics

Patient ID	Age	Sex	% predicted FEV_1	PC_{20} (mg/ml)	fig. 4-6 and fig. 4-7	fig. 4-1	fig. 4-2	fig. 4-8
BG088	60	M	70	-	V		V	
BG110	44	F	82	-	V		V	V
BG111	49	F	68	-	V		V	V
BG113	56	M	70	-	V	V	V	
BG157	41	F	80	-			V	
BG169	47	F	91.4	-		V	V	
BG189	41	F	109	-		V	V	
DS45	64	F	69.3	-	V		V	
DS52	36	F	95.5	0.42	V	V	V	
DS53	42	M	68.7	1.69	V		V	
Syn B33	23	M	103	-	V		V	
Syn C25	52	F	102	1	V		V	
Syn C43	30	F	110	2.07	V		V	
Syn D13	24	F	58	-	V		V	V
VK009c	23	F	87.8	-			V	
DS47	27	F	102.9	17				V
Average	**41.2**		**85.5**					

table 2-1. Characteristics of BECs donors.
Also indicated are the samples that were specifically used for each figure.

2.5 Propagation of HRVs.

HRV-1B was a gift of Dr. Nicole Bedke (Brooke Laboratories, School of Medicine, Southampton). HRV-16 was a gift of Dr. Jens Madsen (School of Medicine, Southampton). HRV-1B was grown on HeLa cells at low passage number (<50) while HRV-16 was grown on HeLa cells at high passage number (>50). This difference is due to the fact that higher titre virus was obtained this way for both viruses (personal communication, Dr. Nicole Bedke and Dr. Jens Madsen). However, both viral stocks were prepared following the same protocol.

HeLa cells were grown in the appropriate growth medium, up to around 70-80% confluency. Cells were washed once with HBSS (GIBCO) and then HRV was added together with additional infection medium (see table 2-2 for volumes and composition of infection medium used). The cell culture vessel was then kept at room temperature on a plate rocker at 30 oscillations per minute (o.p.m.) for 1 hour. Subsequently, more infection medium was added and finally the cell culture vessel was incubated at 33°C (in a humidified incubator, in air with 5% CO_2) for 16-24 hours. After performing three cycles of freeze-thaw at -80°C, the supernatant (containing the virus) was recovered, cell debris were removed by centigugation at 800xg at 4°C and used to inoculate more HeLa cells. The virus was amplified according to this procedure for 4 passages, diluting the virus-containing medium 1:4 with infection medium, and using bigger sized flasks at each passage. Finally, the virus containing medium was centrifuged at 800xg at 4°C and then filtered through a 0.2 μm syringe filter, in order to remove as much cell debris as possible. The viral suspension so obtained was then titrated by TCID50 assay.

Flask	Virus	Infection medium added at inoculation	Infection medium added after rocking	Final volume of infection medium in flask
T25	1ml	1ml	2ml	4ml
T75	2ml	2ml	4ml	8ml
T175	5ml	5ml	10ml	20ml

Infection medium	
MEM with Glutamax I for HRV-1B DMEM with L-glutamine for HRV-16	500ml
HEPES (1M – Sigma HO887)	8ml
$NaHCO_3$ solution 7.5% (Sigma S8761)	5ml
Tryptose phosphate broth solution (Sigma T8159)	20ml
$MgCl_2$ (3M – from powder, filter-sterilised)	5ml
Non Essential Aminoacids 100x (GIBCO 11140-050)	5ml
Pen/Strep 100x (GIBCO 15070-063)	5ml
FBS (GIBCO 10108-165)	20ml (4% final concentration)

table 2-2. Dilutions and medium composition for preparation of virus stock.

2.6 TCID50

Tissue culture infectious dose, at which virus particles will infect 50% of cells (TCID50) were determined by limiting dilution in 96 well plates and calculated by using the Spearman-Karber formula. HeLa cells at high passage number (>50) were cultured until confluent. Cells were detached by trypsin treatment, diluted at $1x10^5$ cells/ml and then seeded in 96-well plates (200µl/well=$2x10^4$ cells/well) and incubated at 37°C, 5% CO_2. After three hours, medium was replaced with 180 µl/well of DMEM infection medium (DMEM supplemented with 2% (v/v) heat inactivated foetal bovine serum (FBS), 50 IU/ml penicillin, 50 mg/ml streptomycin, 2 mM L-glutamine). A 10-fold serial dilution was then performed (in 200µl/well final volume) directly in the 96-well plate. After 1 hour at room temperature on plate rocker (30 o.p.m.), cells were incubated at 37°C, 5% CO_2 for 5 days. Subsequently, live cells were stained by adding 50µl/well of crystal violet staining solution (0.13 w/v crystal violet, 5% v/v formaldehyde, 5% ethanol in 1x PBS). Plates were then incubated for 30 minutes in the dark. Wells were then washed with tap water and air dried.

Formulae used to determine TCID50 and MOI for infections:

$TCID50 = [10 \wedge {}^{-(l-(d(s-0.5))}]/0.18$ ml

where:

$l = Log_{10}$ of lowest dilution (highest concentration of virus, generally -1)

$d = Log_{10}$ difference between successive dilutions

s = number of wells fully or 50% covered by live (stained) cells/number of wells in each row

1 multiplicity of infection (MOI of 1) is defined as a cell culture condition where there is 1 infectious virus particle per cell.

MOI = number of infectious virus particles/number of cells

Being TCID50= number of infectious virus particles/ml

MOI=(TCID50 x ml)/number of cells

and

ml = (MOI x number of cells)/TCID50

Following this protocol, the TCID50 of the HRV-1B stock obtained was determined to be 1.7 x 10^5/ml. This value was used to calculate the MOI used for all the infections performed, after determining the cell number/well.

2.7 Infections with HRV-1B.

2.7.1 HeLa cells and THP1MΦ.

Infection medium for HeLa cells: DMEM supplemented with 2% (v/v) heat inactivated foetal bovine serum (FBS), 50 IU/ml penicillin, 50 mg/ml streptomycin, 2 mM L-glutamine.

Infection medium for THP1MΦ: RPMI with Glutamax I supplemented with 2% FBS.

HeLa cells were grown until confluence, detached by trypsin treatment and seeded at 10^5 cells/ml/well in 12 well plates. 16 hours later they were infected with HRV-1B at MOI of 0.1 or 0.01. THP1MΦ were obtained as described previously and infected with HRV-1B at MOI of 0.1 or 0.01.

In both cases, before infection, the cells present in two wells were counted using an improved Neubauer 0.1 mm hemocytometer. Cells were detached by trypsin treatment and re-suspended

in 1ml/well. The cell count/well, obtained as a mean of the cell count from two wells, was used in the formula previously reported, in order to find out the volume of virus suspension necessary for an MOI of 0.1. The latter was then diluted 10 times and used to infect cells at an MOI of 0.01. All the necessary dilutions were done using the appropriate infection medium.

Cells to be infected were first washed with 1ml/well of HBSS (GIBCO), and then 200µl/well of the virus suspension at the appropriate dilution was added. The plates were then incubated at room temperature, on a plate rocker (30 o.p.m.) for one hour. At this point, residual virus was removed and cells were washed as above. Then, either 1ml/well infection medium was added, or cells were harvested (0 hours post-infection) using 500µl/well of TRI-Reagent (Ambion). Plates were then incubated at 37°C, 5% CO_2. Samples were then collected at the indicated time point as follows:

1) supernatants were collected and kept on ice until stored at -80°C
2) cells were washed with 1ml/well HBSS and then harvested in 500µl/well of TRI-Reagent (Ambion). The lysates were incubated at room temperature for 10 minutes, vortexed briefly and stored at -80°C until further processing.

Time points are indicated as hours post-infection (pi). Note that 0 hours pi is immediately after the 1 hour-incubation at room temperature on the plate rocker.

2.7.2 BEAS-2B cells.

Starvation / infection medium for BEAS-2B: RPMI with Glutamax I supplemented with 2% FBS.

BEAS-2B cells were infected as described for HeLa cells but cells were seeded in 24-well plates and 24 hours prior to infection, growth medium was replaced with starvation medium.

2.8 siRNA transfections.

A negative control siRNA and an anti-*DICER* siRNA were purchased from Ambion (Silencer® Select Validated siRNA) see table 2-3 for more details.

Ambion siRNA ID	sense strand sequence (5'-3' sequence)	antisense strand sequence (5'-3' sequence)
s23754 (Anti-DICER)	GAUCCUAUGUUCAAUCUAAtt	UUAGAUUGAACAUAGGAUCga
Negative control #2 (Catalog #: 4390846)	Not provided	Not provided

table 2-3. Details of the anti-DICER siRNA used (Applied Biosystems)

2.8.1 Transfection of THP1MΦ.

THP-1 cells were resuspended in plain RPMI at $5x10^5$ cells/ml and were seeded in 12-well plates using 0.8 ml/well ($4x10^5$ cells/well). The negative control siRNA and the *DICER1*-targeting siRNA were transfected using Oligofectamine (Invitrogen) according to the manufacturer's protocol. For each well transfected, the following quantities were used: 0.2 µl of 50 µM siRNA were diluted in 80 µl of plain RPMI. In a different eppendorf, 5µl of Oligofetamine were added to 20 µl of plain RPMI mixing well by pipetting several times. The tubes were left for 5 minutes at room temperature, and then the contents were mixed together by pipetting. After 20 minutes at room temperature, the mixture was finally added to the cells (100 µl/well giving a final siRNA concentration of 10nM). Three hours later, 100 µl/well of 2µM PMA-containing FBS (10 µl of 200µM PMA/ml of FBS) was added. Cells were further incubated overnight at 37°C, 5% CO_2, after which the medium was replaced with 5%FBS RPMI and then treated as previously described for infection with HRV-1B.

2.8.2 BEAS-2B transfection

Transfections of siRNAs.

BEAS-2B cells were seeded at 0.75 x 10^5 cells/well in 24-well plates. 24 hours later, the culture medium was replaced with 200µl/well of growth medium. For each well to be transfected, 1.5µl of Oligofectamine were diluted in 10µl of plain RPMI and mixed by pipetting. In a separate eppendorf 0.15µl of 50µM siRNA were diluted in 40µl of plain RPMI and mixed by pipetting. The eppendorfs were left at room temperature. After 5 minutes, the contents of the two eppendorfs were mixed together by pipetting and left at room temperature. 20 minutes later, the mixture was mixed again by pipetting and dispensed on the cells (50µl/well giving a final concentration of siRNA of 30 nM). The following day the medium present in the wells was replaced with fresh starvation medium. BEAS-2B cells were transfected every 36 hours (3 days) following the protocol just described. This required that 48hours post-transfection cells were detached by trypsin treatment and seeded at the density used earlier. The day after the last transfection medium was replaced with starvation medium rather than growth medium. Cells were then infected with HRV-1B 24 hours later (in total, 48 hours after the third transfection).

Transfections of antimiRs.

Transfection was performed using INTERFERin, as recommended by the manufacturer's protocol. BEAS-2B cells were seeded at 0.75 x 10^5 cells/well in 24-well plates. 24 hours later, the culture medium was replaced with 500µl/well of growth medium. For each well to be transfected, 1.2µl of 50µM antimiR were diluted in 100µl of plain RPMI and mixed by

pipetting. Immediately after, 4µl of INTERFERin were added and mixed by pipetting. The eppendorfs were then left at room temperature. 20 minutes later, the mixture was mixed again by pipetting and dispensed on the cells (100 µl/well giving a final concentration of antimiR of 100 nM). The following day the medium present in the wells was replaced with fresh starvation medium. Cells were therefore either infected with HRV-1B or treated with TGF-β.

2.8.3 Transfections of BECs

BECs had been seeded in 24-well plates as described previously.

Oligofectamine was used on BECs as optimized on BEAS-2B. Again, the quantities reported refer to each well. When cells reached about 80% confluence, BEC culture medium was replaced with 200µl/well of fresh BEGM. 1.5µl of Oligofectamine were diluted in 10µl of plain RPMI and mixed by pipetting. In a separate eppendorf 0.15µl of 50µM siRNA were diluted in 40µl of plain RPMI and mixed by pipetting. The eppendorfs were left at room temperature. After 5 minutes, the contents of the two eppendorfs were mixed together by pipetting and left at room temperature. 20 minutes later, the mixture was mixed again by pipetting and dispensed on the cells (50µl/well). 24 hours later the medium was replaced with 0.5ml/well of BEGM. 24 hours later (48 hours after transfection) cells were detached by trypsin. Trypsin activity was stopped by adding 10% DMEM. Cells were spun down, re-suspended in BEGM and 1/3rd was seeded in wells pre-coated with Collagen I (at 0.029 mg/ml for 30 minutes). Next day transfection was repeated as above.

2.9 RNA extraction and RT-qPCR

RNA was extracted with TRI-Reagent (Ambion) using 500µl/well for 12-well plates or 300µl/well for 24-well plates. RNA purification was performed according to the manufacturer's protocol. Briefly, cells were lysed in TRI-Reagent and lysis was helped by passing the lysate several times through the pipette tip. Lysates were collected in RNAse-free eppendorfs, incubated for roughly 10 minutes and then either processed straightaway or stored at -80°C until further use. Chloroform was then added in the measure of 20% compared to the volume of TRI-Reagent used. Samples were then mixed thoroughly by vortexing for 15 seconds, incubated for 5 minutes and then centrifuged at top speed in a bench top centrifuge at 4°C for 20 minutes. This separates the organic phase, containing DNA and proteins, from the aqueous phase which contains the total cellular RNA. The aqueous phase of each sample was then carefully collected using RNAse-free filter tips, and transferred into fresh RNAse-free eppendorfs. 10µg of glycogen were then added to each sample to help in the visualiation of the precipitate in the next

step. RNA was precipitated by adding isopropanol in the measure of 50% compared to the amount of TRI-Reagent used. Samples were vortexed for 15 seconds and then incubated at -20°C for at least 20 minutes. The precipitated RNA was then collected by centrifugation at top speed (13000rpm = 15000xg) in a bench top centrifuge at 4°C for 30 minutes. The supernatants were discarded while the precipitated RNA was washed by adding 1ml of ice-cold 75% ethanol (v/v in water). Samples were centrifuged as before for 10 minutes. After discarding the supernatant, the pellets were allowed to air-dry and finally they were re-suspended in RNAse-free water (GIBCO) generally 50µl or 30µl for samples from 12-well or 24-well plates respectively.

RNA samples were quantified using the spectrophotometer Nanodrop 1000 (Thermo Scientific). Briefly, after starting the instrument and setting the blank with milliQ water, as little as 2µl of each sample are read at the spectrophotometer whose software calculates and displays the RNA concentration. The Nanodrop measures the absorption of the sample between the instrument pedestals over a range of light wavelengths. For RNA quantification, this range goes from 220 to 350 nm (UV light). The concentration of nucleic acids is proportional to the absorption at 260nm (A_{260}). RNA concentration (ng/µl) is therefore calculated by multiplying this value by 40. Moreover, the ratios A_{260}/A_{280} and A_{260}/A_{230} give a measure of the purity of the preparation, compared to the presence of proteins or other residues. The RNA purified using the protocol described had always A_{260}/A_{280} ratios between 1.7 and 2 while A_{260}/A_{230} ratios were between 1 and 2, values widely accepted as a measure of good quality RNA for RT-qPCR.

Reverse transcription reactions (RT) were performed using the same amount of RNA for all samples. Complementary DNA (cDNA) of total cellular RNA was used to quantify expression of protein-encoding genes (such as GAPDH) by qPCR. Such cDNA was obtained by reverse transcription, using the High-Capacity cDNA Reverse Transcription Kit (Applied Biosystems part number: 4368813) with random hexamers as primers. MicroRNA RT-qPCR was performed using Taqman microRNA assay kits from applied biosystems (part number: 4427975) that contain a specific RT primer and Taqman qPCR primers and probe necessary to quantify expression of a specific microRNA (see table 2-5 for recipes and amount of RNA used). In both cases, the cDNA obtained was used to perform qPCR using TaqMan® Universal PCR Master Mix, No AmpErase® UNG (Applied Biosystems part number: 4364341) on a 7900HT Real-Time PCR machine (Applied Biosystems) with the standard Taqman thermal cycling conditions (table 2-6).

Fold differences in gene expression were calculated using the comparative Ct method for relative quantification (Livak & Schmittgen 2001).

For more information about the primers used see table 2-4.

Gene	Company	Type of assay	Part n.	Assay ID
COL1A1	Applied Biosystems	Taqman	4331182	Hs00164004_m1
COL1A2	Applied Biosystems	Taqman	4331182	Hs01028956_m1
CCL26	Applied Biosystems	Taqman	4331182	Hs00171146_m1
DICER1	Applied Biosystems	Taqman	4331182	Hs00229023_m1
EIF2C2 (AGO2)	Applied Biosystems	Taqman	4331182	Hs01085579_m1
GAPDH	Applied Biosystems	Taqman	4352934	
HRV-16	Primer design	Taqman		
HRV-1B	Primer design	Taqman		
IFNB1	Primer design	Perfect probe		
IL13RA1	Primer design	Taqman		
PU.1	Primer design	Taqman		
SMAD2	Applied Biosystems	Taqman	4331182	Hs00183425_m1
TGFB1	Applied Biosystems	Taqman	4331182	Hs00998133_m1
TGFB2	Applied Biosystems	Taqman	4331182	Hs00234244_m1
TGFB3	Applied Biosystems	Taqman	4331182	Hs00234245_m1
SERPINE1	Applied Biosystems	Taqman	4331182	Hs01126606_m1
SOCS1	Applied Biosystems	Taqman	4331182	Hs00705164_s1
IL8	Applied Biosystems	Taqman	4331182	Hs99999034_m1

microRNA (miRBase name)	Type of assay	Assay name (on tube)	Assay ID
hsa-miR-106b	Taqman	hsa-miR-106b	000442
hsa-miR-128	Taqman	hsa-miR-128a	002216
hsa-miR-140-5p	Taqman	mmu-miR-140	001187
hsa-miR-142-3p	Taqman	hsa-miR-142-3p	000464
hsa-miR-155	Taqman	hsa-miR-155	002623
hsa-miR-16	Taqman	hsa-miR-16	000391
hsa-miR-18a	Taqman	hsa-miR-18a	002422
hsa-miR-19b	Taqman	hsa-miR-19b	000396
hsa-miR-30a	Taqman	hsa-miR-30a-5p	000417
hsa-miR-34a	Taqman	hsa-miR-34a	000426
hsa-miR-93	Taqman	mmu-miR-93	001090

NB: All taqman microRNA kits have the same part number: 4427975

table 2-4. Details about primer and probes used for RT-qPCR.
Note that the sequences were not provided by the manufacturer.

Random hexamers reverse transcription	
10x RT buffer	1.00
25x dNTPs (100mM tot)	0.40
10x Random primers	1.00
RNAse inhib. (Ambion 20U/μl)	0.50
Multiscribe (RT enzyme)	0.50
RNA (200ng) + water	**6.60**
total	10.00

microRNA reverse transcription	
10x RT buffer	0.75
25x dNTPs (100mM tot)	0.08
5x specific primer	1.50
RNAse inhib. (Ambion 20U/μl)	0.10
Multiscribe (RT enzyme)	0.50
water	2.08
RNA (2 ng/μl)	**2.50**
total	7.50

qPCR	
qPCR mastermix (2x)	2.50
primers and probe (20x)	0.25
water	1.00
1/10 diluted cDNA	**1.25**
total	5.00

microRNA qPCR	
qPCR mastermix (2x)	2.50
primers and probe (20x)	0.25
water	1.90
undiluted cDNA	**0.35**
total	5.00

table 2-5. Reverse transcription and qPCR recipes.

Reverse transcription thermal cycling conditions – random hexamers

	Step 1	Step 2	Step 3	Step 4
Temperature (°C)	25	37	85	15
Time (minutes)	10	120	5	hold

Reverse transcription thermal cycling conditions – microRNA

	Step 1	Step 2	Step 3	Step 4
Temperature (°C)	16	42	85	15
Time (minutes)	30	30	5	hold

qPCR thermal cycling program (for any taqman assay)

	Temperature (°C)	Time	Function
	95	10 min	Denaturing and enzyme activation
Cycle for (40 cycles)	95	15 sec	Denaturing
	60	1 min	Annealing/extension/data collection

qPCR thermal cycling program (for perfect probe assays)

	Temperature (°C)	Time	Function
	95	10 min	Denaturing and enzyme activation
Cycle for (40 cycles)	95	15 sec	Denaturing
	50	30 sec	Annealing / Data collection
	72	15 sec	Extension

table 2-6. Thermal cycling conditions for RT-qPCR

2.10 AGO2 co-immunoprecipitation (co-IP)

2.10.1 Protocol

Only RNAse-free filter tips and eppendorfs were used during this procedure.
All the buffers used and the optimised conditions chosen are summarised in table 2-7 and table 2-8.

Beads preparation

Protein G-coated sepharose beads (Amersham) were prepared for IP reactions as follows, either the day before use or stored at 4°C for maximum one month. Beads were always collected by centrifugation in a bench top centrifuge, at 3000 rpm (= 800xg) for 1 minute at 4°C.

Briefly, the ethanol contained in the storing buffer was first removed, by washing the beads 3 times with ice-cold lysis buffer. Finally, beads were blocked with a final concentration of 1µg/µl of BSA and 1µg/µl of sonicated salmon sperm DNA (sspDNA) for at least 1 hour at 4°C.

A more detailed description follows.

1ml of beads was centrifuged in an ice-cold eppendorf. The supernatant was discarded, while the collected beads were washed by adding 1ml of ice-cold lysis buffer and by inverting the tube several times. Collection and washing was repeated 3 times in total. The volume of the collected beads was estimated by eye (generally about 650µl) and an equal volume of ice-cold lysis buffer was added. Finally, 150µl of BSA (10mg/ml) and 150µl of sspDNA (10mg/ml) were added in order to block aspecific binding and the eppendorf was left at 4°C, rotating end over end, for at least 1hour, generally overnight. After this incubation, beads were collected by centrifugation and washed three times as above and resuspended in an equal volume of ice-cold lysis buffer. Therefore, beads ready to be used were always roughly 50% (v/v) in the appropriate lysis buffer (without DTT or inhibitors).

Step 1 cell lysis

THP1MΦ or BEAS-2B cells were first trypsinised to detach them from the plastic. Trypsin was then inhibited by adding growth medium (containing 10% FBS) and cells were then collected by centrifugation as above. In both cases, cells were then washed twice in sterile ice-cold PBS (GIBCO) and finally the cell pellet was resuspended in 50µl/10^6 cells of ice-cold complete lysis buffer, incubated on ice for 10 minutes and then placed at -80°C.

Pause point

Cell lysates were either stored at -80°C until further processing or thawed on ice (after at least 10 minutes at -80°C) and processed immediately. This freeze-thaw step proved useful in aiding cell lysis and it was recommended in also other RNA co-IP protocols (Keene et al. 2006).

Step 2 antibody binding

Cell lysates were kept on ice during the entire procedure and this included chilling all the eppendorfs on ice for a few minutes, before use.

Cell lysates, were thawed on ice and vortexed briefly before being passed through a G26 sterile needle several times (about 10 times) to complete the lysis process. Finally, they were cleared of the residual cell debris by centrifugation, at top speed in a bench top microcentrifuge, at 4°C for 15 minutes. Pellets were discarded while supernatants were collected and diluted ten times, so that 1ml of lysate would correspond to $2x10^6$ cells. 1ml aliquots were dispensed in pre-chilled eppendorfs, while 10µl were placed into 500µl of TRI-Reagent and constitute the input sample, useful for calculating fold enrichment (see next section). The same amount of anti-Ago2 specific antibody or the corresponding IgG negative control isotype antibody was then added to each 1ml-aliquot of cell lysate at this stage and finally, the samples were left rotating end over end on a wheel at 4°C overnight.

Antibody coupling to beads

50 µl of protein G-coated sepharose beads, prepared as described above, were added to each co-IP reaction, and incubated rotating end over end on a wheel at 4°C for 2 hours. Beads were then collected by centrifugation and then washed as already described, using 1ml of the appropriate ice-cold washing buffer for the appropriate amount of times. Beads were then washed once more with ice-cold PBS (1x) and resuspended in 100µl of RNAse-free water. 2.5µl of proteinase K (20mg/ml) was added to each eppendorf (final concentration of proteinase K about 0.5µg/µl). Beads were incubated for 15 minutes at 37°C, flicking the tubes every 5 minutes to keep beads in suspension (or in a rotomixer at 1000rpm).

Purification of Co-immunoprecipitated RNA

500µl of TRI-Reagent (Ambion) were added to the beads in each eppendorf. Beads were then vortexed briefly and incubated at room temperature for about 10 minutes. Eppendorfs were then spun at top speed in a bench-top centrifuge for 1 minute. Supernatants were transferred into new eppendorfs while the collected beads were discarded. Indeed, Proteinase K and TRI-Reagent treatments freed any RNA from proteins, breaking obviously also the link to the beads, which therefore are not needed anymore and can be removed at this stage. RNA isolation was thereafter performed

following the TRI-Reagent protocol given previously (paragraph 2.9). After precipitation, the RNA pellet was resuspended in 30µl of RNAse-free water.

Pause point

The isolated RNA, was then either used straightaway for RT-qPCR reactions, or stored at -80°C for later use.

RT-qPCR

Quantification of co-immunoprecipitated RNAs (mRNA or microRNAs) was performed as usual, using either 3.3µl of RNA for random primer based RT, or 0.5µl for microRNA RT.

Lysis buffers	Washing buffers
Lysis B PBS 1x NP-40 0.5% EDTA pH8 2 mM DTT 0.5 mM Glycerol 20%	**Wash 1a** PBS 1x NP-40 0.05% Glycerol 10%
IPLB Tris-HCl pH7.5 20 mM NaCl 150 mM NP-40 0.5% EDTA 2 mM DTT 0.5 mM Glycerol 20%	**Wash 1b** PBS 1x NaCl 160 mM NP-40 0.05% Glycerol 10%
PXL PBS 1x NP-40 0.5% Na-Desoxycholate 0.5% SDS 0.1%	**IPWB** Tris-HCl pH7.5 50 mM NaCl 300 mM $MgCl_2$ 5 mM NP-40 0.05% Glycerol 10%
	Wash 1M PBS 1x NaCl 860 mM NP-40 0.05% Glycerol 10%
	PXLW Same composition as PXL But with PBS 5x

Note

PBS (1x):	**Complete lysis buffer:**
NaCl 140 m M Na_2HPO_4 8 mM KH_2PO_4 1 mM KCl 3 mM pH 7.5	Lysis buffer composed as specified above and containing 100U/ml RNAse inhibitor (Applied Biosystems) and 1x complete cocktail protease inhibitor (Roche). Where required, **DTT** was added just before use.

table 2-7. Composition of buffers used for AGO2 co-IP experiments.

	THP-1	BEAS-2B
Amount of cells (10^6)	2	2
Lysis buffer	Lysis B	Lysis B
Washing buffer	Wash 1b (5 times)	Wash 1M (5 times)
µg of Ab	1 µg	1 µg

table 2-8. Reagents and conditions chosen for co-IP reactions (after optimization).

2.11 Calculations for Ago2 co-IP

The calculations used here were adapted from the delta delta Ct method for qPCR. Moreover, table 2-9 and table 2-10 are an example of how the raw data has been used and constitute indeed the calculations performed for fig. 3-11 and fig. 3-12 respectively.

For all co-IP results shown:

Over input: DCt using Ct (Input) as reference, e.g. Ct(Ago2) – Ct(Input)

Fold: $2^{(-\text{Over input})}$

Fold enrichment: Fold normalized to the Fold of one IgG sample

Only for table 2-9 (fig. 3-11):

No Ab: average Ct value from sample where no antibody was used

Only for table 2-11 (fig. 3-14 E):

DCt: DCt using always Ct (IgG(**0.5x10^6**)) as reference,

e.g. Ct (Ago2(**2x10^6**)) - Ct(IgG(**0.5x10^6**))

Absolute fold: $2^{(-\text{DCt})}$

PU.1						
Ct	**Sample**	**average Ct**	**No Ab - AGO2**	**over input**	**fold**	**fold enrichment**
27.407335 27.443405	LysisB-A AGO2	27.43	0.96	2.06	0.24	1.94
28.36186 28.407854	LysisB-A No Ab	28.38		3.02	0.12	1.00
28.18089 28.064384	LysisB-B AGO2	28.12	4.69	2.76	0.15	1.20
32.88936 32.73173	LysisB-B No Ab	32.81		7.45	0.01	0.05
28.001936 27.795507	IPLB AGO2	27.90	2.38	2.15	0.23	1.83
30.579348 29.982925	IPLB No Ab	30.28		4.53	0.04	0.35
29.529188 29.220678	PXL AGO2	29.37	5.27	3.67	0.08	0.64
34.77094 34.51458	PXL No Ab	34.64		8.94	0.00	0.02
25.293058 25.433088	LysisB input	25.36				
25.566805 25.931477	IPLB input	25.75				
25.732935 25.667847	PXL input	25.70				
Undetermined Undetermined	LysisB-input no RT					

table 2-9. Calculations performed for fig. 3-11

In fig. 3-11 **A** the plotted values are from column “fold enrichment”. In fig. 3-11 **B** the plotted values are from column “No Ab - AGO2”.

PU.1						
Ct	**Sample**	**average Ct**	**IgG - AGO2**	**over input**	**fold**	**fold enrichment**
24.757038 24.953346	Lysis B Input	24.86				
30.33447 29.83714	Lysis B IgG 0.01 µg	30.09	0.55	5.23	0.027	1.00
29.578262 29.498785	Lysis B AGO2 0.01 µg	29.54		4.68	0.039	1.46
30.35973 Undetermined	Lysis B IgG 0.1 µg	30.36	2.34	5.50	0.022	0.83
27.97714 28.065699	Lysis B AGO2 0.1 µg	28.02		3.17	0.111	4.18
29.75894 29.821234	Lysis B IgG 1 µg	29.79	2.06	4.93	0.033	1.23
27.732868 27.725945	Lysis B AGO2 1 µg	27.73		2.87	0.136	5.12
29.697363 29.44025	Lysis B IgG 2 µg	29.57	2.04	4.71	0.038	1.43
27.645033 27.422325	Lysis B AGO2 2 µg	27.53		2.68	0.156	5.86
29.9582 29.780846	Lysis B IgG 4 µg	29.87	1.88	5.01	0.031	1.16
27.969751 28.001276	Lysis B AGO2 4 µg	27.99		3.13	0.114	4.29

table 2-10. Calculations performed for fig. 3-12.
Plotted values are from column “fold enrichment”

Ab saturation test					
SMAD2					
Ct	**Sample**	**average**	**IgG - AGO2**	**DCt**	**Absolute fold**
30.764034 30.683296	**Input 0.5x10^6**	30.72			
28.682013 28.71569	**Input 2x10^6**	28.70			
28.139954 27.750428	**Input 4x10^6**	27.95			
Undetermined 36.53989	**IgG 0.5x10^6**	36.54	-0.32	0.00	1.00
36.431057 37.2816	**AGO2 0.5x10^6**	36.86		0.32	0.80
35.050323 35.595604	**IgG 2x10^6**	35.32	1.17	-1.22	2.32
34.18051 34.122597	**AGO2 2x10^6**	34.15		-2.39	5.24
35.85522 34.736015	**IgG 4x10^6**	35.30	2.02	-1.24	2.37
33.279015 33.273697	**AGO2 4x10^6**	33.28		-3.26	9.60

table 2-11. Calculations performed for fig. 3-14 E.
Plotted values are from column “Absolute fold”

2.12 Generation of lentivirally transduced BEAS-2B cell lines.

2.12.1 Plasmids

The lentiviral inducible knock-down system adopted was obtained from Tronolab (see (Wiznerowicz & Trono 2003) and http://tronolab.epfl.ch/). It consists of two lentiviral vectors that need to be co-transduced in the same cell for the system to be inducible (fig. 2-1). The names and functions of all the plasmids used are reported in table 2-12.
This system was used in order to constitutively over-express miR-155 in BEAS-2B cells. The same system was used in order to obtain inducible knock-down of *EIF2C2* (*AGO2*) or *DICER1* in BEAS-2B cells. The lentiviral vectors transduced into BEAS-2B cells in order to obtain the cell lines used for this study are listed in table 2-14.
pLVTHM_BIC encodes the gene for *miR-155* (*BIC*) and had been previously generated by our group (Martinez-Nunez et al. 2009). Also BEAS-2B cells constitutively over-expressing *miR-155* (B2B-155) had been previously generated by our group (unpublished data). B2B-155 and B2B-C cell lines were generated by Ana Francisco Garcia in collaboration with Dr Fethi Louafi and Victor Paky Bondanese, during a project carried out during her MRes at the University of Southampton, under the supervision of Dr. Tilman Sanchez-Elsner and Prof. Donna Davies.

All the other pLVTHM-derived plasmids were generated as follows. The pairs of ssDNA oligonucleotides listed in table 2-16 (designed as explained in table 2-15) were annealed by mixing them in a 1:1 ratio and incubated in a thermal cycler with the program in table 2-17. The dsDNA fragments obtained (inserts) were cloned into pSUPER between BglII and HindIII. The whole sequence containing H1 promoter and the insert was then excised from pSUPER, using EcoRI and ClaI, and inserted into pLVTHM between the same couple of restriction sites (fig. 2-3). These constructs are expected to express short hairpin RNA molecules (shRNA) inside the cell, allowing for the knock-down of the desired target gene (as schematically shown in fig. 2-2).

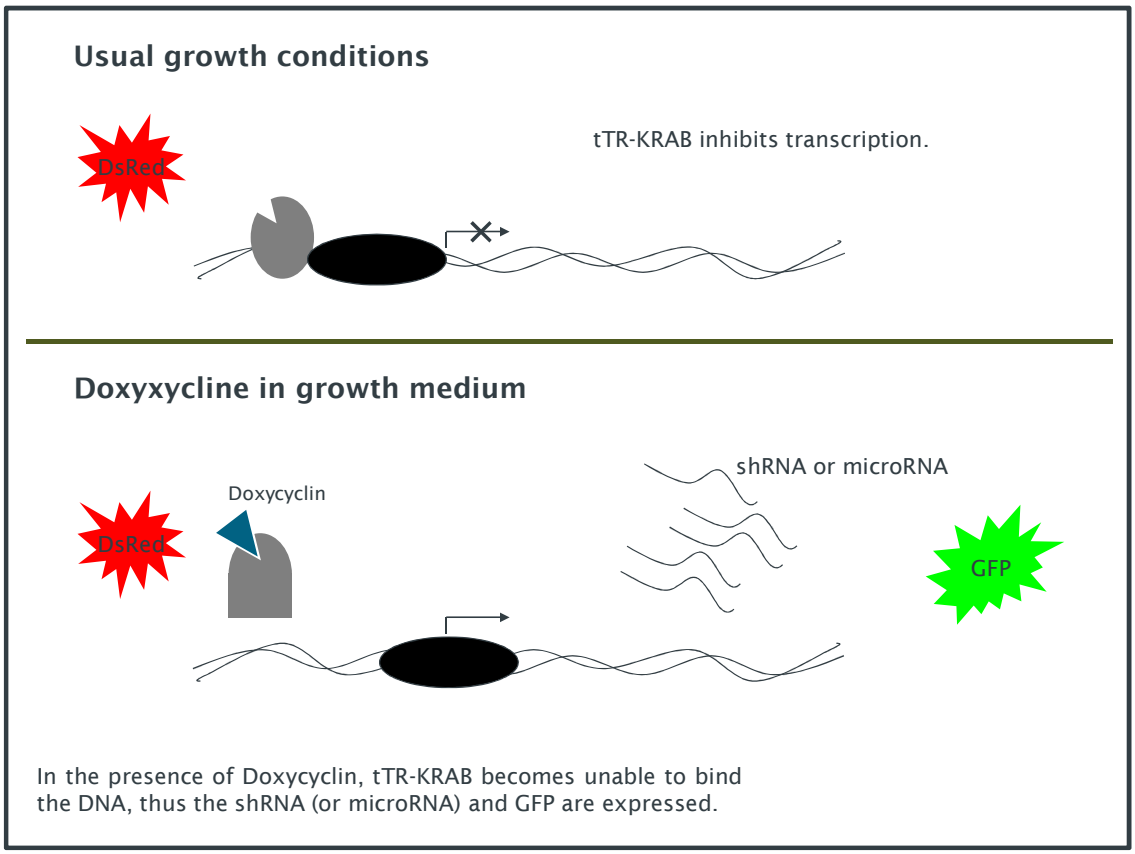

fig. 2-1. Schematic representation of how the inducible system adopted works.

Plasmid	Function	Main elements or gene/s encoded
psPAX2	Packaging	HIV-1 genes necessary for lentivirus production: gag, pol, rev, tat.
pMD2.G	Packaging	Membrane glycoprotein from Vescicular Stomatitis virus (VSV-G).
pLV-tTRKRAB-red	Lentiviral vector. It allows transcriptional regulation of transgenes.	tTR-KRAB, tetracycline-dependent transcriprional trans-inhibitor; DsRed2, red fluorescent protein, as a marker.
pLVTHM	Lentiviral vector. It expresses the transgene (shRNA or microRNA).	H1 (RNA polIII) expression cassette; tetracycline operator (tetO) allows for regulation by tTR-derived proteins (tetracycline repressor); GFP (marker);
pSUPER	Subcloning	tetO and H1 promoter.

table 2-12. Plasmid used for cloning and generation of lentiviral particles.

Plasmid	Insert
pLVTHM_BIC	BIC (miR-155 gene)
pLVTHM_neg	sh_neg
pLVTHM_AGO2	sh_AGO2
pLVTHM_DCR	sh_DCR

table 2-13. pLVTHM-derived plasmids generated and relative inserts.

Cell line name	Lentiviral plasmids transduced
B2B-155	pLVTHM_BIC
B2B-C	pLVTHM_neg
BEAS-2B LV_neg	pLV-tTRKRAB-red; pLVTHM_neg
BEAS-2B LV_AGO2	pLV-tTRKRAB-red; pLVTHM_AGO2
BEAS-2B LV_DCR	pLV-tTRKRAB-red; pLVTHM_DCR

table 2-14. Transduced BEAS-2B cell lines and lentiviral vectors they harbour.

In order to have an inducible system, target cells need to be cotransduced with both pLVTHM-derived vector and pLV-tTRKRAB-Red. Transduction of pLVTHM alone gives constitutive expression of shRNA or microRNA.

Common sequences		Specific sequences	
S		**sh_neg**	
5' end	GATCCCC	**SENSE**	ATACTCCGTTCGTGTCACG
Linker	TTCAAGAGA	**ANTISENSE**	CGTGACTCGTTCGGAGTAT
3' end	TTTTTGGAAA		
AS		**sh_AGO2**	
5' end	AGCTTTTCCAAAAA	**SENSE**	GCAGGACAAAGATGTATTA
Linker	TCTCTTGAA	**ANTISENSE**	TAATACATCTTTGTCCTGC
3' end	GGG		
		sh_DCR	
		SENSE	GATCCTATGTTCAATCTAA
		ANTISENSE	TTAGATTGAACATAGGATC

Restriction enzymes		
Enzyme	**Restriction site**	**Adaptor**
HindIII	A'AGCT,T	AGCTT
BglII	A'GATC,T	
BamHI	G'GATC,C	GATCC

table 2-15. Sequences used to design the inserts.
All the sequences are written in the direction 5'-3'.
Common sequences: the 5' and 3' ends of the sense and antisense oligonucleotides, allow for directional cloning into pSUPER. The linker forms the loop of the shRNA.
Specific sequences: the sense and antisense sequences are complementary to each other. They form the stem of the shRNA. The terms "sense" and "antisense" are relative to the sequence of the target mRNA. Therefore, the mature RNA (that enters the RISC) is expected to have sequence derived from the one referred to as "antisense" in this table. The specific sequences were obtained from Ambion siRNA s23754 for sh_DCR, from (Schmitter et al. 2006) for both sh_AGO2 and sh_neg. The sequence of each S/AS couple of oligonucleotides shown in table 2-16 was assembled by joining the sequences shown here in the order:
(S or AS) 5'end – sense – (S or AS) linker – antisense – (S or AS) 3'end.

Oligo	Gene targeted / sequence
sh_DCR	*DICER1*
S	GATCCCCGATCCTATGTTCAATCTAATTCAAGAGATTAGATTGAACATAGGATCTTTTTGGAAA
AS	AGCTTTTCCAAAAAGATCCTATGTTCAATCTAATCTCTTGAATTAGATTGAACATAGGATCGGG
sh_AGO2	*EIF2C2* (AGO2)
S	GATCCCCGCAGGACAAAGATGTATTATTCAAGAGATAATACATCTTTGTCCTGCTTTTTGGAAA
AS	AGCTTTTCCAAAAAGCAGGACAAAGATGTATTATCTCTTGAATAATACATCTTTGTCCTGCGGG
sh_neg	None (negative control shRNA)
S	GATCCCCATACTCCGTTCGTGTCACGTTCAAGAGACGTGACTCGTCGGAGTTTTTTTTGGAAA
AS	AGCTTTTCCAAAAAATACTCCGTTCGTGTCACGTCTCTTGAACGTGACTCGTCGGAGTTTGGG

table 2-16. DNA oligonucleotides cloned into the lentiviral vector.
Annealing the paired oligonucleotides gives a dsDNA fragment with protruding ends. Therefore there is no need to digest before inserting it into plasmid.

95°C for 5 min
to 80°C in 15min (-1°C/min)
to 70°C in 20min (-0.5°C/min)
to 55°C in 150min (-0.1°C/min)
to 10°C in 90min (-0.5°C/min)

table 2-17. Annealing thermal cycling program.
These steps were adopted to anneal correctly the pairs of oligonucleotides listed in table 2-16 and obtain the inserts used for cloning. 3µg of each oligonucleotide were mixed together in a total of 50µl of annealing buffer (100 mM NaCl, 10mM Tris pH7.4)

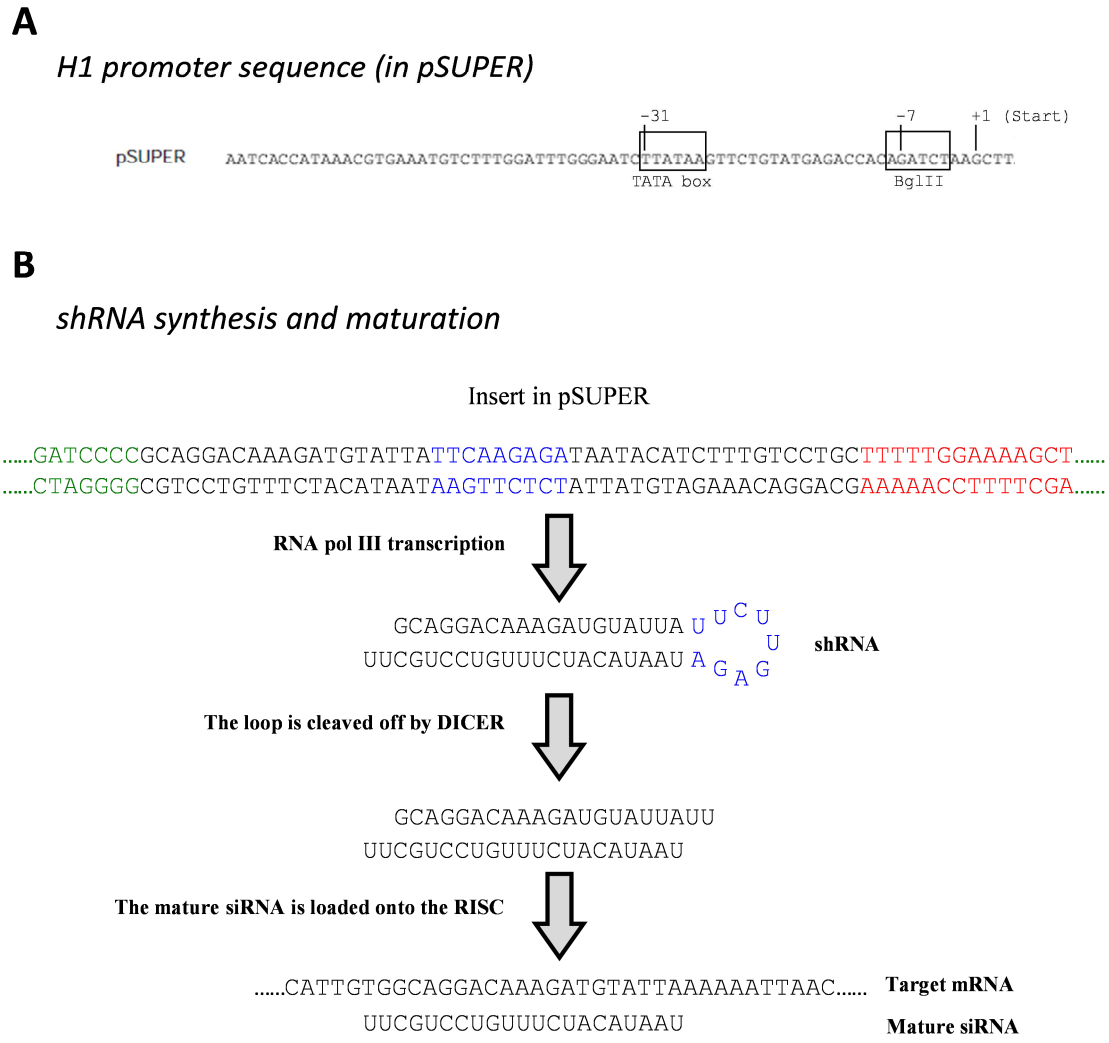

fig. 2-2. Schematic of H1 promoter in pSUPER and expected shRNA synthesis.
What shown here is also valid for the final lentiviral constructs. In fact, the whole expression cassette is subcloned from pSUPER. The RNA produced by RNA polymerase III folds into a hairpin, the shRNA. The latter is recognised by Dicer which cleaves off the loop, generating the mature short RNA that will be loaded onto the RISC complex and that will be responsible for silencing of the target. The sequences used in this diagram are from shAGO2 and the target sequence shown is from AGO2 transcript variant 1 (accession number NM_012154).

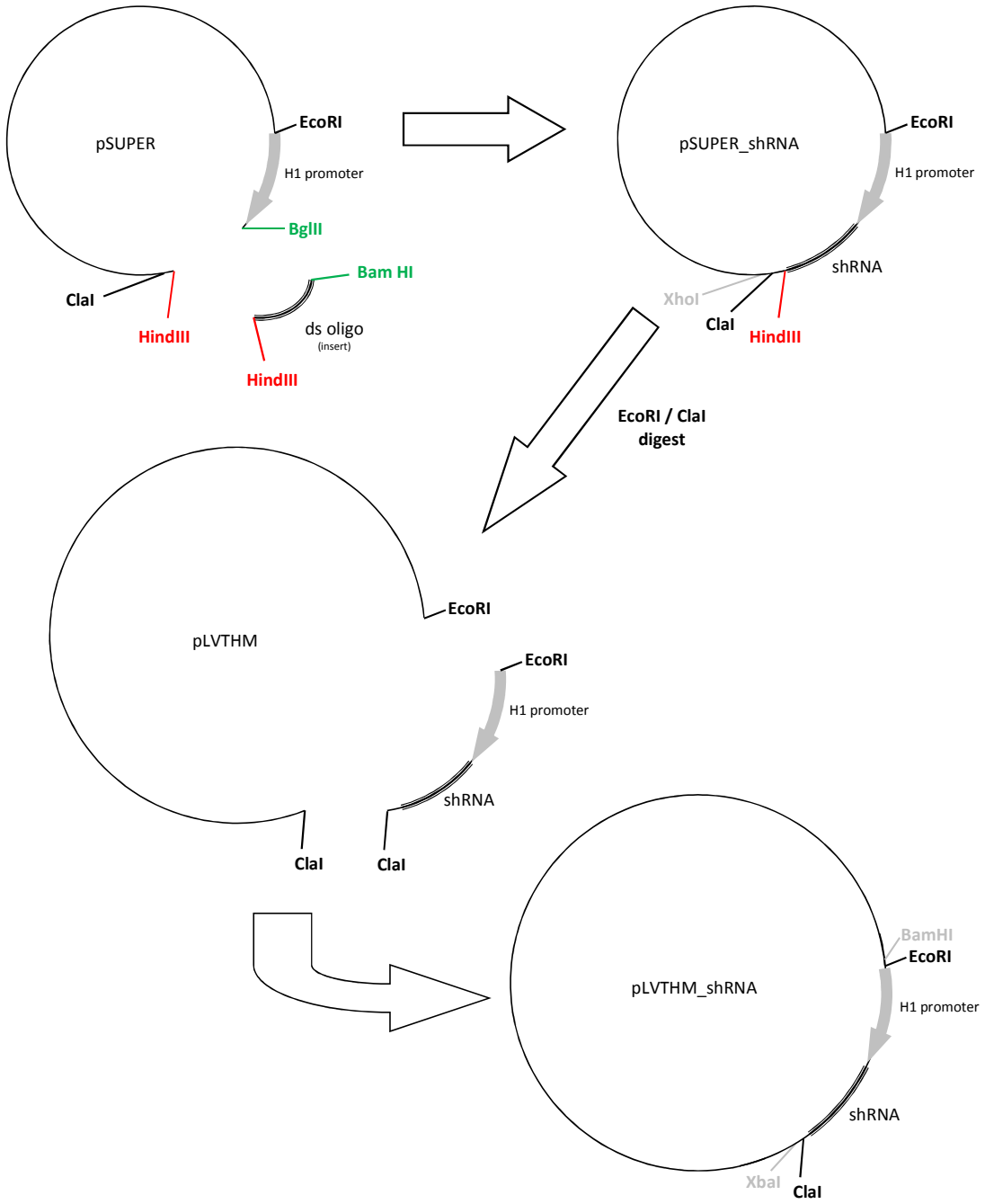

fig. 2-3. Schematic representation of the cloning strategy.
Restriction enzymes in grey were used for screen digest. Note that BglII and BamHI generate compatible protruding ends. However, their ligation gives rise to a sequence that is not recognised by any of the two enzymes. Therefore positive clones (pSUPER_shRNA) are BglII resistant. This was exploited for screening purposes. Positive clones identified this way were also confirmed by EcoRI/XhoI digest. pLVTHM_shRNA positive clones were identified by digestion with BamHI/XbaI. Finally, plasmids extracted from two different clones per pLVTHM-derived construct were sequenced, confirming that the constructs obtained were as designed (data not shown). During all the subcloning steps, bands were purified from from agarose gel using QIAquick Gel Extraction Kit, following the manufacturer's instructions.

2.12.2 Transduction of BEAS-2B cell lines

Overview

BEAS-2B cells were transduced with lentiviral particles containing the pLVTHM-derived vectors listed in table 2-14 following the workflow in fig. 2-4. Briefly, HEK293T cells are co-transfected with the two packaging plasmids, which are psPAX2 and pMD2.G, and the appropriate lentiviral vector or pLV-tTRKRAB-red (see also table 2-12 for more information about the plasmids). Lentiviral particles shed in the medium are collected and applied on target cells, in this case BEAS-2B cells. When the virus infects the latter cells, viral genomic RNA is first retro-transcribed and then it integrates into the cellular genomic DNA. This guarantees high efficiency of gene delivery (referred to as transduction) and high frequency of stable integration of the construct into cellular DNA. A few days later, successful transduction can be monitored by expression of the markers (fluorescent proteins) encoded in the lentiviral vectors.

Lentiviral genes, necessary for viral replication, are encoded only in the packaging plasmids. Co-transfecting a lentiviral vector and the packaging plasmids into HEK cells, makes those cells produce and shed in the medium lentiviral particles that contain RNA synthesised from the lentiviral vector (pLVTHM-derived or pLV-tTRKRAB-red). The latter are the only constructs that are delivered by mature virions. In fact, they are the only ones to encode the viral packaging site (the RNA sequence that is bound by viral capsid proteins ensuring correct virus assembly). This design guarantees bio-safety of the system used (2^{nd} generation). In fact it is very unlikely that mature virions will bear also the structural and functional genes necessary for viral replication, because all the elements necessary to successful viral assembly are spread across three different plasmids. Therefore, the lentiviral particles produced are infectious but replication-deficient.

Lentivirus transduction with TRONOSYSTEM plasmids

Superfect (Qiagen cat. No. 301305) was used to transfect HEK293T cells according to the following protocol.

Day 1: Plate $2x10^6$ cells (HEK293) in 10cm dish.

Day 2: Transfect the 3 plasmids required with SUPERFECT (Qiagen).

Protocol:

a) Use sterile FACS tubes for mixing SUPERFECT with the DNA

b) Add to 300µl of OptiMEM (or plain DMEM):

- 5µg pLVTHM (or pLV-tTRKRAB-Red)
- 3.75µg pPAX2
- 1.5µg pMD2G (VSV)

Mix by pipetting a few times

c) Add 60µl of SUPERFECT

Mix by pipetting a few times or by vortexing for 10sec

d) Incubate for 10 min at room temperature

e) Wash cells carefully with PBS

f) Add 3ml of complete growth medium (10%FBS DMEM) to DNA complexes

g) Put DNA complexes on cells (cells will be with only these 3ml)

h) Place in incubator

i) After 3-4 hours remove medium and replace with 6ml of growth medium (no need to wash cells)

Day 3: Check transfected cells. If possible check under fluorescence microscope for the expression of either GFP or DsRed2.

Seed target cells (to transduce). Plate them in order to have less than 50% confluency on next day (i.e. for BEAS-2B seed in 6-well plates 2.5ml per well at $6x10^4$ cells/ml).

Day 4: Transduce target cells.

Protocol:

a) Remove medium from target cells. Replace with 2ml of growth medium supplemented with about 8µg/ml Polybrene.

Put cells in incubator (and leave them for about 30 mintes).

b) Collect supernatant from HEKs and centrifuge it at 2000rpm (=800xg) for 15min. Carefully collect the supernatant, leaving pelletted material at the bottom. Replace HEK medium with 6ml of fresh growth medium

c) **OPTIONAL:** filter supernatant-containing medium (0.22um filters. Pre-wet the filter)

d) Remove medium from cells in 6-well plate

e) Add virus-containing medium supplemented with Polybrene at same concentration as above

f) Centrifuge plate at about 800xg for 90minutes at 37ºC
(this is referred to as "spinoculation").

g) Put plates in incubator for a few more hours

h) Replace medium of target cells with 3ml of growth medium (without washing with PBS)

Day 5: repeat procedure at day 4

Day 6: **OPTIONAL** repeat procedure as at day 5

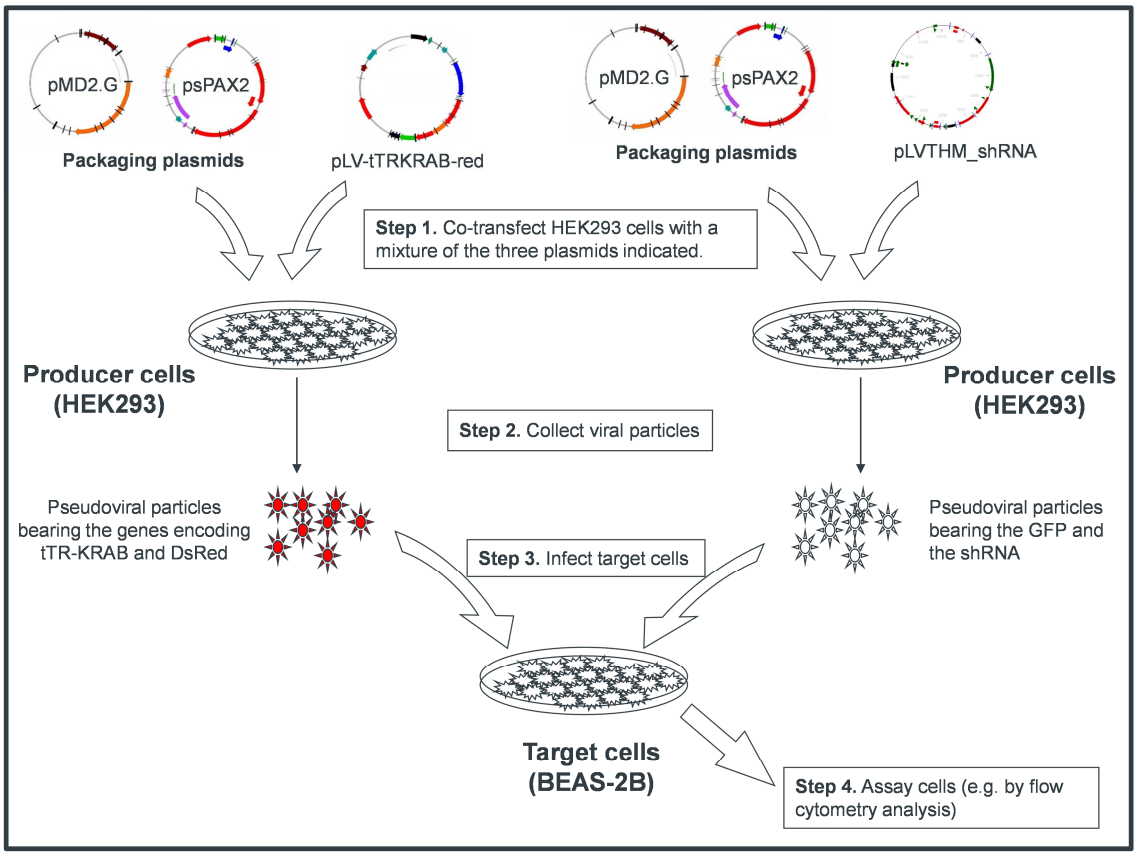

fig. 2-4. Transduction workflow.

2.12.3 Selection of transduced BEAS-2B cells.

In order to generate the cell lines BEAS-2B LV_neg, BEAS-2B LV_AGO2, BEAS-2B LV_DCR, BEAS-2B cells were first transduced with lentiviral particles containing the vector pLV-tTRKRAB-red. Cells transduced with this vector constitutively express tTR-KRAB, a tet-dependent transcriptional repressor that prevents expression of the transgenes from pLVTHM-derived plasmids. pLV-tTRKRAB-red also encodes the gene for DsRed2 a red fluorescent protein, useful for selection of transduced cells. Selection of all the transduced cell lines was achieved by cell sorting, performed on a BD FACSAria III cell sorter. DsRed2 positive BEAS-2B cells were sorted (data not shown) and grown. These cells were then transduced with one of the pLVTHM-derived plasmids, namely pLVTHM_neg or pLVTHM_AGO2 or pLVTHM_DCR (see table 2-13 and table 2-14). Because they had already been transduced with pLV-tTRKRAB, expression of both GFP and the shRNA was repressed in the absence of doxycycline (fig. 2-1). Therefore, double-transduced cells were grown in the presence of 50ng/ml of doxycycline for three days prior to selection of GFP-DsRed2 double positive cells (fig. 2-5). Sorted cells were kept in culture for one month in the absence of doxyxycline, in order for them to recover from induction before further characterization, and several vials of frozen stocks were made and stored in liquid nitrogen.

In order to generate the cell lines B2B-155 and B2B-C, BEAS-2B cells were transduced with only pLVTHM_BIC or pLVTHM_neg respectively (table 2-14). Transduced cells were then selected by sorting GFP-positive cells (data not shown) after which, several vials of frozen stocks were made and stored in liquid nitrogen. These cells were used within one month after thawing.

BEAS-2B wt

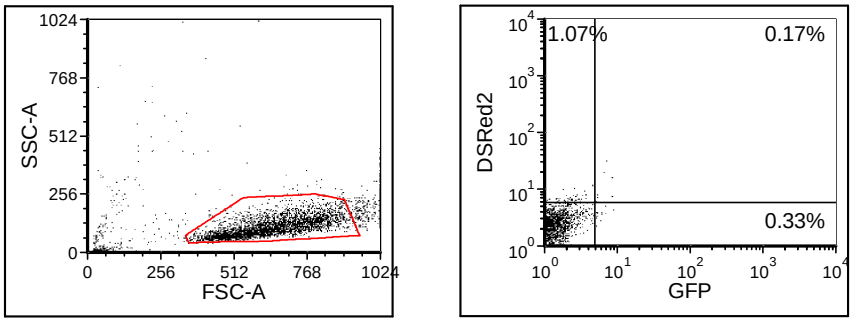

Set up: red + green

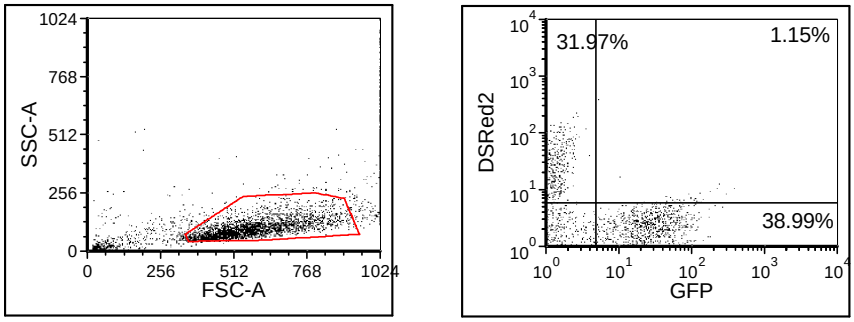

BEAS-2B LV_neg

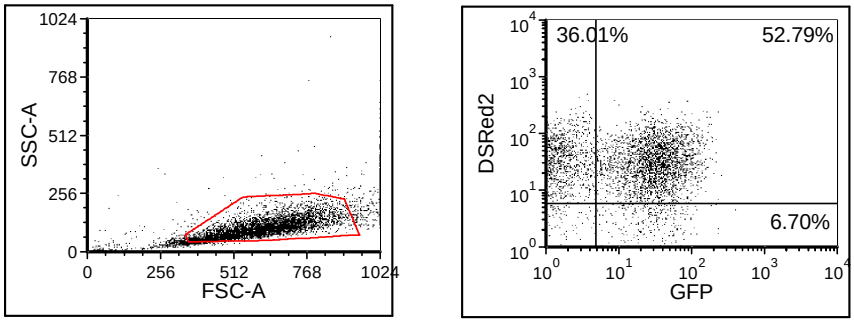

BEAS-2B LV_neg
post-sorting

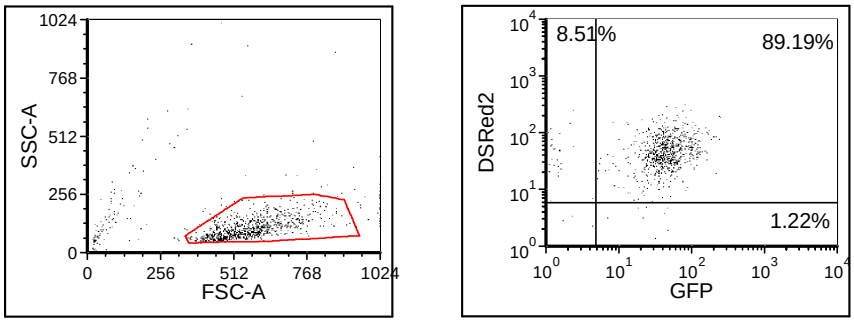

fig. 2-5
(Continues on next page)

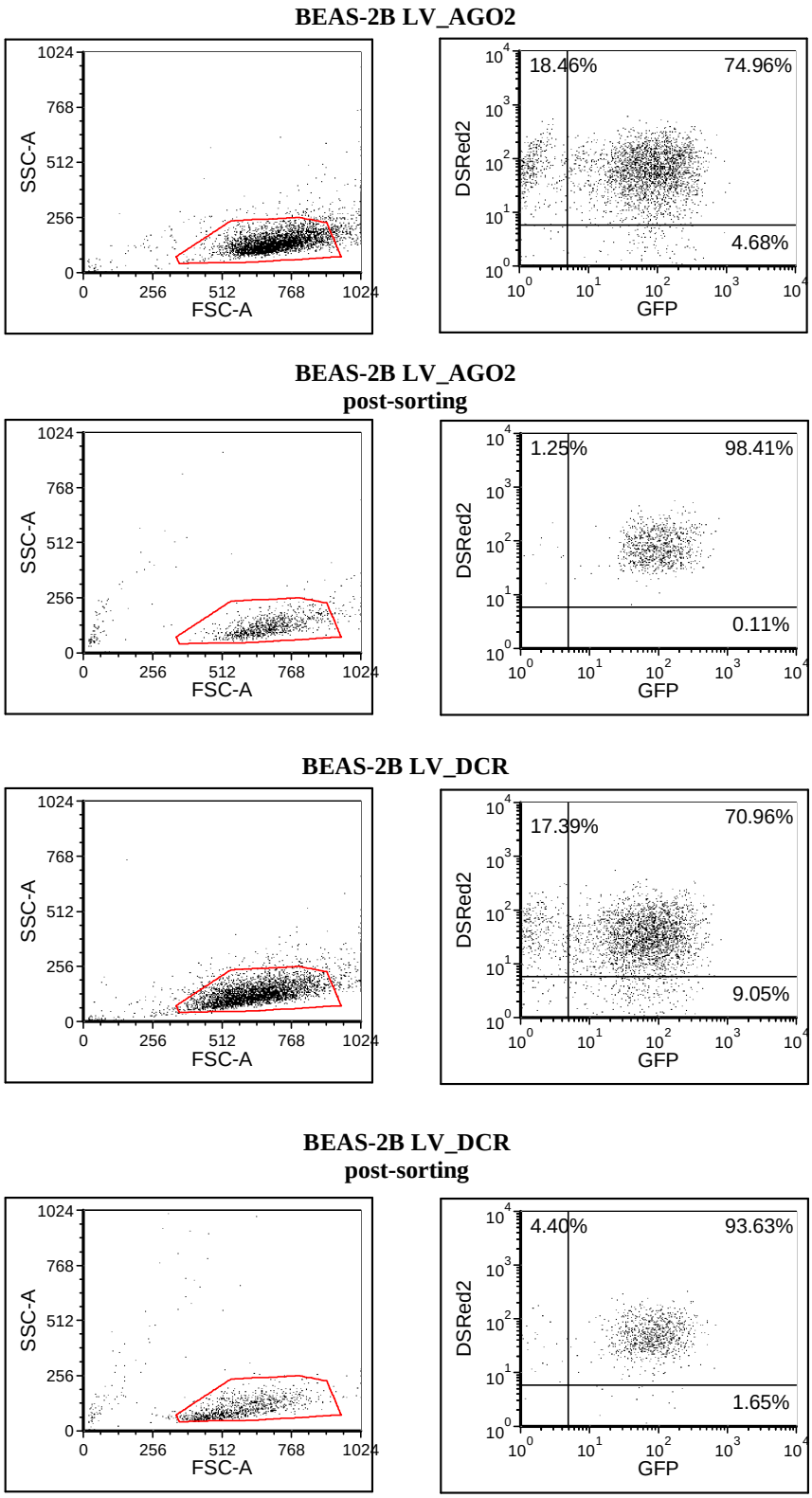

fig. 2-5. Selection of transduced BEAS-2B cells by FACS.
Double-positive cells were sorted. A part from the control cells (wt and mixed red+green cells) pre- and post-sorting plots are shown for each cell line sorted.

2.13 microRNA RT-qPCR arrays

In order to perform RT-qPCR microRNA arrays the Applied Biosystems TaqMan® Low Density Array system was used, following the manufacturer's instructions. Briefly, 400 ng of total cellular RNA extracted as described above, was used to generate cDNA using the Megaplex™ RT Human Pool A (see table 2-18 for recipes and programmes). The data were then analysed with Sequence Detection System v2.4 Enterprise Edition (Applied Biosystems). All the microRNAs that had a Ct value higher than 32.5 in at least 2 out of 4 samples were discarded. Therefore out of the 377 microRNAs detectable in each plate, 173 were kept for further analysis. Relative expression of all the microRNAs considered was calculated using the delta delta Ct method, using RNU44 as reference gene. All microRNAs were calibrated using the average ΔCt. Therefore the expression of a given microRNA was calculated using the formula $2^{-(\Delta CT \text{ individual miRNA} - \text{mean of 173 miRNAs})}$.

Megaplex RT recipe	
10x RT buffer	0.8 µl
25x dNTP (100mM tot)	0.2 µl
Megaplex RT primers	0.8 µl
Multiscribe	1.5 µl
RNAse inhib (Ambion) 20U/µl	0.1 µl
MgCl2 (25mM)	0.9 µl
RNA + water (350ng to 1µg)	3.2 µl
Total	**7.5 µl**

RT thermal cycling programme

	Temperature (°C)	Time
40 cycles	16	2 min
	42	1 min
	50	1 sec
	85	5 min
	4	Hold

qPCR array recipe	
Master mix (2x)	450 µl
Megaplex RT product (cDNA)	6 µl
Water	444 µl
Total	900 µl

qPCR array thermal cycling programme
Load and run the array using the 384-well TaqMan Low Density Array default thermal-cycling conditions. See the *TaqMan® Array User Bulletin* (PN 4371129)

table 2-18. Summary for Taqman microRNA arrays.
Adapted from the manufacturer user's guide.

2.14 Statistical analysis

All the experiments performed at least three times were analysed for statistical significance using the tools integrated in the software GraphPad Prism. The test used is indicated in the specific figure captions.

In general, the unpaired t-test was used when the sample number was lower than 10 (all the experiments with cell lines) and the comparison was between only two conditions. If the variance of the two groups was significantly different then the Welch's correction was applied. If multiple conditions were compared altogether, one-way ANOVA with Bonferroni post-test correction was used. When human primary cells were used and the sample number was higher

than 10, the distribution was assumed to be non-normal and therefore Mann-Whitney test was used.

2.15 Bioinformatic analysis

The prediction programme developed at the Segal lab (Kertesz et al. 2007) was used with default options. The executable version was used, called PITA executable, available at http://genie.weizmann.ac.il/pubs/mir07/32bit_exe_pita_prediction.tar.gz.

PITA was used in order to predict microRNAs binding to HRV genomes. All the microRNAs included in the database MiRBase v11 were used. The output files consist of a list of predicted target sites for each genome. In each list, all the target sites were ordered according to increasing values of ddG, and sites with a ddG value higher than "-9" were discarded. Therefore, only the microRNA names were kept, and the duplicates were removed. Finally, only those microRNAs that were present in all the lists so obtained were kept. These microRNAs are listed in table 3-1 and are referred to as candidate anti-HRV microRNAs, throughout the present thesis. They represent in fact the microRNAs predicted to effectively target all the viral genomes submitted for analysis, namely HRV-1B, 2, 3, 14, 16, 44, NAT001. The genome sequences used were downloaded from NCBI databases and the relative accession numbers are listed in table 2-19.

Also the predictions shown in table 4-1 were performed using the same programme. In this case, only the microRNAs selected from the arrays and plotted in fig. 4-1 B were used against the genomes of only HRV-1B and HRV-16. All target sites with ddG higher than -9 were discarded and only the common microRNAs are listed in table 4-1 C.

HRV serotype	Accession number	Immunological group	Genomic group
1B	D00239.1	minor	A
2	X02316.1	minor	A
3	EF173422.1	Major	B
14	K02121.1	Major	B
16	L24917.1	Major	A
44	DQ473499.1	minor	A
NAT001	EF077279.1	-	C

table 2-19. Details of HRV genomic sequences used for bioinformatics analyses.

Chapter 3

RESULTS: microRNAs target HRV-1B.

3.1 Establishing a cell model to study the role of microRNAs on HRV replication.

3.1.1 MicroRNAs are predicted to bind to HRV genomes.

MicroRNA activity has been widely studied in the context of post-transcriptional regulation of gene expression. Many algorithms have been developed aiming to predict whether a microRNA can target a given gene. Generally, these programs predict base-pairing between a microRNA and the 3' UTR of a given mRNA, calculating the stability of the possible duplexes. The latter stability is crucial for the efficacy of a microRNA, and the more stable the duplex the more likely is that the gene is regulated by the microRNA. In addition, these prediction algorithms take into account also the conservation of the target sequence across different vertebrates. This is done because it is conceivable that if the sequence involved had a regulatory role it would have undergone positive selection during evolution.

The prediction programme developed by Kertesz et al. was used in order to have a first proof of concept about whether microRNAs can target HRVs. This programme calculates not only the strength of the interaction between microRNA and target sequence but also the site accessibility (Kertesz et al. 2007) a very interesting feature for this investigation, considering that HRV genomes present complex secondary structures. In the output, the strength of the base-pairing between miR and target sequence is referred to as "**dGduplex**". The energy required to open the secondary structure of the target (the site accessibility) is instead referred to as "**dGopen**". Therefore, the sum of the two energies, the "**ddG**", represents the overall likelihood of the predicted interaction to happen. The lower the ddG, the more likely is that the microRNA successfully binds to the predicted target sequence. A ddG of -10 is considered typical of good miR-target interactions (Segal Lab).

MicroRNAs have been shown to bind viral genomes throughout the whole sequence, e.g. (Lecellier et al. 2005, Pedersen et al. 2007). Therefore, the entire genome of several HRV serotypes (1B, 2, 3, 14, 16, 44, NAT001) were submitted for analysis against all the microRNAs included in the database miRBase v11 (for an example of results obtained see table 3-2).

The results obtained suggest that many microRNAs may target HRVs. In order to refine this search, all the target sites with a ddG value higher than -9 were eliminated and only the microRNAs predicted to target all the HRVs analysed were kept (table 3-1). One of these candidate anti-HRV microRNAs is miR-155, a microRNA extensively studied in our group. In addition, also other bio-informatic programmes (table 6-1 and table 6-2 in appendix) predict that

miR-155 targets both HRV-1B and HRV-16, viruses that belong to the minor and major groups respectively and were available to be used for this investigation.

hsa-let-7b	hsa-miR-181d	hsa-miR-601
hsa-miR-103	hsa-miR-193a-5p	hsa-miR-602
hsa-miR-107	hsa-miR-197	hsa-miR-608
hsa-miR-1182	hsa-miR-198	hsa-miR-614
hsa-miR-1183	hsa-miR-296-3p	hsa-miR-615-5p
hsa-miR-1202	hsa-miR-297	hsa-miR-616
hsa-miR-1207-5p	hsa-miR-299-3p	hsa-miR-619
hsa-miR-122	hsa-miR-302a	hsa-miR-636
hsa-miR-1225-5p	hsa-miR-302d	hsa-miR-637
hsa-miR-1229	hsa-miR-323-5p	hsa-miR-638
hsa-miR-1231	hsa-miR-324-5p	hsa-miR-648
hsa-miR-1244	hsa-miR-331-5p	hsa-miR-654-5p
hsa-miR-1248	hsa-miR-339-5p	hsa-miR-658
hsa-miR-1254	hsa-miR-342-5p	hsa-miR-659
hsa-miR-1257	hsa-miR-34a	hsa-miR-661
hsa-miR-125a-3p	hsa-miR-383	hsa-miR-663
hsa-miR-1275	hsa-miR-431	hsa-miR-671-5p
hsa-miR-1291	hsa-miR-432	hsa-miR-744
hsa-miR-1292	hsa-miR-453	hsa-miR-760
hsa-miR-1293	hsa-miR-491-5p	hsa-miR-767-5p
hsa-miR-1295	hsa-miR-502-5p	hsa-miR-769-3p
hsa-miR-1296	hsa-miR-509-3p	hsa-miR-770-5p
hsa-miR-1308	hsa-miR-512-3p	hsa-miR-886-3p
hsa-miR-134	hsa-miR-516b	hsa-miR-886-5p
hsa-miR-138	hsa-miR-541	hsa-miR-939
hsa-miR-149	hsa-miR-574-5p	
hsa-miR-155	hsa-miR-584	

table 3-1. Preliminary prediction of HRV-targeting microRNAs.
Description of the method used in paragraph 2.15.
HRV-16 (A)/ 1B (A)/ 2 (A)/ 14 (B)/ 3(B)/ 44 (A)/ NAT001 (C)

virus	microRNA	Start	End	dGduplex	dGopen	ddG
HRV-1B	hsa-miR-1182	773	765	-26.40	-3.29	-23.10
HRV-1B	hsa-miR-1293	4574	4568	-23.60	-1.88	-21.71
HRV-1B	hsa-miR-1183	4597	4589	-27.20	-5.54	-21.65
HRV-1B	hsa-miR-886-5p	455	447	-28.20	-6.99	-21.20
HRV-1B	hsa-miR-939	4572	4564	-22.80	-2.00	-20.79
HRV-1B	hsa-miR-658	4896	4890	-27.41	-6.65	-20.75
HRV-1B	hsa-miR-939	97	91	-23.50	-4.14	-19.35
HRV-1B	hsa-miR-661	776	768	-22.76	-3.45	-19.30
HRV-1B	hsa-miR-608	40	32	-33.60	-14.36	-19.23
HRV-1B	hsa-miR-296-3p	102	94	-20.30	-1.30	-18.99
HRV-1B	hsa-miR-1287	793	785	-22.70	-4.45	-18.24
HRV-1B	hsa-miR-885-3p	4900	4892	-23.80	-5.63	-18.16
HRV-1B	hsa-miR-574-5p	2022	2014	-20.63	-2.62	-18.00
HRV-1B	hsa-miR-296-3p	103	95	-18.70	-0.87	-17.82
HRV-1B	hsa-miR-1287	5296	5288	-22.16	-4.57	-17.58
HRV-1B	hsa-miR-744	4572	4564	-19.53	-2.00	-17.52
HRV-1B	hsa-miR-663	4897	4889	-23.63	-6.17	-17.45
HRV-1B	hsa-miR-323-5p	4282	4274	-27.02	-9.59	-17.42
HRV-1B	hsa-miR-525-3p	249	241	-25.32	-8.42	-16.89
HRV-1B	hsa-miR-1207-5p	96	88	-20.95	-4.07	-16.87
HRV-1B	hsa-miR-1244	2048	2040	-25.00	-8.20	-16.79
HRV-1B	hsa-miR-654-5p	4577	4571	-18.55	-1.89	-16.65
HRV-1B	hsa-miR-1207-5p	4504	4498	-26.30	-9.66	-16.63
HRV-1B	hsa-miR-1231	5863	5855	-22.76	-6.12	-16.63
HRV-1B	hsa-miR-608	2028	2020	-22.10	-5.55	-16.54
HRV-1B	hsa-miR-219-1-3p	669	661	-23.31	-6.89	-16.41
HRV-1B	hsa-miR-550	2833	2825	-24.45	-8.13	-16.31
HRV-1B	hsa-miR-1301	5840	5832	-26.60	-10.53	-16.06
HRV-1B	hsa-miR-574-5p	5712	5704	-20.90	-4.87	-16.02
HRV-1B	hsa-miR-658	93	85	-20.30	-4.45	-15.84
HRV-1B	hsa-miR-618	6569	6561	-24.50	-8.66	-15.83
HRV-1B	hsa-miR-1270	4586	4578	-21.30	-5.58	-15.71
HRV-1B	hsa-miR-181b	7082	7074	-20.71	-5.00	-15.70
HRV-1B	hsa-miR-103	3949	3941	-22.79	-7.27	-15.51
HRV-1B	hsa-miR-221	5524	5517	-21.82	-6.36	-15.45
HRV-1B	hsa-miR-383	3795	3787	-20.63	-5.23	-15.39
HRV-1B	hsa-miR-107	1456	1448	-21.90	-6.69	-15.20
HRV-1B	hsa-miR-296-3p	4909	4901	-21.50	-6.34	-15.15
HRV-1B	hsa-miR-1292	2872	2864	-23.60	-8.52	-15.07

table 3-2. Example of prediction results obtained from the programme developed by Kertesz et al.

Start and end refer to the positions on the viral RNA that base-pair with the microRNA seed. These results were obtained submitting the whole genome sequence of HRV-1B to be scanned against all the microRNAs included in the database MiRBase v11 (see paragraph 2.15 for more details).

3.1.2 HRV-1B replication in HeLa cells and THP1-derived macrophages (THP1MΦ).

We have hypothesised that microRNAs can hamper HRV replication by directly binding to the viral genome. Conceivably, anti-HRV microRNAs would limit synthesis of viral proteins and in turn limit the amount of new genomic RNA produced.

In order to investigate whether microRNAs can affect HRV replication, it seemed convenient to have two cell lines to be used as cell models. Ideally, one cell line had to be very permissive to the virus and poor in antiviral microRNAs, while the other cell line had to be less permissive to the virus and be rich in antiviral microRNAs. HeLa cells were chosen as the permissive cell model; while THP-1 derived macrophages (THP1MΦ) were chosen as the less permissive one. HeLa cells have been used for long time to detect HRV and grow viral preparations, implying the virus replicates very efficiently in these cells. On the contrary, macrophages have been shown to be infected by HRV but not allow its replication (Laza-Stanca et al. 2006). The two cell models also satisfy the second condition, to express different levels of antiviral microRNAs. This was known for at least one of the candidate anti-HRV microRNAs identified, miR-155. In fact, from previous experience in our group, it was known that THP-1 cells express about 10000 fold more miR-155 compared to HeLa cells (see fig. 3-1). For these reasons it was expected that HRV-1B replicated much more in HeLa cells than in THP1MΦ.

Cells were infected with HRV-1B at MOI of either 0.01 or 0.1, and samples were collected up to 10 hours post-infection (hours pi) for HeLa cells, and up to 24 hours pi for THP1MΦ. The aim was in fact to monitor the first round of viral replication, which should occur in about 8-10 hours. In the case of THP1MΦ however, samples were collected up to 24 hours pi, in order to cover the possibility that the viral life cycle was longer in those cells. Supernatants were collected and cells were harvested in Tri-Reagent for RNA extraction. Supernatants were stored at -80°C, and then used to determine the infecting viral titre by limiting dilution assays (TCID50), while the RNA was used to quantify HRV-1B genomic RNA by RT-qPCR. The results obtained confirmed that both cell lines were infected by the virus, since its RNA was consistently detected throughout the time course.

In both HeLa cells and THP1MΦ, the amount of viral RNA detected at 0 hours pi reflected the viral load used for infection. Indeed, about 10 times more viral RNA was detected when an MOI of 0.1 was used, as compared to an MOI of 0.01. During the following hours, HRV-1B RNA decreased gradually from 0 to 3 hours pi in both HeLa cells and THP1MΦ. However, while in HeLa cells it then increased markedly after 3 hours pi, in THP1MΦ HRV-1B RNA never reached a comparable fold increase or a level significantly higher than at 0 hours pi (fig. 3-2).

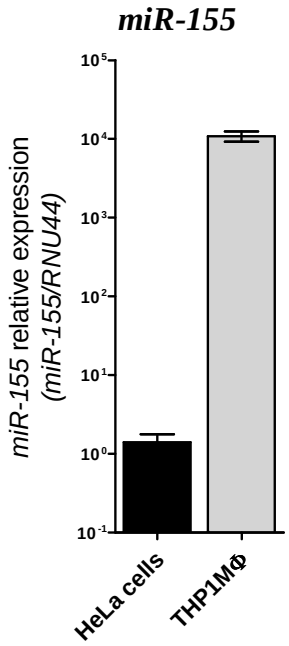

fig. 3-1. THP1MΦ express several fold more miR-155 compared to HeLa cells.
MiR-155 expression was measured from the indicated cell lines by RT-qPCR. The same amount of RNA was used for each cell line. MiR-155 relative expression was calculated using RNU44 as reference gene. The values plotted represent the average, the error bars represent the SD obtained from at least 3 biological replicates.

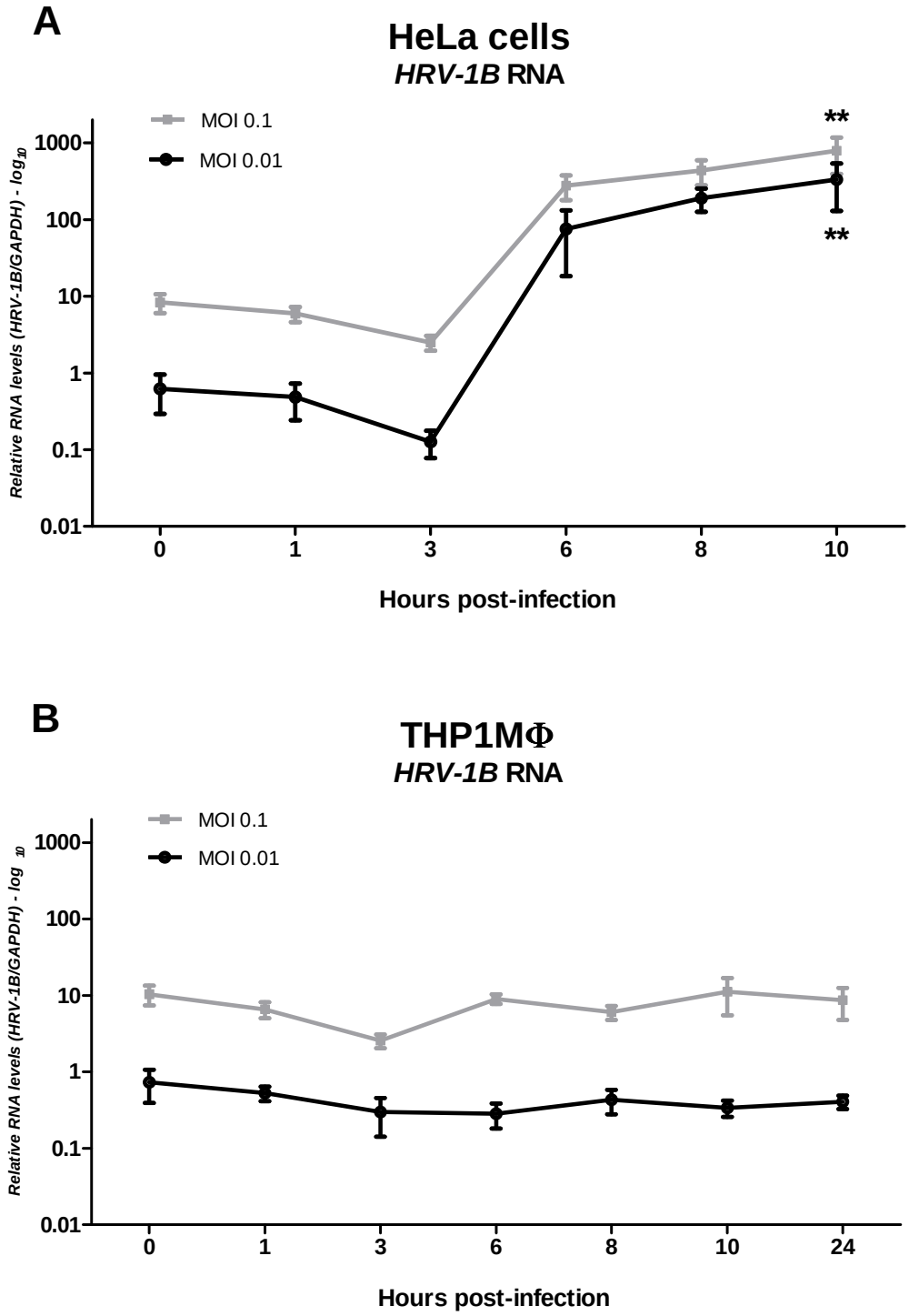

fig. 3-2. HRV-1B replication in HeLa and THP1MΦ.
HeLa (**A**) and THP1MΦ (**B**) were infected with HRV-1B at an MOI of 0.1 or 0.01, and viral RNA was measured by RT-qPCR at the time points indicated. The values plotted represent the average, the error bars represent the SD obtained from 3 independent experiments. **=p<0.01; if nothing is indicated, difference was not significant as compared to 0 hours post-infection of the same MOI. p values were calculated using one way ANOVA with Bonferroni post-test correction.

Viral titre in the supernatants was then determined by TCID50 (fig. 3-3), showing that the amount of virus shed by THP1MΦ infected with an MOI of 0.01 was always below the detection limit of the technique. Viral titre was in fact measurable only in supernatants from THP1MΦ infected with MOI 0.1, collected at 10 and 24 hours pi, with an estimated viral titre of about 100 viral particles/ml.

Regarding HeLa cells, when MOI of 0.01 was used, viral titre was below the detection limit until 3 hours pi, after which it increased and remained constant, at around 100 viral particles/ml, between 6 and 10 hours pi. With MOI of 0.1 instead, the starting titre was higher but decreased gradually up to 3 hours pi and then it increased progressively, reaching the maximum (around 500 viral particles/ml) at the end of the time course, 10 hours pi.

These results confirmed that the two cell lines showed what was expected regarding their permissiveness to HRV-1B. The latter replicated indeed much more in HeLa cells compared to THP1MΦ. These results also show that RT-qPCR can be used to accurately detect viral RNA and monitor how the virus replicates during the very first hours after infection. Limiting dilution titration (TCID50) instead was found to be less sensitive and overall unnecessary within the first round of infection (up to 10 hours). For these reasons, RT-qPCR was the method of choice for this investigation.

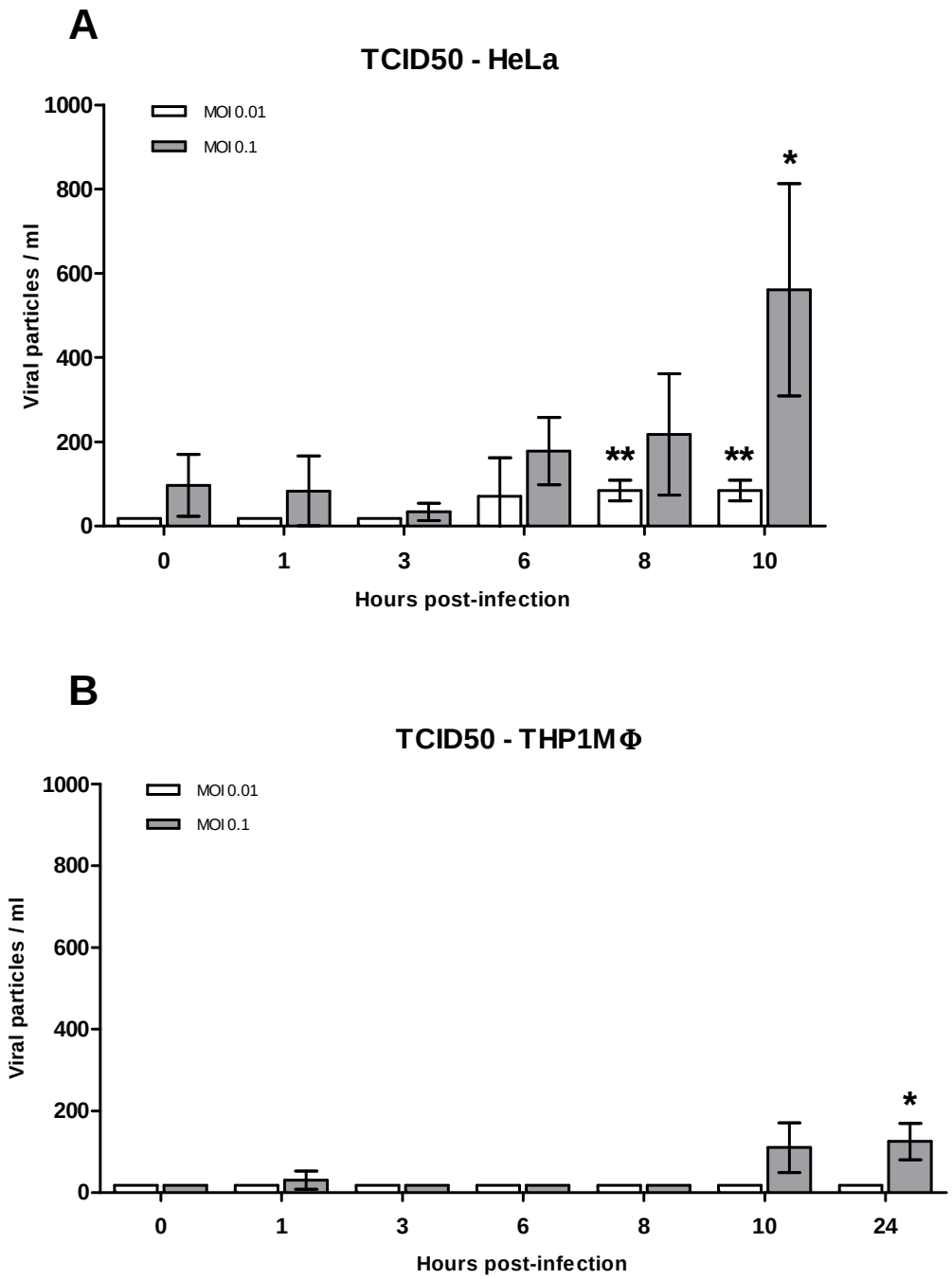

fig. 3-3. HRV-1B replication in HeLa and THP1MΦ.

HeLa (**A**) and THP1MΦ (**B**) were infected with HRV-1B at an MOI of 0.1 or 0.01, and viral titre in the supernatants at the time points indicated, was estimated by limiting dilution (TCID50).

The values plotted represent the average, the error bars represent the SD obtained from 3 independent experiments. *=$p<0.05$; **=$p<0.01$; if nothing is indicated, difference was not significant as compared to 0 hours post-infection of the same MOI. p values were calculated using one way ANOVA with Bonferroni post-test correction.

3.1.3 *DICER* knock-down in THP1MΦ.

As shown in the previous paragraph, HRV-1B replicates more in HeLa cells than in THP1MΦ. We hypothesised that THP1MΦ are less permissive to the virus because they express higher levels of anti-HRV microRNAs compared to HeLa cells, such as miR-155. If this is true, lowering the load of microRNAs expressed in THP1MΦ would allow higher replication of HRV-1B. Therefore, in order to assess this possibility, it was decided to knock-down *DICER1* (hereafter *DICER*) in THP1MΦ, employing siRNA technology. Indeed, Dicer is central in microRNA biogenesis, being responsible for their final maturation (Filipowicz et al. 2008). It was expected that reducing its expression would reduce the levels of mature microRNAs (Kuehbacher et al. 2007, Matskevich & Moelling 2007, Otsuka et al. 2007, Suarez et al. 2007, Tang et al. 2007, Triboulet et al. 2007) and in turn the virus would replicate more.

THP-1 cells were transfected with either a negative control siRNA or an anti-*DICER* siRNA and then differentiated in macrophages. 48 hours post-transfection, cells were infected with HRV-1B at an MOI of 0.1. *DICER* mRNA was measured at 0 hours pi confirming that its expression was reduced by the targeting siRNA to about 25% compared to negative control (fig. 3-4 B). Viral genomic RNA was measured by RT-qPCR at 0, 3, 6 and 24 hours pi (fig. 3-4 A) showing that lower amounts of *DICER* mRNA did not correlate with changes in viral replication. However, it was also noticed that despite the reduction in *DICER* expression, two microRNAs, miR-155 and miR-142 arbitrarily chosen in order to have a general idea about the microRNA biogenesis on the whole, did not show a significant reduction (fig. 3-4 C and fig. 3-4 D).

Hence, it was concluded that the lack of a clear reduction in the expression of cellular microRNAs invalidated this approach.

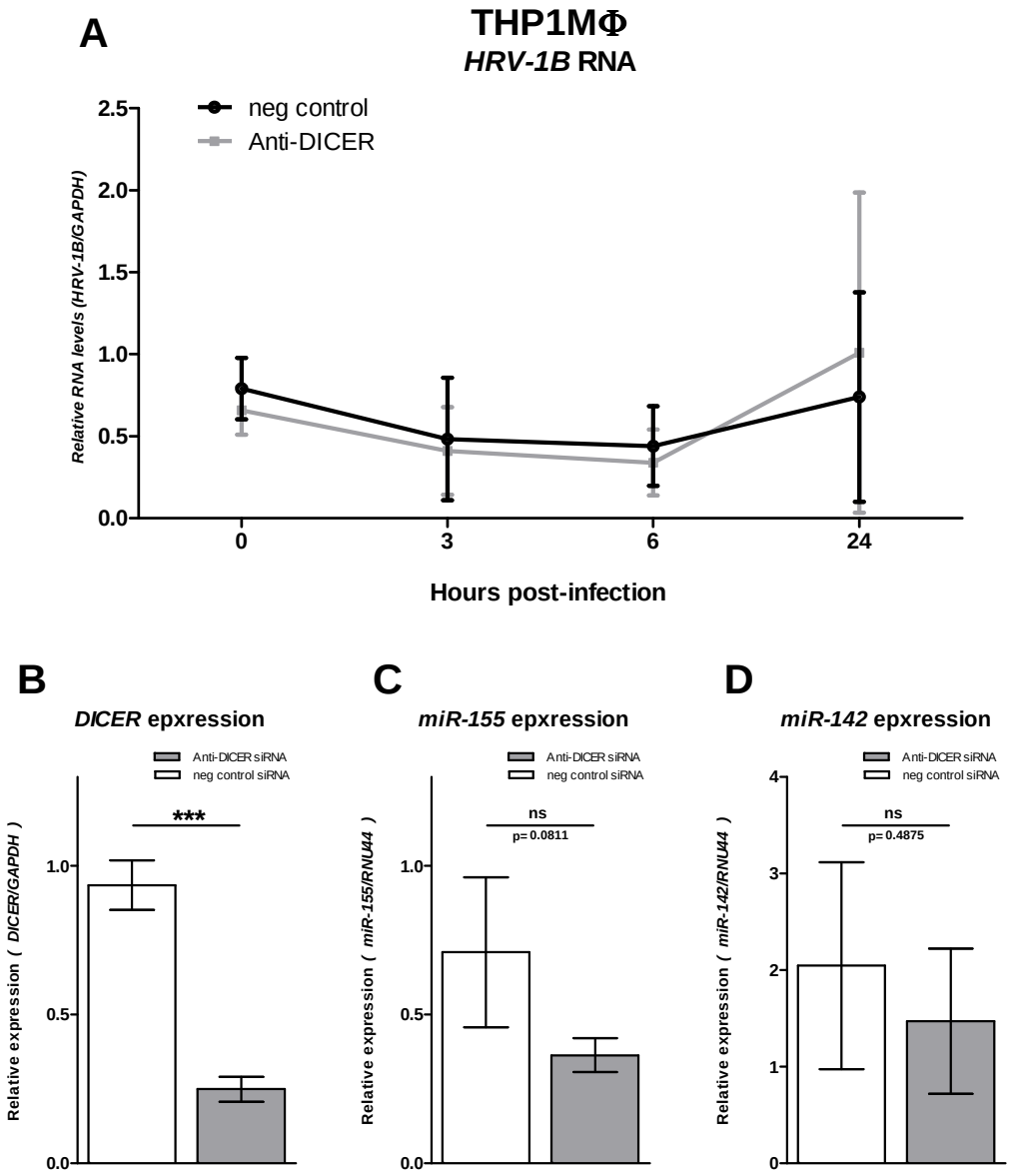

fig. 3-4. Knock-down of DICER did not correlate with higher replication of HRV-1B in THP1MΦ.

THP1MΦ obtained from THP-1 cells transfected with anti-DICER siRNA were infected with HRV-1B at an MOI of 0.1. (**A**) Viral RNA was then measured by RT-qPCR at the time points indicated. The levels of (**B**) DICER mRNA, (**C**) miR-155 and (**D**) miR-142 were measured by RT-qPCR at 0 hours post-infection. The results plotted are the average, while the error bars represent the SD from three independent experiments. ***=p<0.001; where either ns or nothing is indicated difference was not significant. p values were calculated using the unpaired t-test.

3.1.4 Prolonged DICER knock-down increases HRV-1B replication in BEAS-2B cells.

Speculations can be made about why *DICER* knock-down caused only a marginal reduction of mature microRNAs in THP1MΦ. One possibility is that mature microRNAs have a longer half life than expected. This would mean that a longer time with reduced production (lower Dicer activity) is needed in order to actually affect their levels. Also, it is conceivable that the abundance of a microRNA may affect the relative reduction of its concentration, attainable by the strategy used here. Therefore, in order to tackle these difficulties, it was decided to use human bronchial epithelial cells (BECs). THP-1 cells are very rich in miR-155 (see fig. 3-6) not only compared to HeLa cells but also compared to human bronchial epithelial cells (BECs). As a consequence, it seemed more likely to obtain a better reduction of antiviral-microRNAs by a prolonged reduction of Dicer activity in BECs, rather than THP1MΦ.
In addition, as explained in the introduction, HRV infection of BECs constitutes the main interest for the present project.

In order to keep the levels of *DICER* mRNA low for a prolonged period, anti-*DICER* siRNA was transfected several consecutive times. This was first attempted on primary BECs. However, those cells became senescent and died soon after the second round of transfection (fig. 3-5).

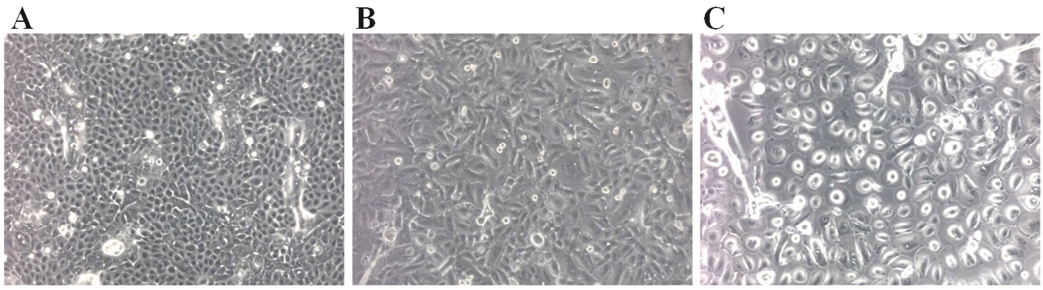

fig. 3-5. Primary BECs do not withstand multiple transfections.
Primary BECs from one healthy donor were grown until confluence (**A**) or transfected once (**B**) or twice (**C**) with negative control siRNA. Pictures were taken two days after transfection.

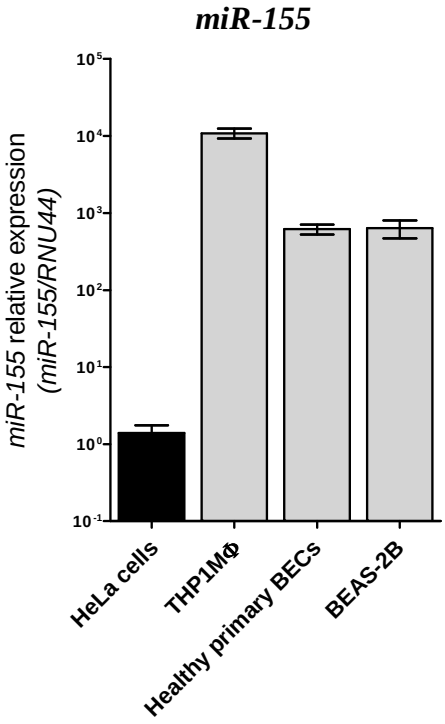

fig. 3-6. Bronchial epithelial cells express less miR-155 compared to THP1MΦ.
MiR-155 expression was measured from the indicated cell lines and primary BECs by RT-qPCR. The same amount of RNA was used for each cell line. MiR-155 relative expression was calculated using RNU44 as reference gene and HeLa cells as calibrator. The values plotted represent the average, the error bars represent the SD obtained from at least 3 biological replicates (three different healthy donors for primary BECs).

Therefore, the next best option was to use BEAS-2B cells, a virally immortalized cell line derived from healthy human BECs (Reddel et al. 1988) that has often been employed as a convenient model for HRV infection of BECs, e.g. (Papadopoulos et al. 2001).

Negative control or anti-*DICER* siRNA were successfully transfected for three consecutive times in BEAS-2B cells (see paragraph 2.8.2 for more details). RNA was purified from those cells at 48 hours after each transfection and expression of *miR-30a-5p* and *DICER* was measured by RT-qPCR (fig. 3-7). *DICER* expression was reduced to around 40-30% compared to negative control, after each of the three transfections performed. The expression of *miR-30a-5p* instead, was reduced only marginally (to 60%) by two rounds of transfection, and it dropped to 40% only after the third round, as compared to negative control. This result reinforced the idea that microRNAs may indeed have a longer half-life than expected, and encouraged further experiments.

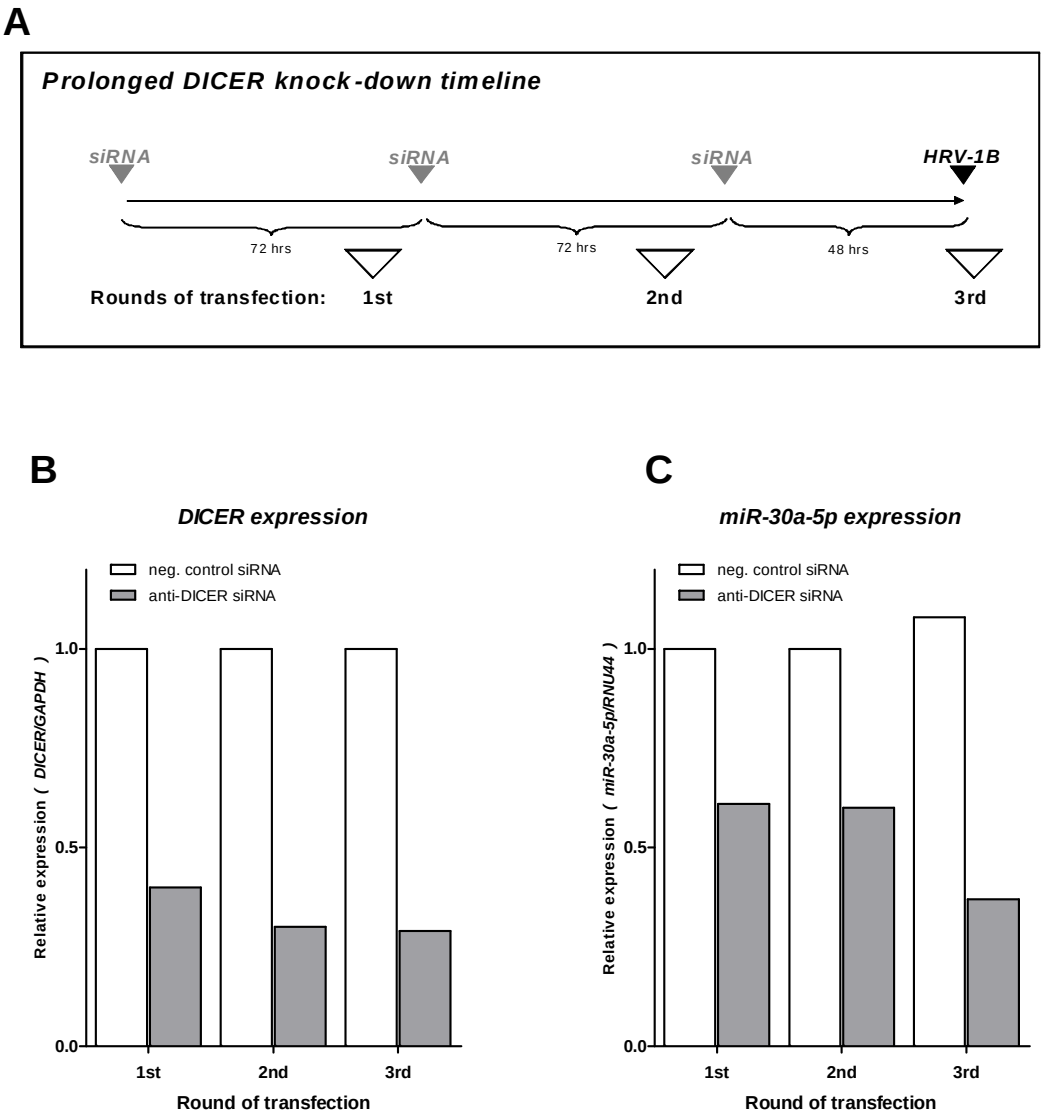

fig. 3-7. Sustained knock-down of DICER is necessary in order to effectively lower the levels of mature microRNAs.

A: global timeline of the experiment. Briefly, cells were transfected every three days (for three times in total) before infection with HRV-1B (see fig. 3-9). Cells were always about 50% confluent at the time of transfection. In order to achieve this, cells were detached and seeded at the correct density every two days. Cells were collected two days after each transfection (more details in materials and methods).

(**B**) DICER and (**C**) miR-30a-5p expression were quantified by RT-qPCR. Each value plotted represents the average of qPCR duplicates obtained from one single experiment, used to explore the feasibility of the repeated siRNA transfection.

BEAS-2B cells were transfected for three rounds, as earlier described. 48 hours after the third transfection, the cells were infected with HRV-1B. Three different MOIs of HRV-1B were used in order to test whether different viral loads may affect the outcome. As expected, regardless of the MOI used, HRV-1B replicated more when *DICER* had been knocked down (fig. 3-8).

Finally, in order to confirm the reproducibility of this finding, the latter experiment was repeated three times using only one MOI (fig. 3-9). BEAS-2B cells were transfected for three rounds. 48 hours after the third transfection, they were infected or not with HRV-1B, at an MOI of 0.01. RNA was purified from both uninfected cells and the infected ones harvested at 0, 3 and 8 hours post-infection. Measuring the expression of *DICER* and *miR-30a-5p* in the uninfected cells (fig. 3-9 A and B) confirmed that their knock-down was similar to what was obtained in the preliminary experiment shown in fig. 3-7. HRV-1B RNA was measured by RT-qPCR in the infected cells, in order to monitor viral replication. As shown in fig. 3-9 C, on average, 1.6 times more HRV-1B RNA was present 8 hours post-infection in cells with lower *DICER* expression. This difference was statistically significant.

These results show that lower expression of mature microRNAs results in an increase of HRV-1B replication in BEAS-2B cells. However, this may still be due to an indirect mechanism, not to the direct interaction of microRNAs with viral genome. As a matter of fact, microRNAs may affect viral replication by affecting the cellular anti-viral response, such as induction of IFNs. Expression of *IFNB1* (the gene for IFN-β) was measured by RT-qPCR (fig. 3-9 D). The results show that the antiviral gene was induced by viral replication and its expression was very similar at each time point considered, regardless of which siRNA had been used.

In conclusion, *DICER* knock-down in BEAS-2B cells does not favour HRV-1B replication by impairing pathways leading to IFN-β induction.

The possibility that microRNAs bind directly the viral RNA, constitute the subject of following paragraphs.

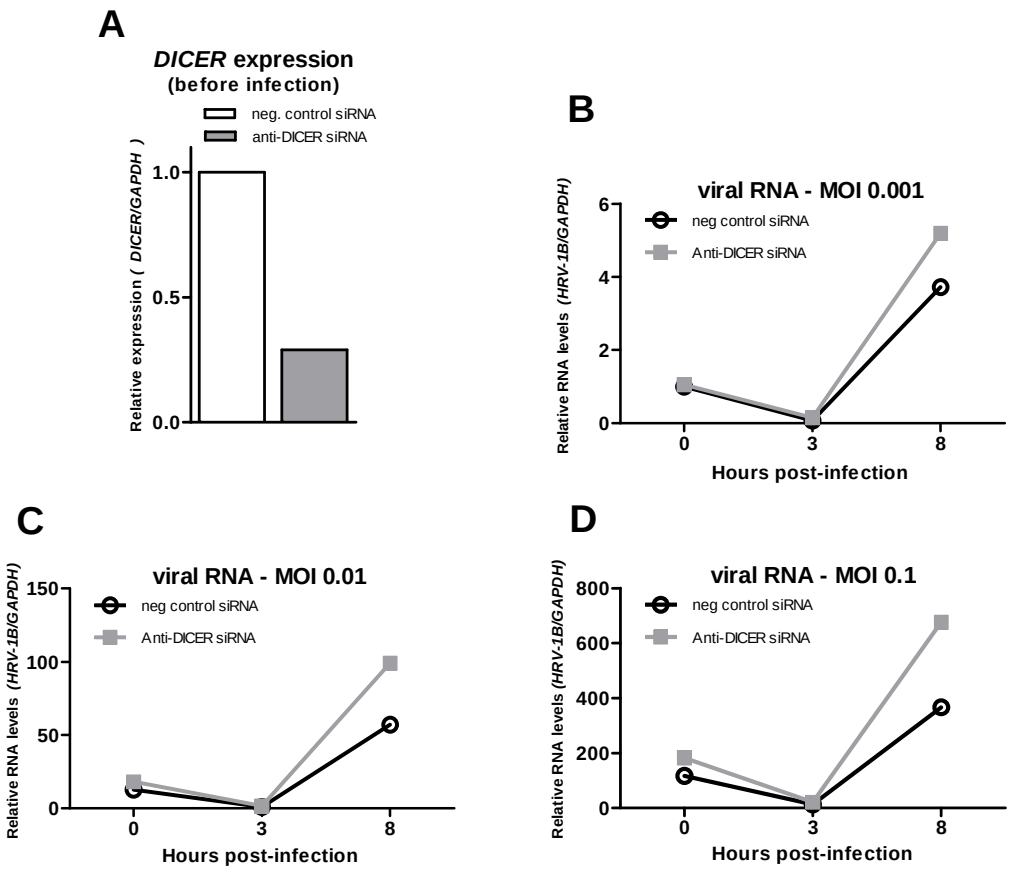

fig. 3-8. Sustained knock-down of DICER allows higher replication of HRV-1B (preliminary experiment).

BEAS-2B cells were treated as summarised in fig. 3-7 A. Cells were transfected for three rounds with either a negative control siRNA or anti-DICER siRNA. 48 hours after the third round of transfection, cells were infected with the indicated MOI of HRV-1B. (**A**) DICER expression was quantified before infection by RT-qPCR. HRV-1B RNA was measured by RT-qPCR 0, 3 and 8 hpi (**B-D**). The values plotted represent the average of qPCR duplicates from one experiment. The relative level of viral RNA were all normalised to the amount detected at 0hpi of MOI 0.001.

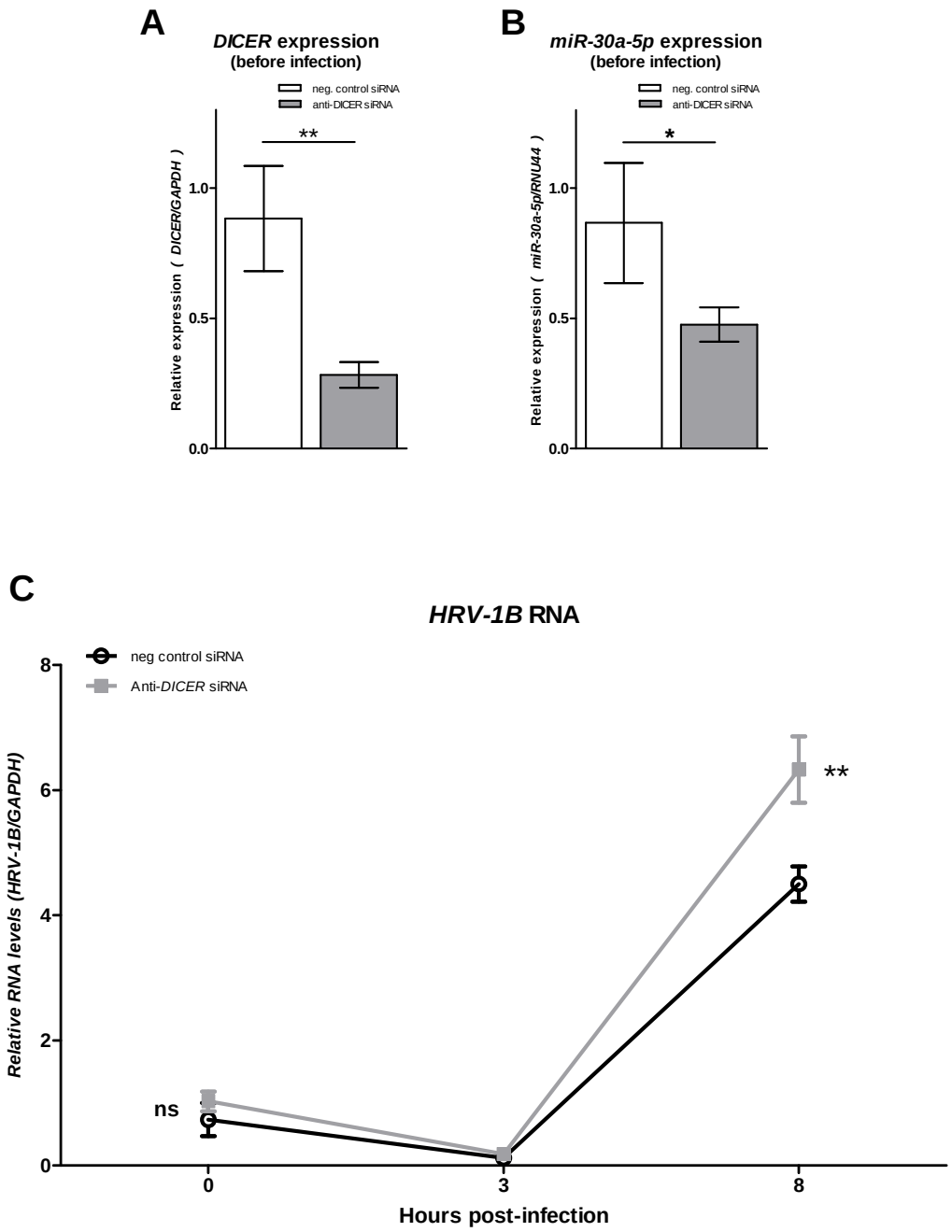

(Figure continues on next page)

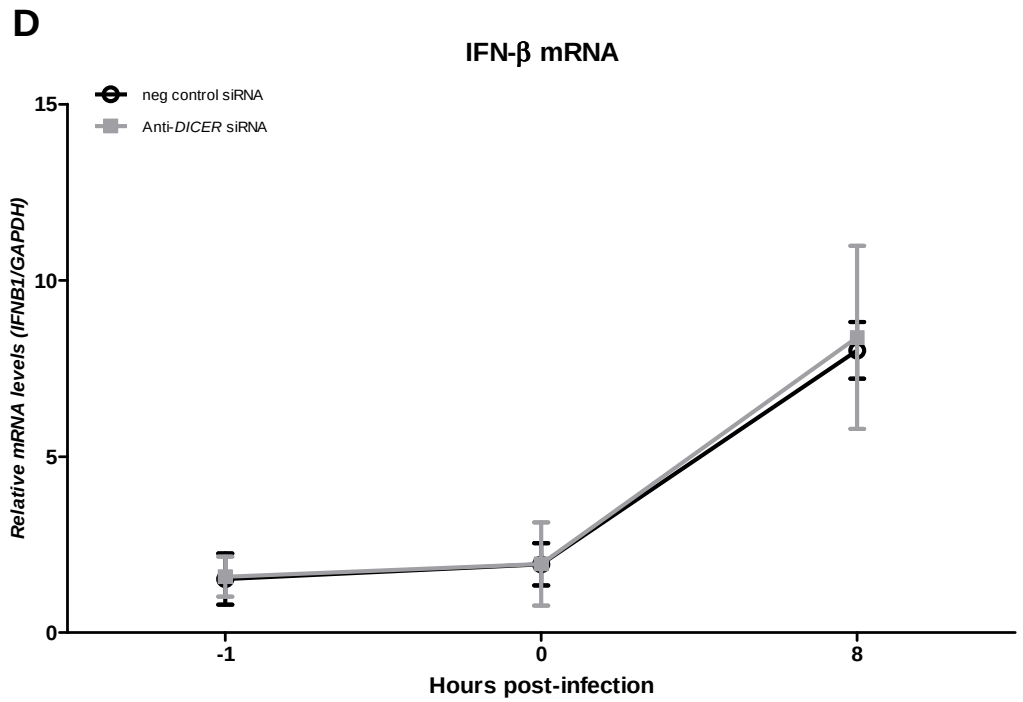

fig. 3-9. Sustained knock-down of DICER allows higher replication of HRV-1B (n=3).

BEAS-2B cells were treated as summarised in fig. 3-7 A. Cells were transfected for three rounds and then infected with HRV-1B at MOI 0.01.

Cells collected just before infection were used to measure (**A**) DICER and (**B**) miR-30a-5p expression by RT-qPCR. HRV-1B RNA (**C**) and IFNB1 expression (**D**) in infected cells were measured by RT-qPCR at the indicated time points. In D the time point "-1" refers to uninfected cells, collected just before infection (same samples as in A and B). The values plotted are the arithmetic mean while the error bars represent SD of three independent experiments. *=$p<0.05$; **=$p<0.01$; if nothing is indicated or ns=difference was not significant compared to cells transfected with negative control siRNA at the same time point. p values were calculated using the unpaired t-test.

3.2 MicroRNAs directly bind to HRV-1B RNA.

3.2.1 Ago2 co-immunoprecipitation (Ago2 co-IP)

3.2.1.1 Rationale

Mature microRNAs exert their effect as part of a ribonucleoprotein (RNP) complex referred to as miRISC, of which Ago proteins are indispensable components (Pillai et al. 2004). Therefore, it is possible to isolate the mRNAs that microRNAs target in a cell, by specifically purifying Ago proteins, a technique called co-immunoprecipitation (see fig. 3-10).

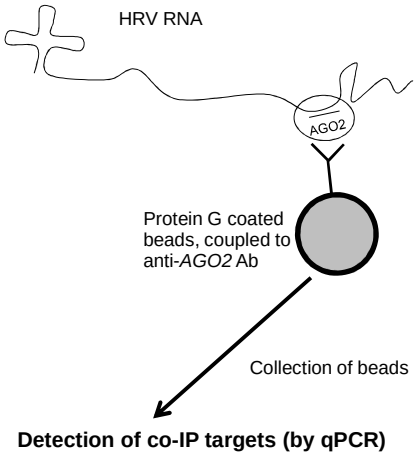

fig. 3-10. Schematic representation of the rationale behind Ago2 co-IP experiments.
Note that target mRNAs are bound to Ago2 protein through their interaction with microRNAs.

3.2.1.2 Optimization

Ago2 co-immunoprecipitations (Ago2 co-IP) had never been performed before in our laboratory. Therefore, it was necessary to optimise the protocol, starting from the procedures described previously (Chi et al. 2009, Keene et al. 2006, Peritz et al. 2006). This optimisation is summarised in the following figures (from fig. 3-11 to fig. 3-14) and it consisted in testing different lysis buffers, washing conditions and antibody concentrations.

The optimal conditions that have been finally chosen, the composition of all the buffers used and the detailed protocol can be found in paragraph 2.10. All the cellular mRNAs detected

in these experiments had already been shown to be directly regulated by microRNAs, and were exploited for this reason as convenient positive controls.

3.2.1.3 THP1MΦ

At first, different combinations of lysis and washing buffers were compared to use with THP-1 cells, while $2x10^6$ cells/IP were always used for Ago2 co-IP experiments. The best combination was chosen by quantifying the amount of *PU.1* mRNA co-immunoprecipitated both specifically (when the antibody against Ago2 was used) and non-specifically (when no antibody was used). LysisB-B was preferred over all the other conditions. In fact, although PXL showed similar specificity (fig. 3-11 B), LysisB-B guaranteed higher absolute recovery of the mRNA (fig. 3-11 A).

Titration of the antibody suggested that 1μg was the optimal amount to use (fig. 3-12). In fact, for both *PU.1* and *SMAD2*, the amount of co-immunoprecipitated mRNA peaked at 2μg of antibody, but then it decreased when 4μg were used. Looking at the co-immunoprecipitated miR-155, it peaked at 1μg of antibody, decreased at 2μg and again increased at 4μg. Although the latter trend regarding miR-155 was not expected, overall the experiment showed clearly that already 0.1μg of antibody could guarantee co-immunoprecipitation of both miR and target mRNA, while more than 2μg were inhibitory. As a matter of fact, a 20-fold increase of antibody (from 0.1 to 2μg) led to only a marginal increase of signal (i.e. amount of mRNA co-immunoprecipitated) and therefore 1μg represents a convenient choice. Also a matched isotype negative control antibody (hereafter IgG) was titrated in the same experiments, confirming the specificity of the antibody used against Ago2, and the specificity of the results obtained.

Finally, three independent Ago2 co-IP experiments confirmed the reproducibility of the method (fig. 3-12 D).

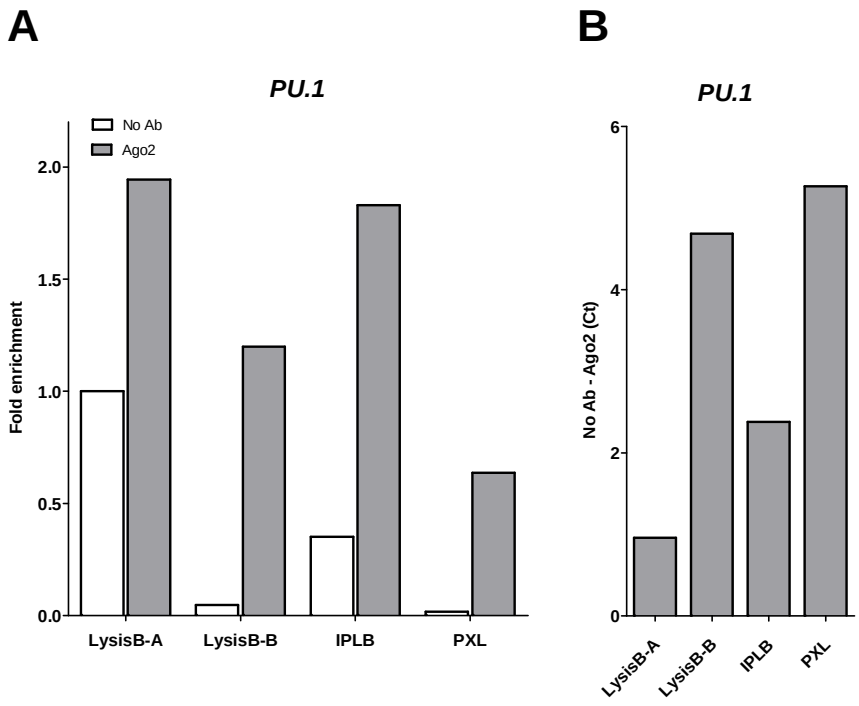

fig. 3-11. Optimization of Ago2 co-IP in THP1MΦ – lysis and washing buffers.
Previous work from our group has shown that PU.1 is targeted by miR-155 (Martinez-Nunez et al. 2009). PU.1 mRNA was measured by RT-qPCR. PU.1 official gene symbol: SPI1.

X axis labels indicate the combination lysis/wash buffer used. 2µg of anti-Ago2 antibody was used, or no antibody at all (No Ab). Beads were washed with the buffer and for the number of times indicated here:

LysisB-A: Wash 1a (x5); **LysisB-B:** Wash 1b (x5); **IPLB:** IPWB (x3); **PXL:** PXLW (x5).

Each bar represents the average of qPCR duplicates from one single experiment.

The calculations adopted can be found in paragraph 2.11.

In **A)** the amount of background mRNA (No Ab) or the amount associated with Ago2 (Ago2) are plotted independently. In **B)** the difference between the Ct value obtained for either "No Ab" or "Ago2" are plotted and used as a measure of the specificity obtained with the buffers adopted.

LysisB-B was chosen as the best condition, since it guarantees a large difference from background (see B) but also high absolute recovery of mRNA (see A).

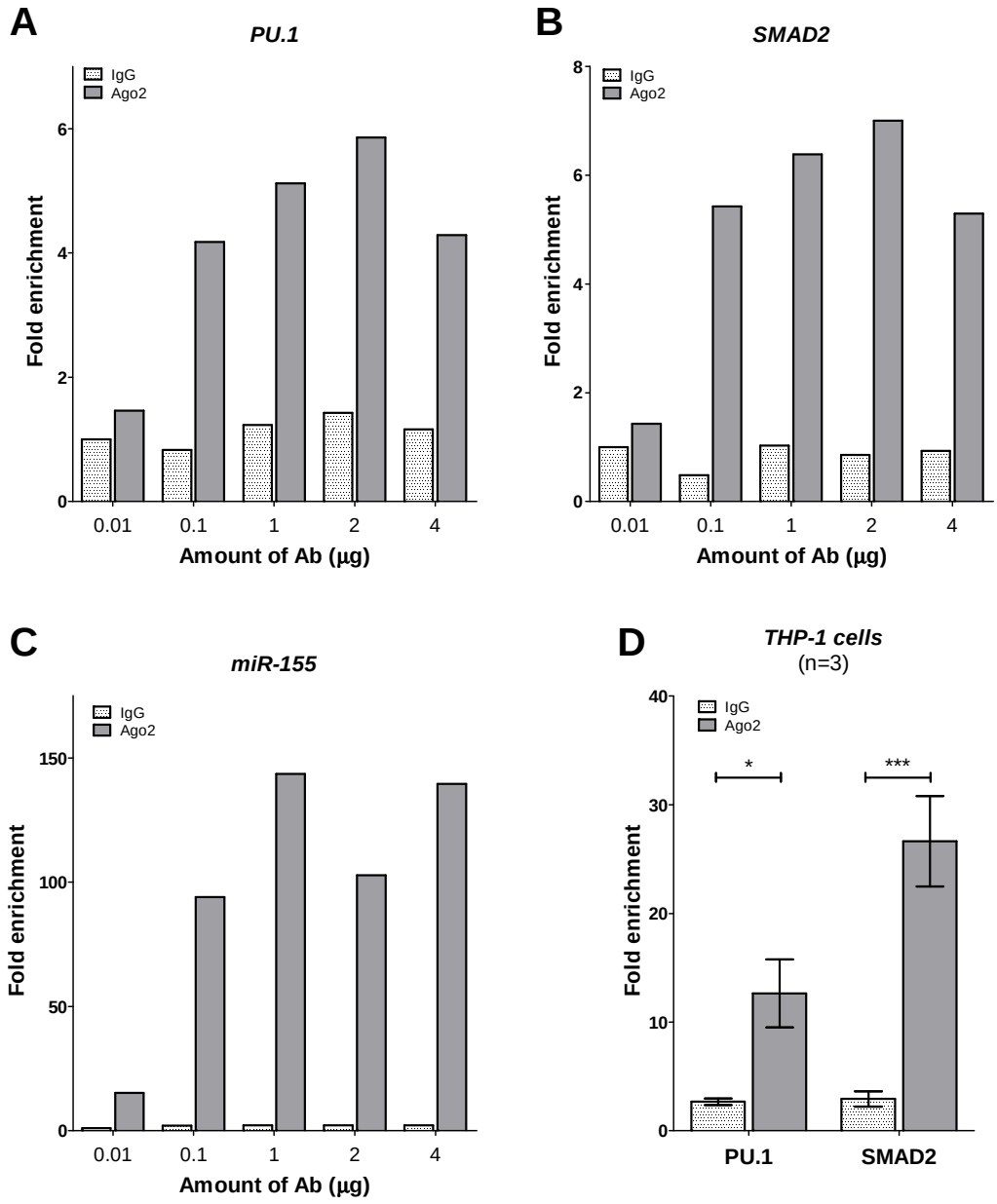

fig. 3-12. Optimization of Ago2 co-IP in THP1MΦ cells – antibody titration.

Previous work from our group has shown that PU.1 and SMAD2 are targeted by miR-155 (Louafi et al. 2010, Martinez-Nunez et al. 2009). In the legend IgG refers to the negative control antibody, Ago2 refers to the anti-Ago2 antibody. Both were always used at the same concentration. The amount of antibody used in panels A to C is indicated on the X axis. 1µg was used in D.

The values plotted in **A**, **B** and **C** represent the average of qPCR duplicates (from one single experiment). 1µg was chosen as the best condition to use.

In **D**, the values plotted represent the average, while the error bars represent the SD, of three independent experiments. *=$p<0.05$; ***=$p<0.001$. p values were calculated using the unpaired t-test.

3.2.1.4 BEAS-2B cells

The protocol optimised for THP-1 cells did not show optimal results with BEAS-2B cells. More stringent conditions were adopted in the washing step, and the concentration of salt (NaCl) in the washing buffer was increased from 0.3M to 1M. In fact, by looking at the amount of *SMAD2* mRNA co-immunoprecipitated, 1M of salt reduced the background, without harming significantly the association with Ago2 (fig. 3-13). An antibody titration experiment, confirmed that 1µg was the optimal amount to use also in this case (fig. 3-14 A to D). Indeed, it guaranteed maximal co-IP and it was not saturated, even when cell lysate was as much as twice more concentrated. In fact, the amount of *SMAD2* mRNA recovered together with Ago2 (but not with IgG) was proportional to the amount of cells used and therefore the total amount of Ago2 protein present (fig. 3-14 E). The amount of cells used was the same for each co-IP experiment ($2x10^6$) and it was changed only for the experiment in fig. 3-14 E.

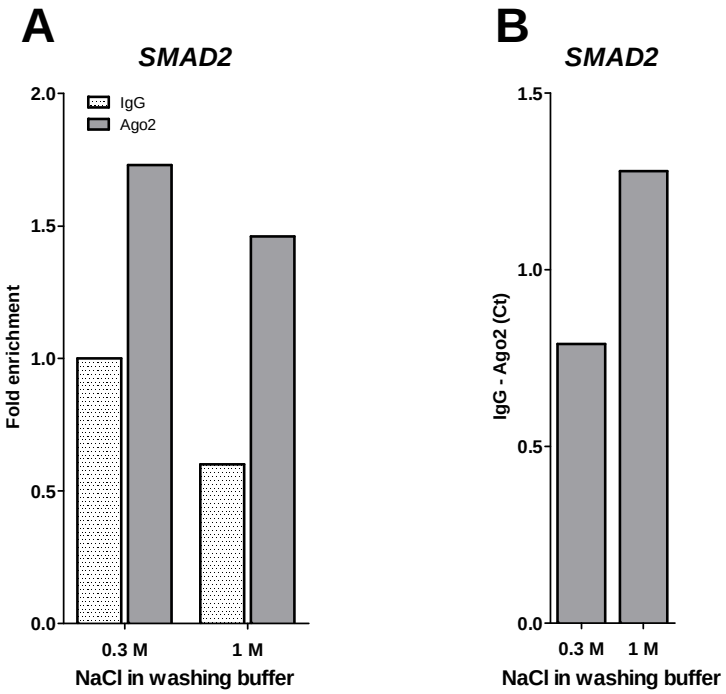

fig. 3-13. Optimization of Ago2 co-IP in BEAS-2B cells – washing buffer.
Values plottes refer to the average of qPCR duplicates from one experiment. Lysis B and 1µg of antibody were used. The two washing buffers compared, differed only for the concentration of NaCl which is indicated on the X axis. 0.3M: Wash 1b; 1M: Wash 1M (see table 2-7 in materials and methods for recipes). For **B**, the same calculations as in fig. 3-11 B were used**.**

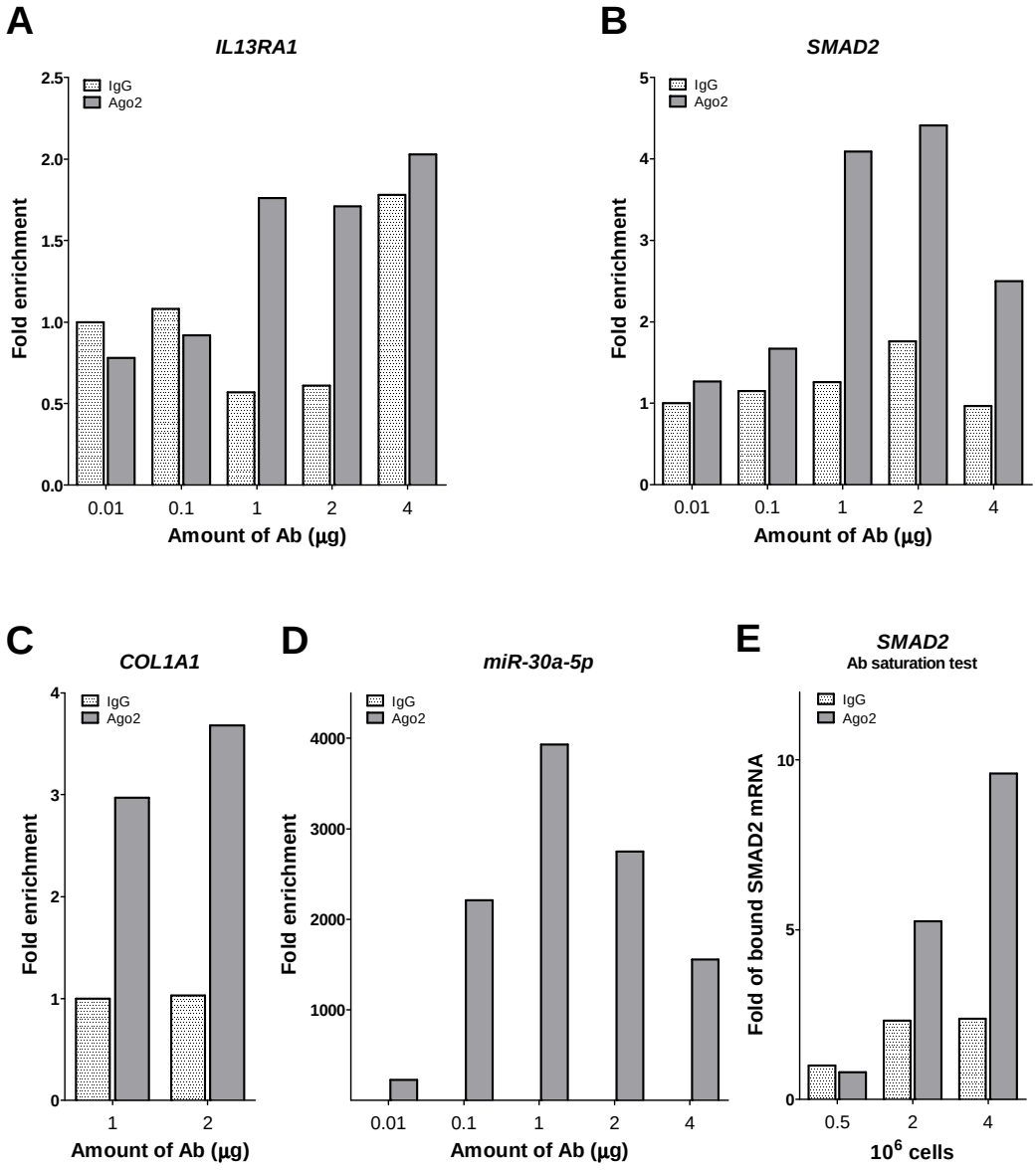

fig. 3-14. Optimization of Ago2 co-IP in BEAS-2B cells – antibody titration and saturation test.

The values plotted, represent the average of qPCR duplicates (from one single experiment). Previous work from our group has shown that also IL13RA1 is targeted by miR-155 (Martinez-Nunez et al. 2011). COL1A1 has been shown to be targeted by miR-29b (Ogawa et al. 2010). Legends as in fig. 3-12. From **A** to **D** antibody titration. 1µg was chosen as the optimal amount. 1µg of antibody was used in **E** which shows that the amount of antibody used is not saturated by the epitope in the usual conditions (when $2x10^6$ cells/IP were used). Calculations for **E** are shown in table 2-11.

3.2.2 Ago2 co-IP in THP1MΦ infected with HRV-1B.

As shown in paragraph 3.1.3, it was not possible to affect expression of mature microRNAs, and in turn HRV replication, in THP1MΦ by knocking down *DICER*. However, Ago2 co-IP could reveal whether microRNAs bind to viral RNA in those cells. THP1MΦ were infected with HRV-1B at an MOI of 0.01. Six hours post-infection cells were lysed in order to perform Ago2 co-IP. As shown in fig. 3-15 A, although HRV-1B RNA was on average enriched in the fraction co-purified with Ago2, as compared to IgG, this difference was not significant. The same experiments confirmed instead that *PU.1* mRNA was significantly associated with Ago2 protein, both compared to negative control antibody and to *GAPDH* mRNA.

3.2.3 Ago2 co-IP in BEAS-2B cells infected with HRV-1B.

In paragraph 3.1.4, it was shown that affecting microRNA maturation in BEAS-2B cells, allows higher HRV-1B replication without affecting IFN-β induction. This suggested that microRNAs hamper viral replication with a direct mechanism. Therefore, Ago2 co-IP was used in order to test whether in BEAS-2B cells, Ago2 (and therefore microRNAs) binds directly to viral RNA during infection.

BEAS-2B cells were infected with HRV-1B at an MOI of 0.01 and were then harvested 6 hours post-infection. HRV-1B RNA and *SMAD2* mRNA resulted to specifically associate to Ago2 (fig. 3-15 B). Indeed, in both cases twice as much RNA was recovered with Ago2 as compared to IgG. In both cases, such difference was statistically significant. In contrast, although slightly more *GAPDH* mRNA was associated with Ago2 compared to negative control, the difference was not significant. Furthermore, HRV-1B RNA was associated to Ago2 with a fold enrichment significantly higher than *GAPDH* and comparable to *SMAD2*, which has already been shown to be a target of miR-155 (Louafi et al. 2010).

In summary these results show that microRNAs bind to both *SMAD2* and HRV-1B RNA in BEAS-2B cells (fig. 3-15 B). This together with previous findings presented in this thesis, reinforces the hypothesis that in BEAS-2B cells microRNAs reduce viral replication by direct binding.

Regarding THP1MΦ instead, Ago2 co-IP experiments could confirm direct interaction of the miRISC with *PU.1* and *SMAD2* mRNAs (fig. 3-12 D). HRV-1B RNA showed the same trend but the results did not reach statistical significance (fig. 3-15 A) and further experiments may be needed to clarify this further.

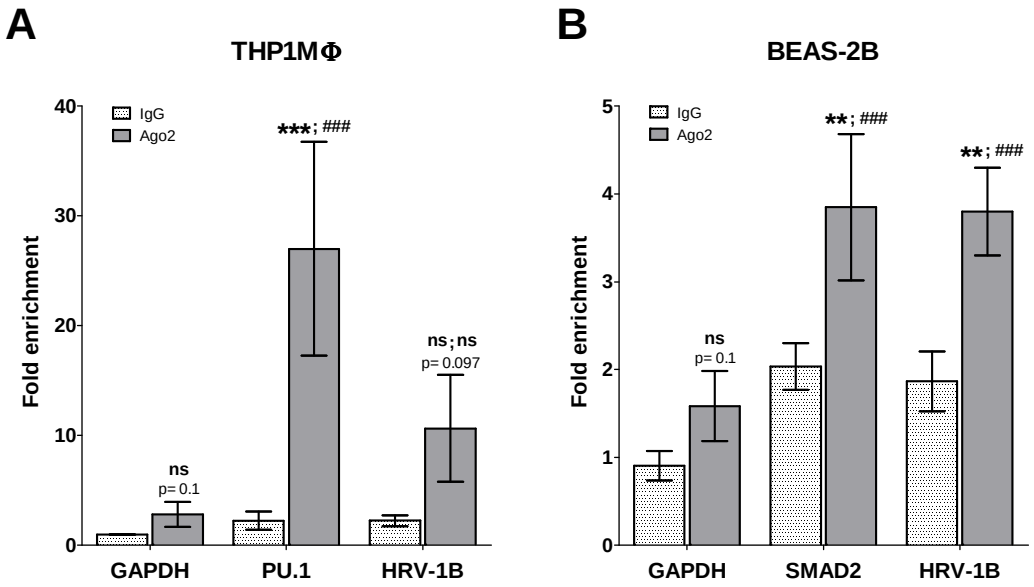

fig. 3-15. HRV-1B RNA co-immunoprecipitates with Ago2 in BEAS-2B cells, but not in THP1MΦ.

(A) THP1MΦ or **(B)** BEAS-2B cells were infected with HRV-1B at MOI 0.01. 6 hours post-infection, cells were collected and Ago2 co-IP was performed following the optimised protocols.

The values plotted represent the average, while the error bars represent the SD, of three independent experiments. ns=not significant ($p>0.05$); ** =$p<0.01$; *** or ## =$p<0.001$. p values were calculated using one way ANOVA with Bonferroni post-test correction.

* symbols represent significance as compared to IgG of same gene.

symbols instead represent significance as compared to Ago2 *GAPDH*.

p-values for the non significant differences between IgG and Ago2 were re-calculated using unpaired t-test with Welch's correction and reported in the figure.

3.3 Do microRNAs reduce HRV-1B replication by directly binding to the viral RNA?

3.3.1 Lentiviral inducible knock-down system.

3.3.1.1 Rationale

The main findings presented so far, support the hypothesis that microRNAs affect rhinoviral replication. As a matter of fact, it has been shown that in BEAS-2B cells:

a) Sustained *DICER* knock-down leads to lower levels of mature microRNAs and higher HRV-1B replication (fig. 3-9).
b) HRV-1B RNA associates with Ago2 (fig. 3-15).

Altogether, these findings suggest that microRNAs inhibit HRV-1B replication by directly binding to the viral RNA. If this was true then it is expected that sustained *DICER* knock-down would also reduce the amount of HRV-1B RNA associated with Ago2. However, large numbers of cells are needed in order to perform this experiment. Therefore, it was decided to generate BEAS-2B cells containing an inducible knock-down system. In those cells, a construct integrated in the chromosomal DNA would allow the inducible expression of shRNAs (functionally identical to siRNA). Therefore, thanks to this system, the prolonged silencing of *DICER* could be achieved in a large number of cells and be more convenient and economical than transfecting several times large number of cells with synthetic siRNAs. In addition, because Ago2 has been shown to bind HRV-1B, reducing the expression of this protein was also expected to favour viral replication. In conclusion, three BEAS-2B-derived cells lines were generated, with inducible expression of either negative control, or anti-*DICER* or anti-*AGO2* shRNAs.

3.3.1.2 Cell line characterization

For this purpose it was decided to employ a lentiviral system that had already been used in our group (Martinez-Nunez et al. 2009). The lentiviral nature of the vectors guarantees efficient integration of the constructs in the cellular genome. It is a so called tet-on system, meaning that expression of the shRNA is possible only in the presence of tetracycline or derivatives, such as doxycycline (Wiznerowicz & Trono 2003). This particular system consists of two different lentiviral vectors, each one expressing a different fluorescent protein as marker. One vector contains the shRNA expression cassette and encodes Green Fluorescent Protein (GFP). The second vector expresses the red fluorescent protein DsRed2. It also expresses tTR-

KRAB, a tet-dependent transcriptional repressor that, in the absence of doxycycline, prevents expression of the shRNA and GFP from the other vector. Therefore, cells containing the full system are constitutively DsRed2 positive. Upon administration of doxycycline, they express both the shRNA and GFP, and become therefore DsRed2-GFP-double positive. More details about generation of the cell lines can be found in paragraph 2.12. However, for the reader's convenience, a schematic of the inducible system (fig. 3-16) and a table with the genes expected to be silenced in each cell line (table 3-3) are also reproduced below.

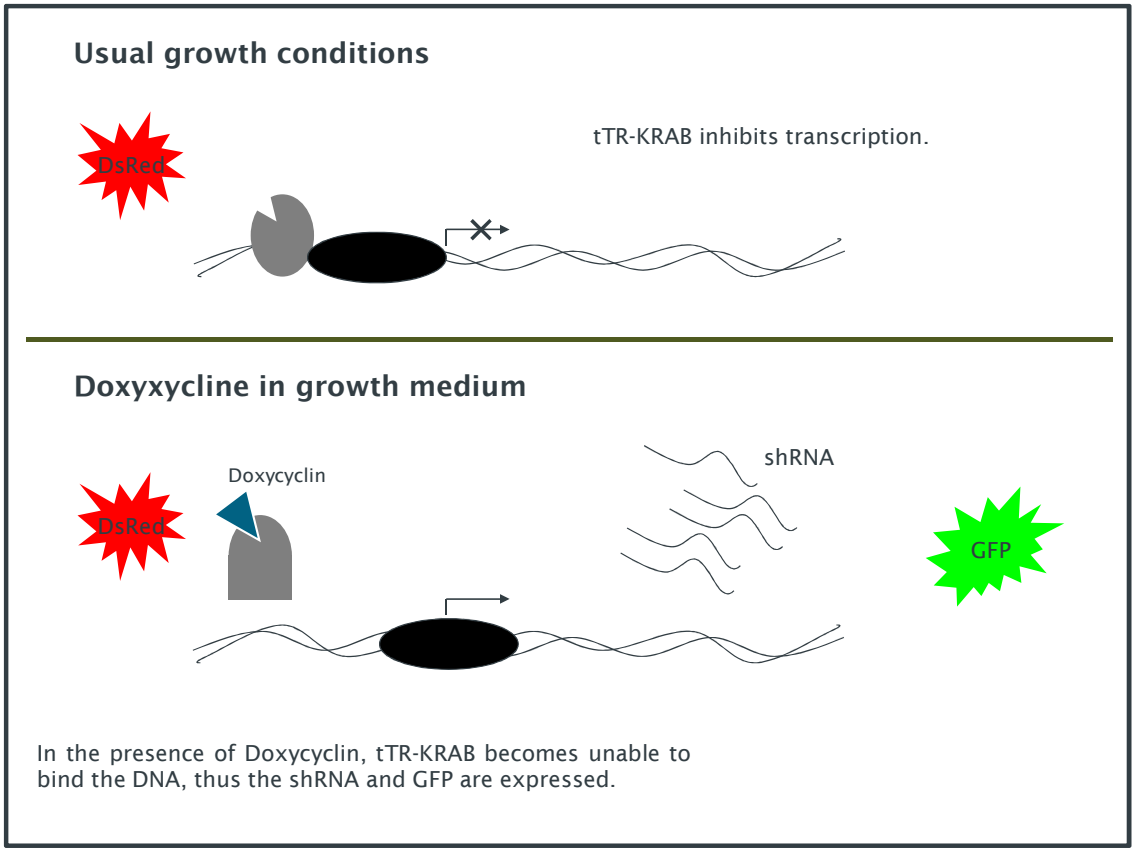

fig. 3-16. Lentiviral cell lines – schematic of inducible system

Cell line name	Plasmid used	Target protein
BEAS-2B LV_neg	pLVTHM_neg	None (negative control cell line)
BEAS-2B LV_AGO2	pLVTHM_AGO2	*EIF2C2* (AGO2)
BEAS-2B LV_DCR	pLVTHM_DCR	*DICER1*

table 3-3. Lentivirally transduced BEAS-2B cell lines generated.

The cell lines generated were further characterised in order to verify that the inducible system was working as expected. Addition of doxycycline in the growth medium should induce expression of GFP together with the shRNA, and therefore cause silencing of the target gene.
Flow cytometry data showed that in all three cell lines, the system was inducible. As expected, most cells became GFP positive between two and three days after induction (fig. 3-17). On the contrary, looking at the expression of both *DICER* and *AGO2*, unexpected results were obtained (fig. 3-18). In the absence of doxycycline, the expression of both genes tends to slightly and gradually decrease over time. This trend was however visible for all the cell lines, and it may be due to cell growth. Therefore more attention was given to differences on the same day post-induction. As expected, in the negative control cell line, shRNA induction did not affect expression of either gene. Doxycycline treatment did not affect *AGO2* expression also in cells expressing anti-*DICER* shRNA. On the contrary, induction of anti-*AGO2* shRNA led to about 50% knock-down of its target gene in two days. However the difference with the non-induced cells diminished over time, until becoming negligible on day 6.
In contrast to the expected observations just mentioned regarding *AGO2*, *DICER* expression was not affected by doxycycline treatment in cells expressing anti-*DICER* shRNA. In those cells *DICER* expression was not different from either non-induced cells or negative control cells. Surprisingly instead, induction of anti-*AGO2* shRNA, caused up-regulation of *DICER* which was, on day 6, 1.5 times higher than before induction or 3 times higher than non-induced cells.

Clearly, despite having a functional inducible system, these cell lines did not have the characteristics wanted: sustained reduction of either *DICER* or *AGO2* expression. Instead, the anti-*DICER* shRNA did not have any effect on the target, and while the anti-*AGO2* shRNA was effective on *AGO2*, it caused strong up-regulation of *DICER*. Whether this translated into increased mature microRNAs has not been tested. Because of time constraints and since the cell lines did not possess the properties they had been generated for, they were not used further.

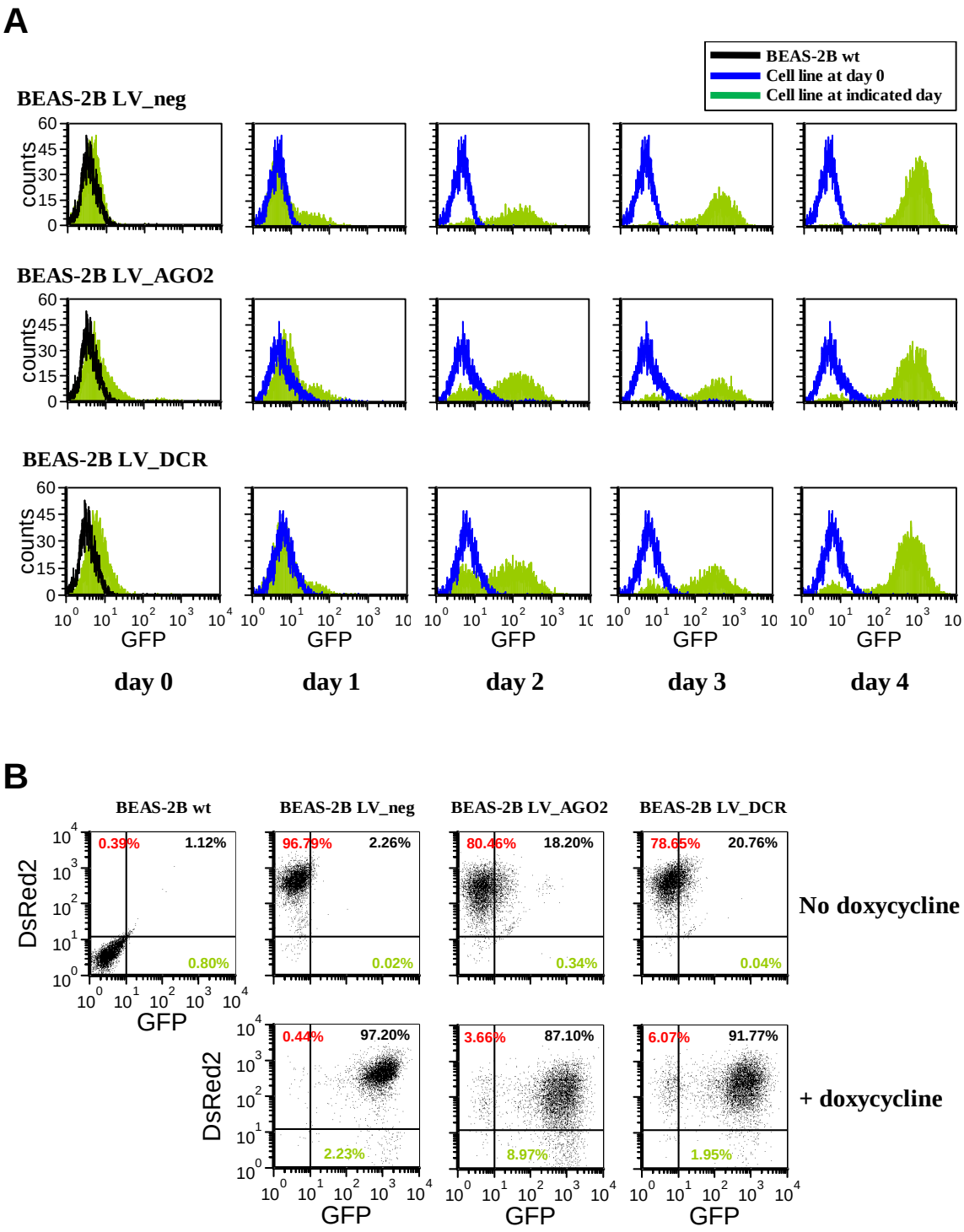

fig. 3-17. Lentivirally transduced BEAS-2B cell lines – inducible expression system. BEAS-2B cell lines, generated as described in paragraph 2.12, were treated with 50ng/ml of doxycycline in order to induce expression of transgenes (GFP and shRNA).
Cells were then collected every 24 hours and the expression of GFP was analysed by flow cytometry. In **A** only GFP signal is plotted, in order to easily compare the shift induced. In **B,** both GFP and DsRed2 fluorescence are plotted from cells treated with doxycycline for four days or mock-treated ("No doxycycline"). From both panels it can be noted some "leakage" in both BEAS-2B LV_AGO2 and _DCR cell lines.

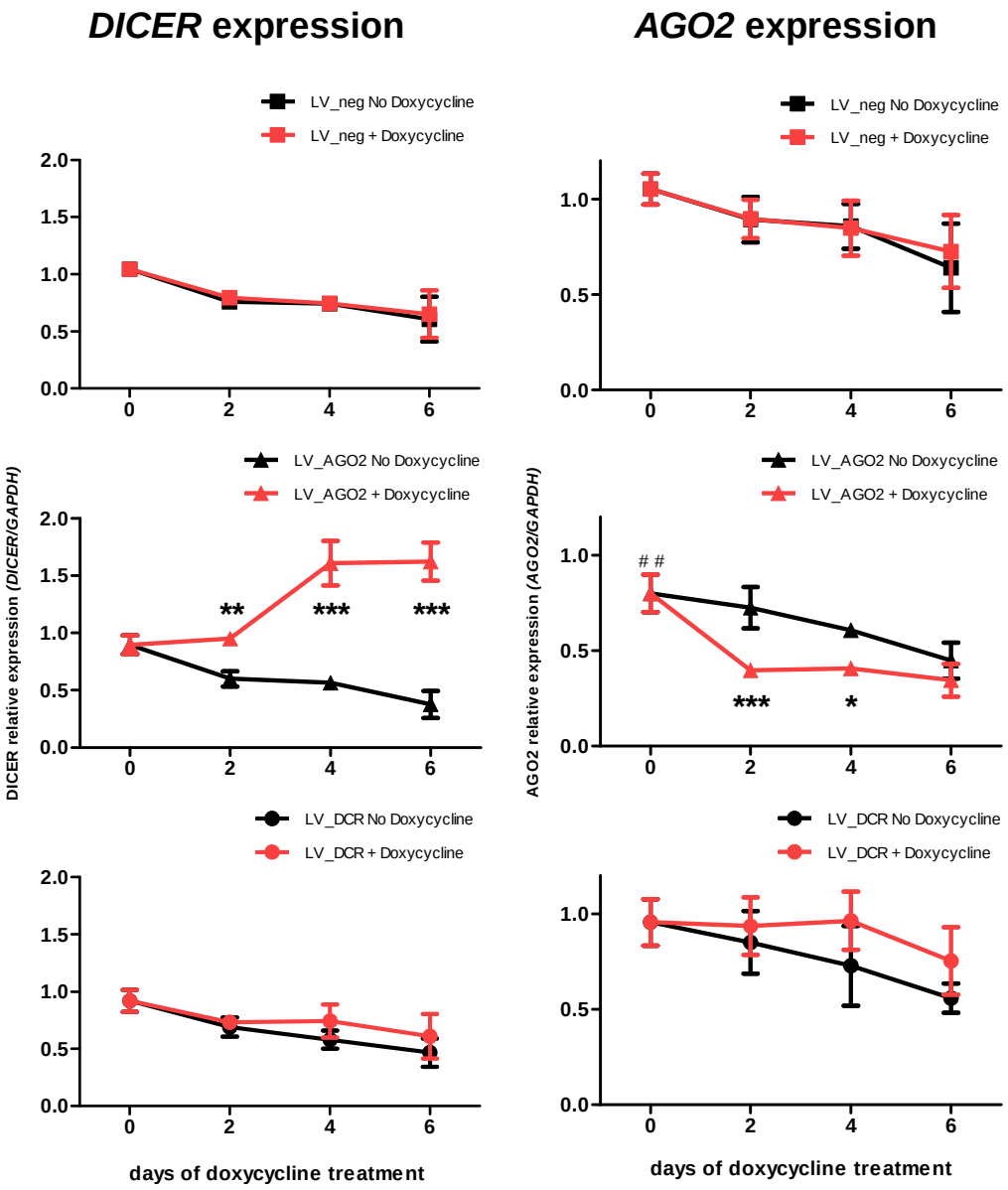

fig. 3-18. Lentivirally transduced BEAS-2B cell lines – expression of *AGO2* and *DICER*.

Cells treated as in fig. 3-17 were also analysed by RT-qPCR in order to quantify expression of the two target genes. The dots represent the average, while the error bars represent the SD from one experiment performed with four biological replicates. All the samples were normalised together, using one sample of BEAS-2B LV_neg as calibrator, each gene was treated separately. * =p<0.05; ** or ## =p<0.01; *** =p<0.001; if nothing is indicated, difference was not significant. p values were calculated using one way ANOVA with Bonferroni post-test correction.

*symbols represent significance as compared to mock-treated of same cell line at the same day of treatment.

symbols instead represent significance as compared to BEAS-2B LV_neg mock-treated at same day of treatment.

3.4 Discussion.

3.4.1 HRV-1B replication in HeLa and THP-1 derived macrophages (THP1MΦ).

The goal of the first part of this investigation was to test whether microRNAs are able to influence the replication of human Rhinovirus (HRV). Therefore, replication of a minor group HRV, namely HRV-1B, was studied in two cell lines: HeLa and THP1MΦ. Viral replication in both cell lines was followed over a time course, both measuring intracellular viral RNA by RT-qPCR (fig. 3-2) and by titrating infectious virus shed in the medium (fig. 3-3) by limiting dilutions (TCID50 assay).

Replication of HRV-1B in Hela cells progressed as expected and it was comparable to what already published, e.g. (Amineva et al. 2011, Fiala & Kenny 1967). In fact, viral RNA decreased during the first hours post-infection but at later time points it increased considerably, reaching plateau around 8 hours post-infection. Also the extracellular viral titre seemed to confirm this trend. However, the extracellular titres were always very close to the detection limit of the technique used, except for the last two time points of the highest MOI. Therefore, for future experiments it was preferred to follow viral replication by measuring the intracellular viral RNA by RT-qPCR. In fact, the main interest of this project is on the replication of viral RNA that is directly a consequence of viral protein production which is what microRNAs act upon. Release of viral progeny is instead a further step that may be influenced and regulated by also other cellular processes.

HRV-1B replicated minimally in THP1MΦ. In fact, viral RNA never reached levels higher than at time 0 and extracellular virus could be detected only at 10 and 24 hours post-infection and only for the highest MOI used. Detection of shed virus suggests that HRV-1B was able to have a productive infection, although small in THP1MΦ. This result was not entirely expected. In fact, Laza-Stanca et al. showed that HRV-16 was able to replicate abundantly in THP1MΦ (Laza-Stanca et al. 2006). Results from the latter paper show that viral RNA peaked at 6 hours post-infection. However, in the same paper they studied replication of the virus also in macrophages derived from peripheral blood mononuclear cells (PBMC-MΦ). Interestingly, in those cells HRV-16 replication was much more similar to what we observed in our THP1MΦ: over time viral RNA gradually decreased and no rise of extracellular virus was evident. The THP1MΦ we used were generated using the same protocol as in the paper from Laza-Stanca et al. Moreover, our cell line was negative to mycoplasma contamination. As a consequence, the discrepancy between our results and theirs may lie in cell line age or other batch-specific differences, or differences pertaining to the HRV strain, HRV-16 in the paper, HRV-1B in our

case. At the same time it is not possible to exclude that our THP1MΦ differentiated more fully into macrophages compared to theirs, or were for other reasons more similar to PBMC-MΦ. In the mentioned paper they suggest that the difference between the two kinds of macrophages rely on the production of type I IFNs. In fact, although in both cell types NF-kB is activated after infection, only PBMC-MΦ produced IFN–α and –β. It is possible then that our THP1MΦ were more differentiated and produced IFNs in response to infection, which contributed to repress viral replication.

However, investigating the reasons behind such a difference was out of the scope of this project. In fact, although in a milder degree than actually registered, THP1MΦ were expected to be less permissive to HRV compared to HeLa cells. The latter speculation had been made because from previous work in our group, it was known that THP-1 cells express substantially more miR-155 than HeLa cells (fig. 3-1). MiR-155 had been identified as an anti-HRV microRNA candidate by our bioinformatic analysis (table 3-1) and this made THP1MΦ an interesting model to work with. We speculated that THP1MΦ may be rich also in other antiviral microRNAs and thus, reducing the expression of cellular microRNAs in these cells was expected to increase viral replication.

In order to achieve this, we decided to silence *DICER*, a key enzyme in microRNA maturation. The latter process involves the activity of two endonucleases that progressively shorten the initial microRNA transcript. Drosha cleaves the primary microRNA (pri-miR) in the nucleus, while Dicer is responsible for cutting the precursor microRNA (pre-miR) in the cytoplasm. The mature microRNA so produced assembles with Ago proteins in order to be functional (Filipowicz et al. 2008, Peters & Meister 2007). Hence, impairing the activity of either Drosha or Dicer has been shown to lead to a reduction of mature microRNAs e.g. (Kuehbacher et al. 2007, Schmitter et al. 2006). We opted to target *DICER* as already done in other published research about antiviral activity by RNAi or microRNAs (Matskevich & Moelling 2007, Otsuka et al. 2007, Triboulet et al. 2007, Wang et al. 2006).

Therefore, a siRNA was transfected into THP1MΦ in order to reduce the expression of *DICER*, and 48 hours later cells were infected with HRV-1B. As assessed by RT-qPCR, the siRNA caused a reduction of *DICER* mRNA between 80 and 90% (fig. 3-4 B) but this did not affect HRV-1B replication (fig. 3-4 A) nor did it lead to a significant reduction of microRNAs (fig. 3-4 C and D). Also other studies showed that 48 hours after transfection of anti-*DICER* siRNA, only a subset of microRNAs were affected, and their reduction was very rarely above 50% (Kuehbacher et al. 2007, Suarez et al. 2007, Winter et al. 2009). Regarding the investigations in virology already mentioned, one was based on mouse cells from knock-out animals (Otsuka et al. 2007) that virtually have no microRNAs (Harfe et al. 2005). In the studies based on human cells instead, they used siRNA against *DICER* but without assessing the effects of its reduction

on cellular microRNAs (Matskevich & Moelling 2007, Triboulet et al. 2007). It is possible that in these cases, *DICER* itself was involved in the protection towards viral infection or that the achieved reduction of microRNAs, although modest, was sufficient to affect viral replication in the systems adopted.

Therefore, although reducing *DICER* expression was expected to cause only a marginal reduction of microRNAs in THP1MΦ, our results were too variable and overall not significant (fig. 3-4). We speculated that if a stronger decrease of microRNAs was achieved, clearer conclusions could be drawn about their impact on HRV replication. Conceivably, at least two features may be responsible for the poor effect on microRNAs obtained by silencing *DICER*: (i) the abundance of microRNAs in a cell, and (ii) a very long half-life of microRNAs. In order to tackle the first point, and assuming that the expression of miR-155 represented also the expression of other antiviral microRNAs, we moved onto bronchial epithelial cells (BECs). In fact, human primary BECs express considerably less miR-155 compared to THP1MΦ (fig. 3-6). In order to tackle the second point (i.e. the possibility that microRNAs have a very long half-life) cells were transfected for three consecutive times with anti-*DICER* siRNA. This was expected to keep *DICER* expression at low levels for a longer period. In summary, it seemed likely that a prolonged *DICER* knock-down in primary BECs would lead to a stronger reduction of cellular microRNAs, as compared to what obtained in THP1MΦ, and in turn unveil whether microRNAs can regulate HRV replication. However, primary BECs did not withstand multiple transfections (fig. 3-5). As a consequence, the bronchial epithelial cell line BEAS-2B was adopted. Transfecting these cells for three rounds with anti-*DICER* siRNA confirmed our reasoning. In fact, a microRNA well expressed in BEAS-2B cells, such as miR-30a-5p, was reduced to less than 50% only after the third transfection (fig. 3-7 C). As expected then, such a reduction proved to enhance HRV-1B replication (fig. 3-9 C). In addition, recently a systematic analysis about microRNA turnover has been published (Gantier et al. 2011). The latter reinforces what we could infer from our results, which is that microRNAs are very stable. This study confirms indeed, that microRNA half-life can be estimated to be in the order of several days.

We have not verified the knock down of Dicer at the protein level by western blotting (i) because of the dramatic reduction of *DICER* mRNA, (ii) because the cells were infected 48 hours post-transfection, as done also in the other papers that used this approach, and (iii) because we were most interested in the effect on microRNAs, rather than Dicer protein per se.

3.4.2 Ago2 co-IP.

Our results shown in fig. 3-9 imply that Dicer, and possibly microRNAs, influence HRV-1B replication. Moreover, impairing the expression of *DICER* did not affect the production of IFN-β by the infected cells (fig. 3-9 D). This supports our hypothesis that microRNAs may act on viral replication through a direct mechanism, i.e. binding to the viral RNA. MicroRNAs regulate translation and stability of their target RNAs by base-pairing with them and therefore bringing them into contact with Ago proteins. In fact the latter associate with mature miRs (in complexes called miRISCs) and are the actual molecules responsible for the effects attributed to microRNAs (Peters & Meister 2007). As a consequence, microRNAs and their targets can be purified by isolating Ago proteins. Since this involves the use of an antibody, this technique is referred to as co-immunoprecipitation (co-IP). Interestingly, around the time this study was started, a few antibodies specific for Ago proteins were developed, which also performed well in co-IP experiments (Ikeda et al. 2006, Nelson et al. 2007, Rudel et al. 2008). Before development of such antibodies, Ago co-IP assays could be performed only by exploiting tagged Ago proteins and using antibodies for the tag moiety. This meant that cells needed to be transfected and made express fusion proteins. Moreover, in these systems both co-immunoprecipitated miRs and mRNAs were those that interacted with the chimeric proteins, e.g. (Landthaler et al. 2008). Antibodies specific for endogenous Ago proteins allowed use of co-IP to target the endogenous miRISCs and targets. This had a strong impact on microRNA investigation and in fact, it promoted the rapid increase in popularity that this technique has seen. A few antibodies specific for Ago2 have been successfully adopted in Ago2 co-IP experiments (Beitzinger et al. 2007, Hassan et al. 2010, Tan et al. 2009). In particular, the antibody we employed for our experiments was also used in a recently published work, where they identified cellular mRNAs targeted by viral microRNAs (Dölken et al. 2010).

Therefore, being a straightforward approach, we opted for Ago2 co-IP in order to test if microRNAs actually bind to viral RNA during HRV-1B replication. The results obtained for BEAS-2B cells show that the amount of HRV-1B RNA associated with Ago2, was significantly higher than in the negative control (fig. 3-15 B). This means that microRNAs bind viral RNA, reinforcing the idea that microRNAs regulate HRV-1B replication by a direct mechanism in bronchial epithelial cells. A similar trend was also obtained for THP1MΦ, but in this case the difference with the negative control did not reach statistical significance (fig. 3-15 A). This is very interesting because the strategy of impairing microRNA maturation was unsuccessful in THP1MΦ. Thanks to the Ago2 co-IP results, it is possible to speculate that in THP1MΦ the interaction between Ago2 and viral RNA is weaker than in BEAS-2B cells and that this could be due to less microRNA binding. For instance, in THP1MΦ *SMAD2* was enriched about twice as much as *PU.1* (fig. 3-12 D). This would fit with bioinformatic analysis, which predict miR-

155 to have two target sequences on *SMAD2* (Louafi et al. 2010) but only one on *PU.1* mRNAs (Martinez-Nunez et al. 2009). Therefore, it seems plausible that microRNAs bind *SMAD2* more tightly than *PU.1* mRNA and that Ago2 co-IP results are able to show such difference. *PU.1* is not expressed in BEAS-2B cells and therefore the comparison made earlier with *SMAD2* was not possible in this cell line. However, while in BEAS-2B cells microRNAs bound HRV-1B as strongly as *SMAD2*, in THP1MΦ microRNAs bound the viral RNA much less than *SMAD2* or *PU.1*. As shown in paragraph 4.2, either increasing or reducing miR-155 expression affects TGF-β signalling in BEAS-2B cells. Therefore, *SMAD2* is a genuine target of miR-155 also in BEAS-2B cells and as a consequence, the strength of the interaction between microRNAs and *SMAD2* as detected by Ago2 co-IP, identifies a functional microRNA target. Hence, because the Ago2 co-IP result for *SMAD2* and for HRV-1B RNA are comparable, also the latter can be expected to be regulated by microRNAs in BEAS-2B cells. Minor group HRVs have been shown to enter the cell through endosomes (Prchla et al. 1994). Macrophages are certainly cells that possess a very high phagocytic activity (Tsuchiya et al. 1982). It is possible then, that cellular characteristics such as active phagocytosis, which is much higher in macrophages than in undifferentiated monocytes or epithelial cells, may be responsible for the remarkably lower viral replication in macrophages compared to epithelial cells. The Ago2 co-IP results we obtained in THP1MΦ may be a consequence of this. In fact, it can be imagined that in macrophages, most virus is prevented from uncoating thanks to the cells' phagocytic activity, and therefore not much viral RNA comes into contact with microRNAs.

Ago co-IP has been widely used in microRNA research. Nevertheless, the use we made of it is original, because in the literature it has only been used to identify cellular mRNAs targeted by microRNAs. This study is instead the first one to show that the RNA of a virus is co-immunoprecipitated with Ago2.

3.4.3 Lentiviral BEAS-2B cell lines.

The observation that it was necessary to silence *DICER* for several days, in order to produce a substantial reduction in microRNA expression, inspired the generation of stably transfected cell lines with inducible siRNA expression. Such a system was ideal for our purposes because it would allow the controlled and prolonged silencing of *DICER* in a large number of cells. Infecting those cells with HRV-1B would have made possible to reinforce and causally link the previous results. In fact, cells with less Dicer would be expected to support higher viral replication, and at the same time have less HRV-1B RNA bound to Ago2.

In addition, we reasoned that if Ago2-bound microRNAs are able to hamper viral replication, then knocking-down *AGO2* would promote HRV-1B replication. For this purpose

BEAS-2B cells were transduced with lentiviral particles bearing inducible short hairpin RNA constructs (shRNA; same activity as siRNA). Three different lentiviral vectors were generated that express three different shRNAs: anti-*DICER*, anti-*AGO2* or negative control. Thus, three cell lines were generated by selecting stably transduced cells (fig. 2-5). In those cells, shRNA expression is induced by adding doxycycline to the medium. Unfortunately, the cell lines obtained were not as wanted, because expression of the two genes of interest (*DICER* and *AGO2*) would not change as expected. All the constructs were inducible as demonstrated by flow cytometry (fig. 3-17), but the anti-*DICER* shRNA did not affect expression of its target. Anti-*AGO2* shRNA was instead functional but repression of *AGO2* triggered the up-regulation of *DICER* (fig. 3-18). This was unexpected. The possibility that cells would react to the silencing of *AGO2*, by inducing *DICER* expression, was not anticipated from the literature. For instance, Schmitter et. al knocked-down either *AGO* (from 1 to 4) or *DICER* in HEK cells, but they did not show the reciprocal influence of such reductions (Schmitter et al. 2006). However, they showed that reduction of either Ago2 or Dicer led to release of microRNA-mediated suppression of luciferase reporters. It is possible that HEK and BEAS-2B cells differ in this, and that *AGO2* knock-down does not trigger *DICER* up-regulation in HEK cells. We have not verified whether microRNA activity was impaired in the Ago2 cells line for technical and time reasons. Moreover, because of these unexpected results, the use of these cell lines was discarded and no further experiments were performed with them. Nevertheless, these results are very interesting and may be highlighting a cellular homeostatic mechanism. It is possible in fact, that in BEAS-2B cells reduction of Ago2 lowers the microRNA activity that is available to the cells. The latter would then try to compensate such loss by producing more Dicer, in order to increase the amount of mature microRNAs. This is an interesting observation that prompts to ask whether there is a feedback mechanism that is able to preserve functionality of the cellular microRNA machinery.

In summary, the experiments performed led us to choose BEAS-2B cells as the cellular model in which to investigate the interaction between HRV and microRNAs. Ago2 co-IP revealed that as hypothesised, microRNAs do bind to HRV-1B genomic RNA, reinforcing the suggestion that microRNAs hamper HRV-1B replication by direct targeting. Although more evidence is still necessary, these results encouraged studying whether differences in the expression of microRNAs between healthy and asthmatic BECs influence the replication of human Rhinovirus in these cells.

Chapter 4

RESULTS: microRNA deficiency in asthmatic bronchial epithelial cells and its possible role in asthma.

4.1 MicroRNAs deficient in asthmatic BECs affect rhinoviral replication.

The results presented in the previous chapter show that microRNAs influence the replication of HRV-1B. This was shown using the bronchial epithelial cell line BEAS-2B. The current chapter presents experiments performed in order to investigate the second hypothesis of this project. In fact, knowing that asthmatic BECs are more permissive to HRV compared to healthy BECs (Wark et al. 2005) we hypothesized that asthmatic cells are deficient in microRNAs that hamper HRV replication.

In order to test whether there is a deficiency in the expression of antiviral microRNAs in asthmatic broncho-epithelium, microRNA RT-qPCR arrays were performed with RNA from healthy and asthmatic BECs. The arrays used were Taqman Array microRNA (card A) from Applied Biosystems, which contains primers to detect 377 microRNAs, among the most commonly studied ones (for more details see materials and methods, paragraph 2.13). For each group, BECs from four different donors were used, and each sample was analysed separately. The results highlighted that the expression of a number of microRNAs was reduced in the asthmatic BECs, as compared to the healthy cells. In particular, a few were expressed less than 50% in asthmatic BECs as compared to the healthy counterparts. These miRs are represented by the dots that fall underneath the double line, in the scatter plots in fig. 4-1. For all the microRNAs, p-values were calculated by unpaired t-test and those with a p-value lower than 0.05 were selected (27 microRNAs in total). This group of microRNAs (fig. 4-1 B) was entered in the prediction algorithm developed by the Segal lab (see paragraph 2.15) in order to predict which one would target HRV-16 or HRV-1B. Proceeding as previously done (see paragraph 3.1.1) only the microRNAs that were predicted to target both viruses were selected (table 4-1).

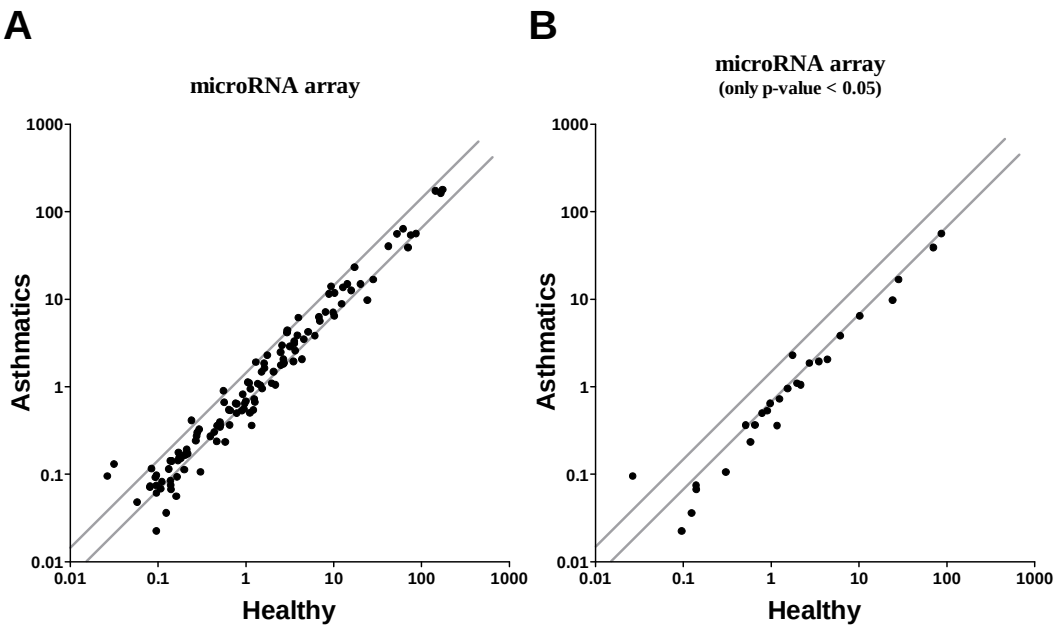

fig. 4-1. MicroRNA RT-qPCR arrays

The axes refer to microRNA expression levels calculated for asthmatic (y axis) or healthy BECs (x axis). Above the two grey lines fall all the microRNAs that are more than 1.5 times more abundant in asthmatic BECs, while underneath the two lines all those that are more than 1.5 times less abundant. MicroRNA expression was calculated using RNU44 as a reference gene, while the average ΔCt of all the microRNAs included was used as a calibrator (to calculate the ΔΔCt) see paragraph 2.13 for more details.

Among all the microRNAs taken into account (**A**) a few were selected (**B**) because they were differently expressed between the two groups, with $p<0.05$ using unpaired t-test. Most of the RNA samples used for this figure (see table 2-1) were kindly provided by Dr. Nicole Bedke. RT-qPCR arrays were preformed by Victor Paky Bondanese.

A

virus	microRNA	Start	End	Seed	dGduplex	dGopen	ddG
HRV-1B	hsa-miR-17	2276	2268	8:1:0	-20.3	-6.29	-14
HRV-1B	hsa-miR-99b	2128	2120	8:1:1	-18.76	-6.35	-12.4
HRV-1B	hsa-miR-20a	2276	2268	8:1:0	-18.3	-6.29	-12
HRV-1B	hsa-miR-140-5p	1535	1527	8:1:0	-17.2	-5.3	-11.89
HRV-1B	hsa-miR-155	2901	2893	8:0:1	-15.12	-3.24	-11.87
HRV-1B	hsa-miR-93	2276	2268	8:1:0	-18.1	-6.29	-11.8
HRV-1B	hsa-miR-128	1562	1554	8:1:0	-16.4	-5.28	-11.11
HRV-1B	hsa-miR-106b	2276	2268	8:1:0	-17.2	-6.29	-10.9
HRV-1B	hsa-miR-34a	2644	2636	8:1:0	-16.2	-5.44	-10.75
HRV-1B	hsa-miR-301a	4633	4625	8:1:1	-15	-5.06	-9.93
HRV-1B	hsa-miR-18a	2124	2116	8:1:1	-14.81	-4.9	-9.9
HRV-1B	hsa-miR-106b	4777	4769	8:1:0	-17.81	-7.96	-9.84
HRV-1B	hsa-miR-99b	2287	2279	8:1:0	-19.2	-10.15	-9.04
HRV-1B	hsa-miR-19b	6668	6660	8:1:0	-14.1	-5.07	-9.02
HRV-1B	hsa-miR-34a	5945	5937	8:1:1	-14.7	-5.69	-9

B

virus	microRNA	Start	End	Seed	dGduplex	dGopen	ddG
HRV-16	hsa-miR-34a	2470	2462	8:1:1	-21.3	-3.4	-17.89
HRV-16	hsa-miR-34a	4950	4944	6:0:0	-20.5	-4.09	-16.4
HRV-16	hsa-miR-34a	1693	1686	7:0:0	-20.04	-7.8	-12.23
HRV-16	hsa-miR-155	3720	3712	8:1:0	-16.6	-5.27	-11.32
HRV-16	hsa-miR-494	564	558	6:0:0	-21.6	-10.86	-10.73
HRV-16	hsa-miR-19b	3666	3658	8:1:1	-18.4	-7.76	-10.63
HRV-16	hsa-miR-125b	5633	5625	8:1:1	-16	-5.66	-10.34
HRV-16	hsa-miR-140-5p	1201	1193	8:1:1	-16.1	-6.18	-9.91
HRV-16	hsa-miR-34a	1805	1797	8:1:1	-15.1	-5.34	-9.75
HRV-16	hsa-miR-125b	4086	4078	8:1:0	-15.9	-6.32	-9.57
HRV-16	hsa-miR-155	717	709	8:1:0	-12.6	-3.22	-9.37
HRV-16	hsa-miR-93	4785	4779	6:0:0	-12.7	-3.34	-9.35
HRV-16	hsa-miR-128	3600	3592	8:0:0	-17.4	-8.15	-9.24
HRV-16	hsa-miR-18a	738	730	8:1:0	-15.3	-6.1	-9.19
HRV-16	hsa-miR-29b	3833	3825	8:1:0	-17.8	-8.67	-9.12
HRV-16	hsa-miR-106b	2901	2893	8:1:1	-16.1	-7.01	-9.08

Continues on next page

C

miRs selected for validation	
1	**hsa-miR-106b**
2	**hsa-miR-128**
3	**hsa-miR-140-5p**
4	**hsa-miR-155**
5	**hsa-miR-18a**
6	**hsa-miR-19b**
7	**hsa-miR-34a**
8	**hsa-miR-93**

table 4-1. MicroRNAs that have low expression in asthmatic BECs are predicted to target both HRV-1B and HRV-16.
The microRNAs plotted in fig. 4-1 B have been used for a target prediction analysis against HRV-16 (A) or HRV-1B (B). Only the microRNAs predicted to target both viruses were selected for further study (C).

Expression of the latter microRNAs was then measured by RT-qPCR (single assay) in the same samples used for the arrays and also additional samples, (in total 13 for healthy and 15 for asthmatics) in order to validate the array results (fig. 4-2). Three microRNAs, namely miR-140-5p, miR-34a and miR-93, were not confirmed to be expressed at significantly different levels between asthmatic and healthy BECs and so they were discarded.

The remainder microRNAs were taken into consideration in order to test whether their lack is able to influence HRV replication. In fact they are (a) less abundant in asthmatic cells and (b) predicted to target HRV genomes. Therefore, BEAS-2B cells were transfected with synthetic microRNA antagonists (antimiRs) one day before infection with HRV-1B. Cells were collected 8 hours post-infection and viral RNA was quantified by RT-qPCR. The results obtained show that silencing either miR-155 or -128 favoured viral replication (fig. 4-3). In fact, when cells were transfected with either antimiR-106b or -18a or -19b, the amount of viral RNA was no different compared to negative control antimiR. Instead, when antimiR-155 or -128 were used, viral RNA was around 50% higher.

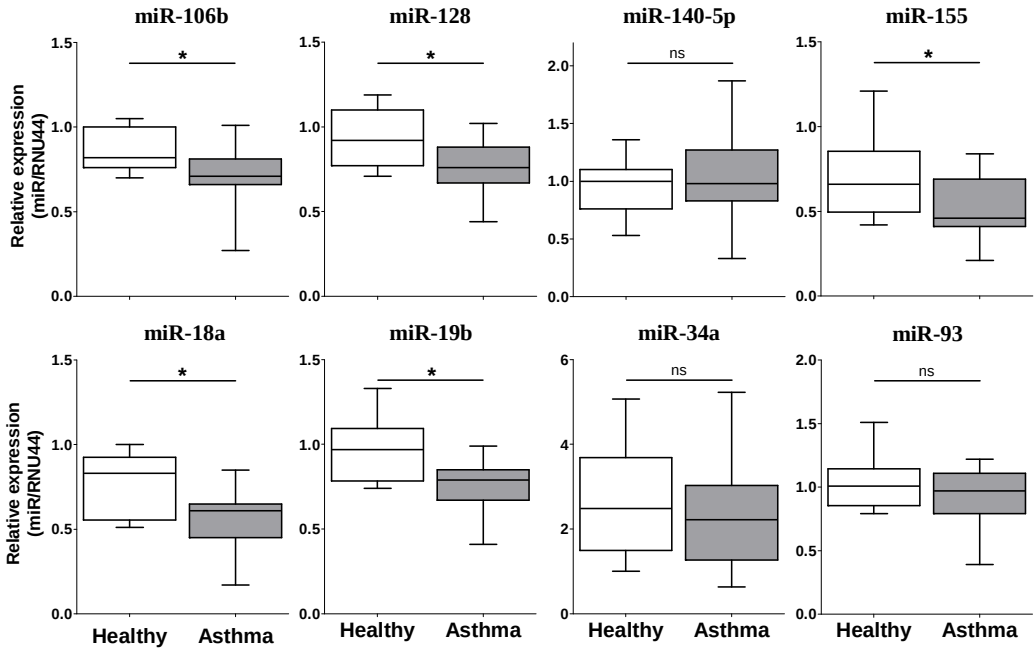

fig. 4-2. Validation of microRNA array results.

Expression of the microRNAs selected (table 4-1 C) was measured by taqman microRNA assays, in order to validate the array results (i.e. they are less abundant in asthmatic BECs). The healthy (n=13) and the asthmatic (n=15) BECs used include also those previously used for the array. Relative expression values were plotted using box and wiskers plots, were 5 to 95 percentiles are shown. ns=not significant ($p>0.05$); *=$p<0.05$; **=$p<0.01$. p values were calculated using Mann Whitney test.

Most of the RNA samples used for this figure (see table 2-1) were kindly provided by Dr. Nicole Bedke. RT-qPCR was preformed by Victor Paky Bondanese.

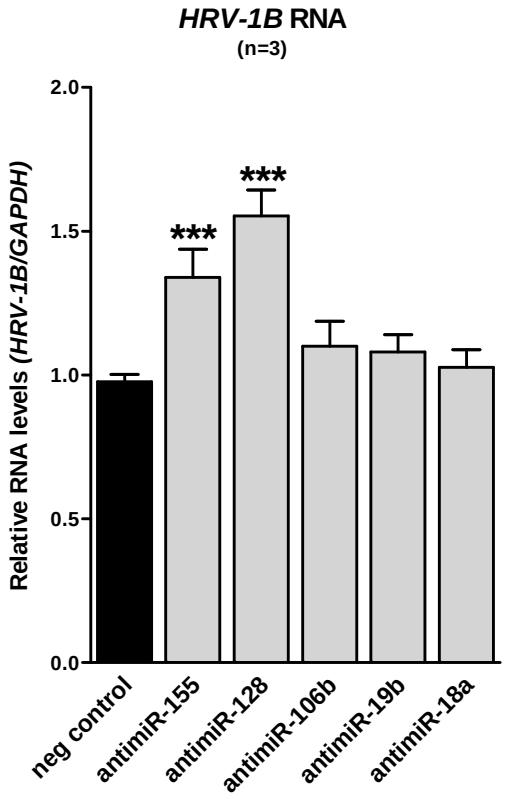

fig. 4-3. Antiviral activity of miR-155 and miR-128 in BEAS-2B cells.
BEAS-2B cells were transfected with the antimiRs indicated. The following day they were infected with HRV-1B at MOI of 0.01. HRV-1B was measured by RT-qPCR from samples collected at 8 hours post-infection. The values plotted represent the average, while the error bars represent the SD, from 3 biological replicates. ***=$p<0.001$; where nothing is indicated the difference was not significant, as compared to negative control antimiR.
P values were calculated using one way ANOVA with Bonferroni post-test correction.

4.2 MicroRNAs deficient in asthmatic BECs modulate downstream effects of IL-13 and TGF-β.

4.2.1 Rationale.

It is widely accepted that IL-13 (Berry et al. 2004, Huang et al. 1995, Humbert et al. 1997) and TGF-β (Torrego et al. 2007) play important roles in asthma. Both cytokines have a dramatic effect on the physiology of lung epithelium, and may be largely responsible for the inflammation and remodelling associated with asthma. Rhinoviral infections are a major trigger of asthma exacerbations. TGF-β has been shown to increase replication of respiratory viruses in fibroblasts (Thomas et al. 2009) and bronchial epithelial cells (McCann & Imani 2007) and also IL-13 has been suggested to favour HRV replication in the asthmatic lung epithelium (Lachowicz-Scroggins et al. 2010).

Very interestingly, in the present investigation it has been found that among others, miR-155 is less abundant in asthmatic BECs. This is potentially of great relevance to asthma, because of the role played by the two cytokines just mentioned. In fact, microRNA-155 has been shown to attenuate the cellular signalling of IL-13 and TGF-β (see fig. 4-4). Specifically, the microRNA directly targets *IL13RA1*, subunit of the receptor for IL-13 (Martinez-Nunez et al. 2011) and *SMAD2*, an important mediator in TGF-β signal transduction (Louafi et al. 2010).

In addition, at least other two microRNAs identified together with miR-155 are predicted to have the same targets, namely miR-18a and miR-128. In particular, while miR-18a is predicted to target *SMAD2*, miR-128 is predicted to target both *SMAD2* and *IL13RA1*. In addition, miR-128 has already been shown to affect negatively TGF-β signalling by targeting one of the receptor subunits, *TGFBR1* (Masri et al. 2010) and it is predicted to target also *SMAD4*. MiR-18a and miR-19b have been shown to be potent inhibitors of TGF-β signalling (Mestdagh et al. 2010). MiR-18a is also predicted to target STAT6, key molecule in IL-13 pathway. Also miR-106b has been shown to affect TGF-β pathway by targeting *TGFBR2* (Wang et al. 2010a). Among the microRNAs that have not been validated yet but the array data suggested being lower in asthmatic BECs, miR-21 has been shown to target the TGF-β receptor subunit *TGFBR2* (Kim et al. 2009). Overall, the array data presented here suggest that the microRNA deficiency uncovered in asthmatic BECs, may be important in asthma by favouring especially TGF-β but also IL-13 signalling. Although the differences measured for each microRNA can be considered modest, intriguingly their individual effects may sum together by converging on the same pathways (see fig. 5-2). Moreover, all the microRNAs identified are abundantly expressed in primary BECs (fig. 4-5).

Hence, we hypothesised that microRNA deficiency in BECs has an important role in asthma, through its ability to modulate the cellular responses to IL-13 and TGF-β. Such deficiency may allow a stronger response to these cytokines and be responsible for important features of chronic asthma besides facilitating viral replication. Because our group had shown that microRNA-155 targets both TGF-β and IL-13 pathways, this microRNA was exploited more than the others mentioned here, in order to test this hypothesis.

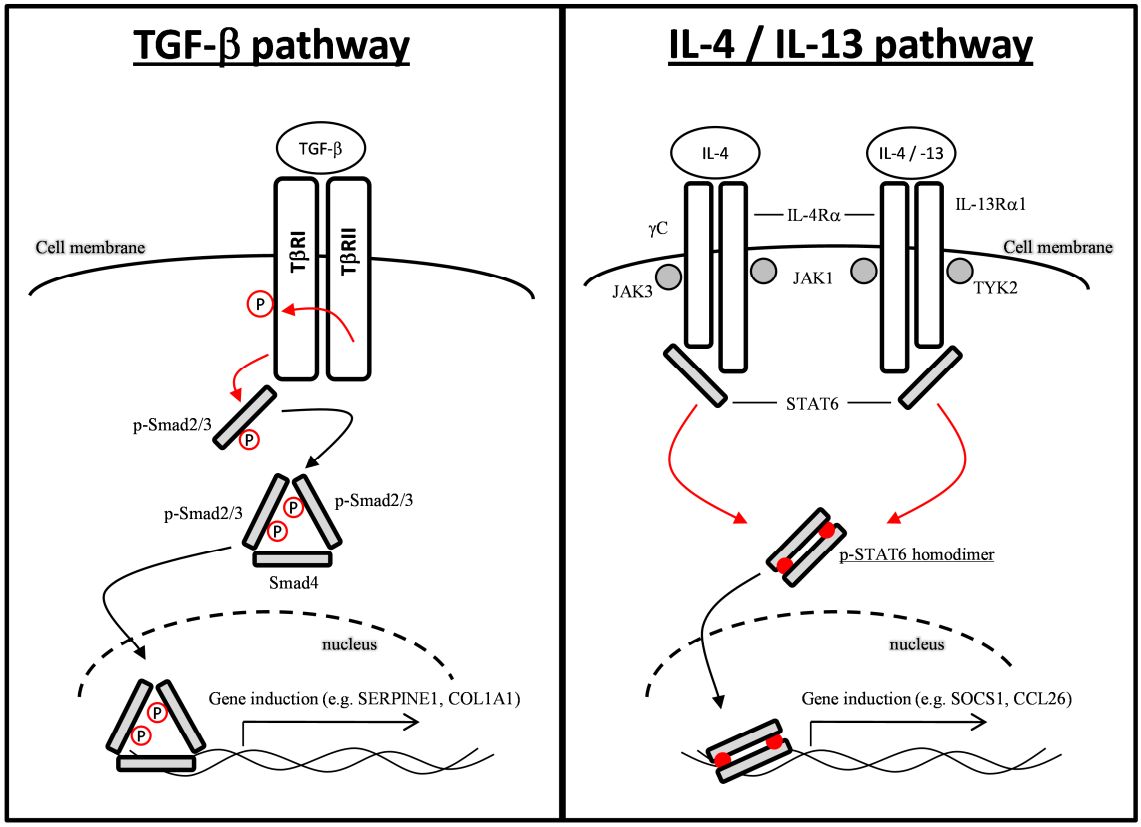

fig. 4-4. Schematic of TGF-β and IL-4 / IL-13 pathways.

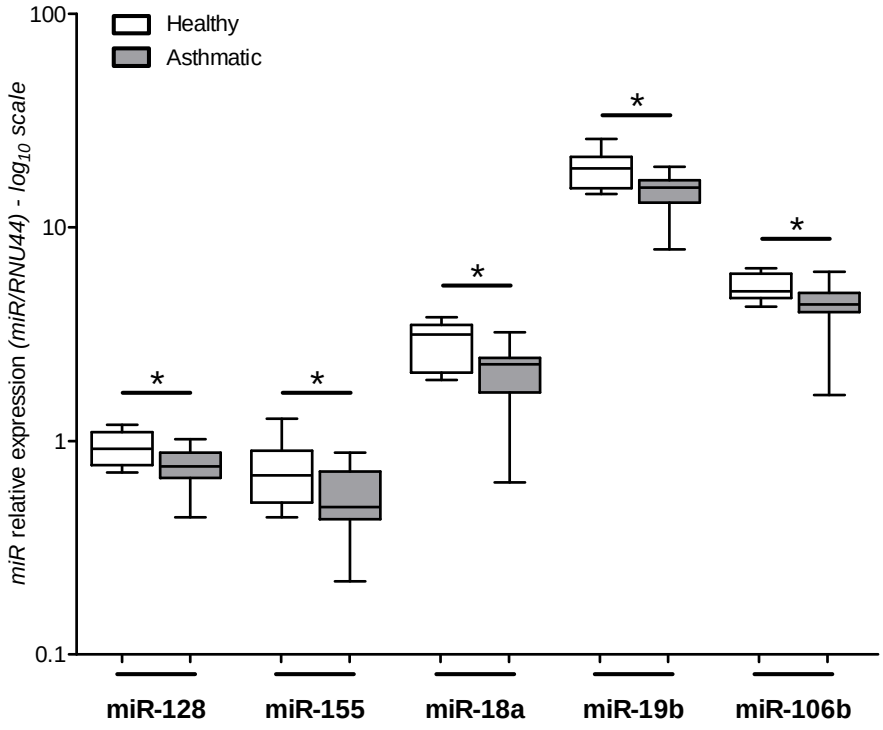

fig. 4-5. MicroRNAs hypothesised to affect TGF-β or IL-13 pathways have similar or higher expression compared to miR-155.

The data plotted are the same as for fig. 4-2 but here the different microRNAs have been normalised altogether, in order to highlight their relative abundance. MiR-128 average Ct value in healthy BECs is 29.7.

*=$p<0.05$. p values were calculated using Mann Whitney test.

4.2.2 Asthmatic BECs express less miR-155 and have higher expression of both its direct targets and genes induced by TGF-β and IL-13.

It was striking also that in the sample set available, expression of *SMAD2* and *IL13RA1* in primary BECs correlated strongly together (fig. 4-6). In particular, as expected from the expression of miR-155 in the two groups, asthmatic cells express these genes more than healthy ones. As a consequence, it was interesting to evaluate whether TGF-β and IL-13 downstream genes also presented a similar trend and specifically if asthmatic BECs expressed them at higher level.

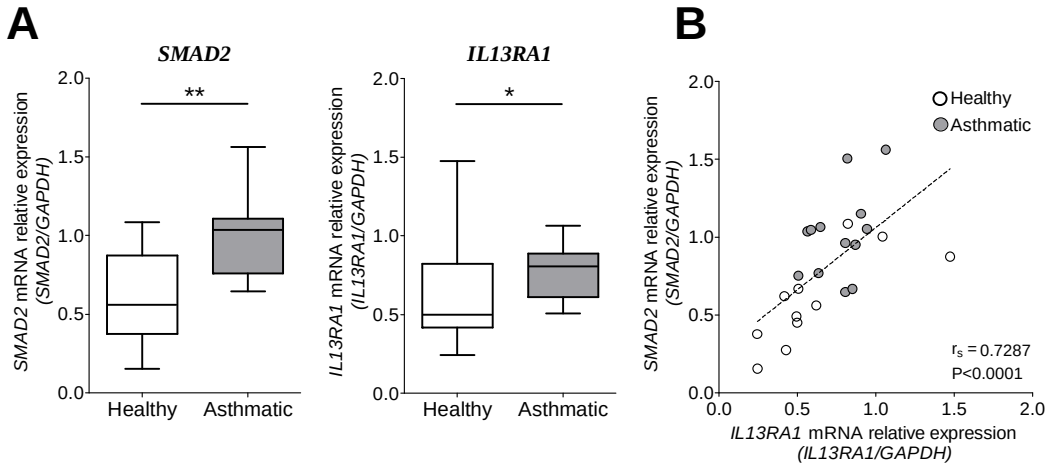

fig. 4-6. *SMAD2* and *IL13RA1* expression correlates in primary BECs and it is higher in asthmatic cells.

Expression of the genes indicated was measured by RT-qPCR, using RNA purified from healthy (n=10) or asthmatic (n=11) cultured primary BECs. (**A**) Relative expression values were plotted using box and wiskers plots, were 5 to 95 percentiles are shown. *=p<0.05; **=p<0.01. p values were calculated using Mann Whitney test. In (**B**) for each sample the expression of each gene is plotted on a separate axis. Nonparametric Spearman correlation analysis confirmed that there is a significant positive correlation between *SMAD2* and *IL13RA1*.

r_s=Spearman correlation coefficient.

All the RNA samples used for this figure (see table 2-1) were kindly provided by Dr. Nicole Bedke. RT-qPCR was preformed by Dr Fethi Louafi.

While *IL13* mRNA was not detectable, the expression of *TGFB1*, *TGFB2* and *TGFB3* could be measured by RT-qPCR (fig. 4-7). Although there was a trend for *TFGB2* to be higher in asthmatic cells, the three isoforms appeared to be expressed at comparable levels in the two groups of cells. The downstream genes measured were *SERPINE1*, *COL1A1* and *COL1A2*, for TGF-β while *SOCS1*, *IL8* and *CCL26* were measured for IL-13 signalling. As anticipated, this revealed a trend for asthmatics to express higher levels of all the genes measured, with *SOCS1* and *COL1A1* reaching statistical significance.

This observation provides an interesting insight on the status of bronchial epithelial cells in asthma, showing that TGF-β and IL-13 pathways are "switched on" already at baseline, promoting the over-expression of genes important in remodelling, such as *SERPINE1* and *COL1A1*, and inflammation such as *CCL26*.

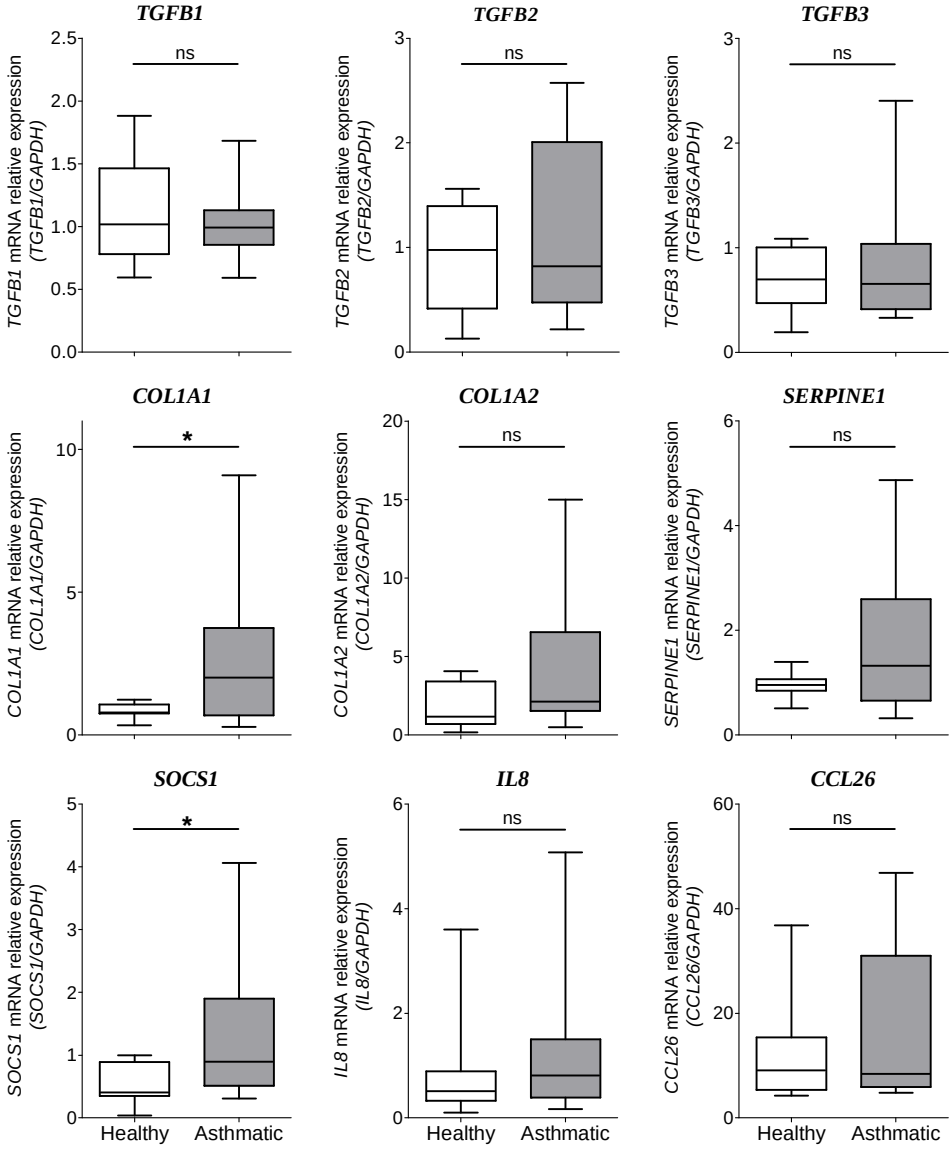

fig. 4-7. Genes responsive to TGF-β and IL-13 tend to be more expressed in asthmatic primary BECs.

Expression of the genes indicated was measured by RT-qPCR, from the same samples as in fig. 4-6. ns=non significant; *=p<0.05. p values were calculated using Mann Whitney test.

All the RNA samples used for this figure (see table 2-1) were kindly provided by Dr. Nicole Bedke. RT-qPCR was preformed by Dr Fethi Louafi.

4.2.3 MiR-155 expression in asthmatic BECs is not influenced by TGF-β.

TGF-β has been shown to either up- or down-regulate miR-155, depending on the cell model (Kong et al. 2008, Martin et al. 2006, Pottier et al. 2009). So it is conceivable that if TGF-β was able to down-regulate miR-155 in BECs, the higher TGF-β activity that is found in asthmatic lungs would be responsible for the lower expression of miR-155 in asthmatic BECs. In order to gather some evidence about this possibility we took advantage of being in a high profile asthma research centre. In fact, the same investigators who provided us with the samples from untreated BECs, which were used for the microRNA array, could show that in asthmatic BECs endogenous TGF-β2 production is responsible for increased p-SMAD2 (Dr Bedke N, unpublished data). In particular, they had treated primary BECs from asthmatics with either TGF-β2 or an anti-TGF-β2 blocking antibody. Measuring the expression of miR-155 in these samples (from 4 different donors) showed that the microRNA was not affected by TGF-β2 (fig. 4-8 B). Although some fluctuation was evident, none of the treatments induced any overall significant difference. Looking at each donor separately it is clear that the fluctuations were not dependent on TGF-β signalling: the direction of the fluctuations was always the same regardless of whether TGF-β2 or the blocking antibody was used. On the opposite, if miR-155 was regulated by TGF-β in these cells, the two treatments would have opposite or at least different effects. This was in fact what happened to *COL1A1* in the same samples. As expected, while exogenous TGF-β2 strongly induced *COL1A1* expression, the blocking antibody slightly reduced it (fig. 4-8 B).

This data encourage thinking that expression of miR-155 in the lung is not influenced by acute asthmatic episodes, and that in particular the microRNA is not influenced by TGF-β in asthmatic BECs, but it is rather an intrinsic characteristic of those cells.

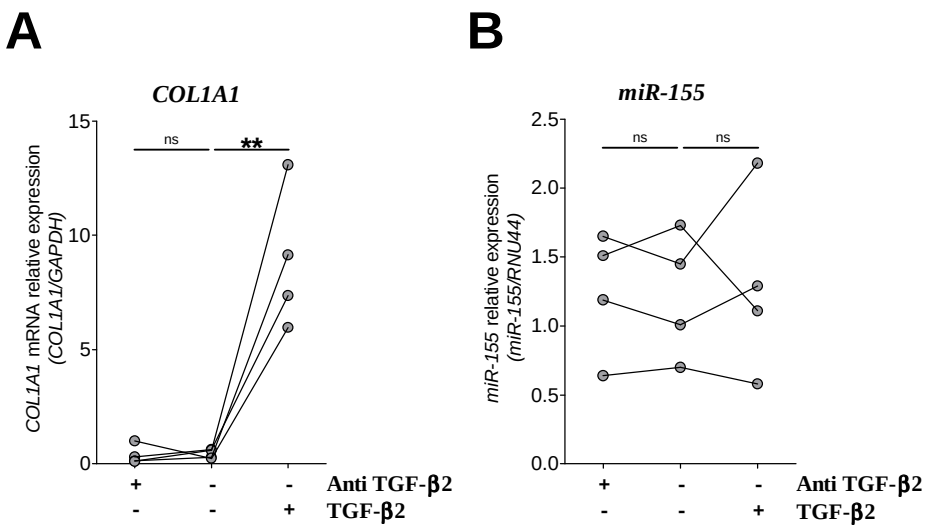

fig. 4-8. The expression of miR-155 in primary BECs from asthmatics is not affected by TGF-β.

Expression of *COL1A1* (**A**) or miR-155 (**B**) was measured by RT-qPCR in cultured primary BECs from 4 different asthmatic donors that were either mock treated, treated with anti-TGF-β2 blocking antibody or treated with TGF-β2 (10ng/ml) for 24 hours. These samples were kindly provided by Dr N. Bedke.

ns=non significant; **=p<0.01. p values were calculated using the repeated-measures (paired) one-way ANOVA test with Bonferroni correction.

All the RNA samples used for this figure (see table 2-1) were kindly provided by Dr. Nicole Bedke. RT-qPCR was preformed by Victor Paky Bondanese.

4.2.4 Over-expression of miR-155 in BEAS-2B cells mimics differences in gene expression between healthy and asthmatic BECs.

In order to study the role of miR-155 in human BECs, two cell lines were generated that differ in the expression of the microRNA. BEAS-2B cells were stably transduced with lentiviral constructs expressing either a negative control shRNA (B2B-C) or miR-155 (B2B-155). The two cell lines were assessed regarding the expression of miR-155 and the same panel of genes shown for primary BECs. This confirmed that as expected, B2B-155 had higher levels of miR-155 compared to B2B-C. In turn, this affected the expression of not only direct targets of miR-155 such as *SMAD2*, *IL13RA1* and *SOCS1* but also *COL1A1* (fig. 4-9).

In summary, altering the levels of miR-155 in BEAS-2B cells, induced changes in gene expression that mirror the differences observed between healthy and asthmatic BECs.

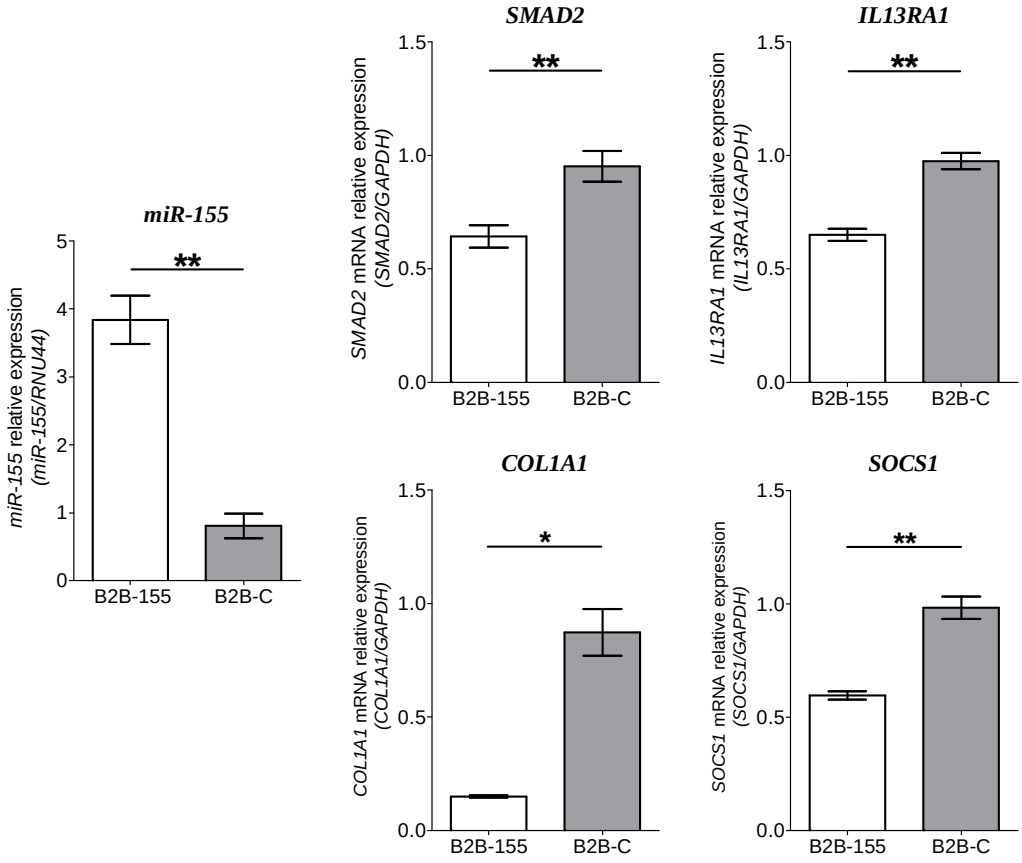

fig. 4-9. Over-expression of miR-155 in BEAS-2B cells reduces the levels of *SMAD2* and *IL13RA1* mRNA.

BEAS-2B cells were stably transduced with lentiviral constructs expressing either a negative control shRNA (B2B-C) or miR-155 (B2B-155). miR-155, *SMAD2*, *IL13RA1*, *SOCS1* and COL1A1 expression were measured by RT-qPCR in the cell lines selected. The values plotted represent the average, while the error bars represent the SD, of three independent experiments.
*=$p<0.05$; **=$p<0.01$. p-values were calculated using the unpaired t-test.
The cell lines B2B-C and B2B-155 were generated as described in paragraph 2.12.1 by Ana Francisco Garcia in collaboration with Victor Paky Bondanese and Dr Fethi Louafi. All the data plotted in this figure have been generated by Dr Fethi Louafi.

4.2.5 Over-expression of miR-155 reduces the response to TGF-β and IL-13.

The BEAS-2B derived cell lines were treated with either TGF-β1, IL-13 or left untreated. RNA was then extracted 24 hours later and expression of responsive genes was measured by RT-qPCR (fig. 4-10). *SERPINE1* and *COL1A1* were used to assess the response to TGF-β, while *SOCS1* and *CCL26* were used to assess the response to IL-13. As expected, after treatment B2B-C cells expressed significantly higher levels of the genes analysed compared to B2B-155.

In fact, following TGF-β treatment, *SERPINE1* mRNA was up-regulated about 12-fold in control cells, but only about 8-fold in B2B-155. Regarding *COL1A1* expression, it was several folds higher in B2B-C than in B2B-155 cells, both before and after TGF-β treatment (fig. 4-10 A).

A similar pattern was also observed following IL-13 treatment. Expression of *SOCS1* was nearly 3-fold increased in B2B-C while it reached only two-fold induction in B2B-155. *CCL26* was up-regulated about 2-fold by IL-13 in B2B-C, while only 1.5 times in the cells over-expressing miR-155 (fig. 4-10 B).

These data demonstrate that in bronchial epithelial cells, miR-155 is able to modulate the cellular response to TGF-β and IL-13. In particular, cells with lower levels of the miR, as it is the case of primary BECs from asthmatic patients, exhibit higher response to both cytokines. This translates into higher expression of genes involved in remodelling (*SERPINE1* and *COL1A1*) and inflammation (*CCL26*) that have been shown to have a role in asthma.

4.2.6 Over-expression of miR-155 is able to counteract the increase in HRV replication induced by TGF-β.

B2B cell lines were treated with 10ng/ml of TGF-β and 48 hours later they were infected with HRV-1B or HRV-16 at MOI of 0.1. Cells were harvested 8 hours post-infection and viral RNA was measured by RT-qPCR. In both cell lines, TGF-β was able to enhance replication of both viruses. However, such increase was higher in B2B-C as compared to B2B-155 cells (fig. 4-11). Over-expression of miR-155 reduced the amount of HRV-1B RNA in treated cells from 2.5 to 1.5 fold (compared to untreated B2B-C cells). Similarly, it nearly halved the amount of HRV-16 RNA in treated cells.

In summary, the last piece of data show that reduced levels of miR155, allowing a stronger TGFβ signalling, lead to higher HRV replication.

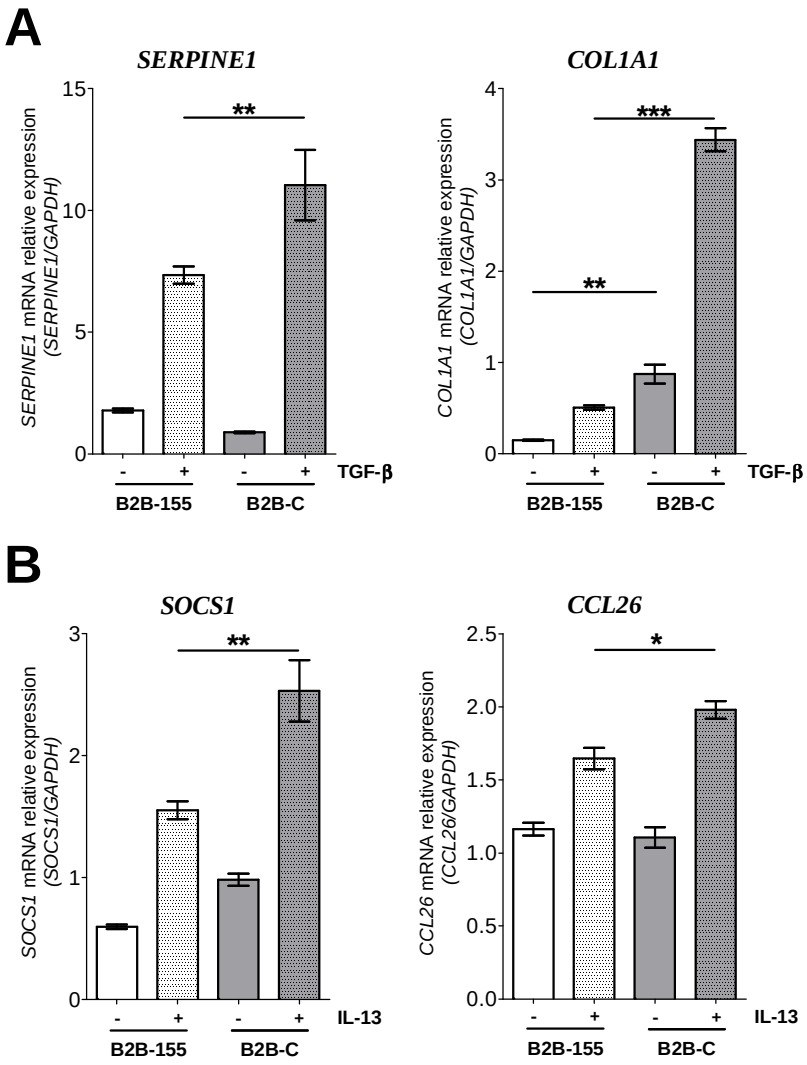

fig. 4-10. Over-expression of miR-155 reduces the effects of TGF-β and IL-13 in BEAS-2B cells.

B2B-C and B2B-155 cells were either mock treated or treated with 10ng/ml of TGF-β1 or 60ng/ml of IL-13. 24 hours after treatment, expression of (**A**) TGF-β responsive genes *SERPINE1* and *COL1A1* or (**B**) IL-13 responsive genes *SOCS1* and *CCL26* was measured by RT-qPCR. The values plotted represent the average, while the error bars represent the SD, of three independent experiments. *=p<0.05; **=p<0.01; ***=p<0.001. p-values were calculated using one-way ANOVA with Bonferroni post-test correction.

All the data plotted in this figure have been generated by Dr Fethi Louafi and Victor Paky Bondanese.

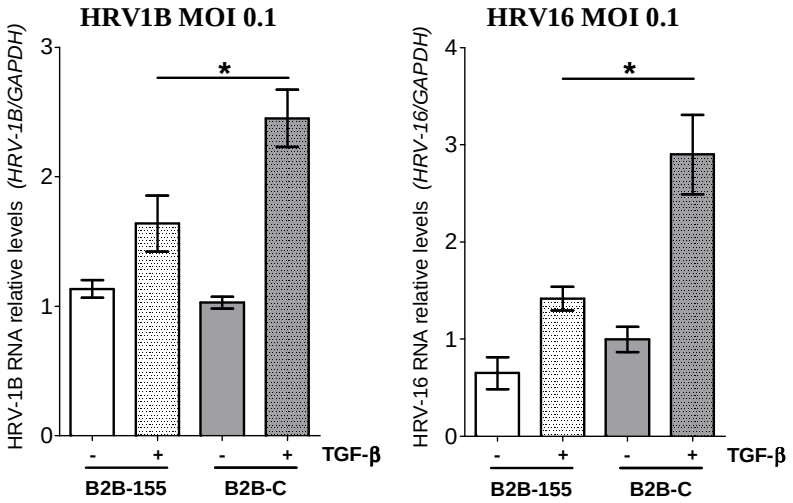

fig. 4-11. Over-expression of miR-155 in BEAS-2B cells counteracts the increased HRV replication induced by TGF-β.

B2B-C and B2B-155 cells were treated with 10ng/ml of TGF-β1. 48 hours later cells were infected with either HRV-1B or HRV-16 at MOI of 0.1. 8 hours post-infection cells were harvested and HRV-1B or HRV-16 RNA was measured by RT-qPCR. The values plotted represent the average, while the error bars represent the SD, of three independent experiments.

*=$p<0.05$. p-values were calculated using one-way ANOVA with Bonferroni post-test correction.

All the data plotted in this figure have been generated by Dr Fethi Louafi and Victor Paky Bondanese.

4.2.7 Inhibiting miR-155 or miR-18a in BEAS-2B cells is able to influence genes downstream TGF-β.

In order to confirm that what was shown by over-expressing miR-155 could be obtained also by inhibiting the activity of the microRNA, BEAS-2B cells were transfected with either a negative control antimiR, or antimiRs specific against miR-155 or miR-18a. 24 hours later cells were treated with either 0.2 or 1 ng/ml of TGF-β1 or mock treated. Further 24 hours later, cells were harvested and mRNA *SERPINE1* was measured by RT-qPCR. As shown in fig. 4-12, inhibiting either microRNA resulted in higher induction of the TGF-β responsive gene. Noteworthy is the intensity of such increase. When miR-18a was inhibited, 0.2ng/ml of the cytokine was able to induce almost as much *SERPINE1* as 1ng/ml of TGF-β did in the negative control (around 6 times higher than negative control mock treated). In other words, inhibiting the microRNA resulted in about 5-fold increase of the efficacy of the cytokine. Also striking was the increase due to silencing the microRNAs of *SERPINE1* expression at baseline (0 ng/ml of TGF-β) which was more than twice higher than the negative control. Finally, when 1 ng/ml TGF-β was used, *SERPINE1* induction went from about 6 in the negative control to about 30 times higher than untreated negative control, in the cells where miR-155 or miR-18a had been inhibited. Although this experiment has been performed only once, it reinforces that miR-155 affects TGF-β signal transduction in BEAS-2B cells, and clearly shows that also miR-18a influences the same pathway.

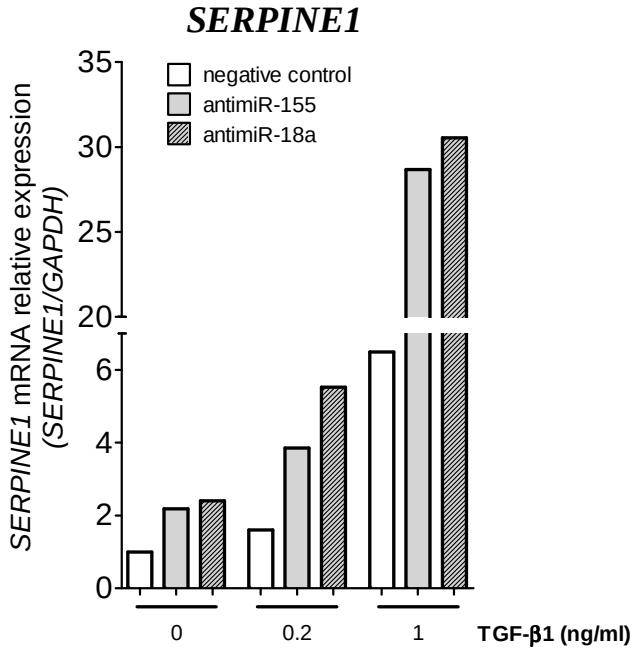

fig. 4-12. Both miR-155 and miR-18a influence TGF-β pathway in BEAS-2B cells.
BEAS-2B cells were transfected with negative control or specific antimiRs against miR-155 or miR-18a. 24 hours later cells were treated with the amount of TGF-β1 indicated (or mock treated). *SERPINE1* expression was calculated using *GAPDH* as reference gene and mock-treated negative control as calibrator sample. The y axis has been broken into two segments in order to highlight that inhibition of the microRNAs caused higher expression of *SERPINE1* already at baseline (more than 2-fold difference). The values plotted are from a single experiment.

4.3 Discussion.

One of the hypotheses that have inspired this project is that there may be differences in microRNA expression between asthmatic and healthy bronchial epithelial cells (BECs) contributing to asthmatic features of this cell type, such as higher viral replication.

In order to investigate this possibility, we performed microRNA RT-qPCR arrays on RNA extracted from cultured primary BECs and we found that indeed there are small differences in the expression of a few microRNAs. Strikingly, most microRNAs differentially expressed are less abundant in asthmatics, while only a few are more abundant (fig. 4-1).

Other groups looked into whether microRNAs are differentially expressed in healthy and asthmatic lungs. For instance, Williams et al. (Williams et al. 2009) performed microRNA arrays from bronchoscopic biopsies, finding no differences between the two groups. However, the authors suggest that their negative results may be explained considering that a biopsy includes many different cell types, and they show that in fact those cell types express microRNAs at different levels. One limitation of that paper is that for this purpose they used a mixture of primary and immortalised cells. For example they used BEAS-2B cells rather than primary BECs. Nevertheless, they convincingly show that the expression of microRNAs is very different in the different cell types that can be found in a biopsy: monocytic cells, fibroblasts, BECs and airway smooth muscle cells. On the contrary, our array data is based on only one cellular type: primary BECs. Those cells were obtained by brushing the bronchial epithelium during bronchoscopies, and were then cultured in-vitro for only two passages. Therefore they are a very precious material and they represent one of the best models to study the epithelial cells of human airways.

Eight microRNAs, under-expressed in asthmatic BECs according to the array results, were also predicted to target both HRV-1B and -16 (table 4-1 C). However, only five of those miRs were validated using single assay RT-qPCR. This means that measuring their expression in a large number of samples, confirmed that they are significantly more abundant in healthy than asthmatic BECs (fig. 4-2).

This finding, together with our previous results, encouraged us to question whether such a microRNA deficiency plays a role in the higher replication that Rhinoviruses have in asthmatic BECs (Wark et al. 2005). In fact, our Ago2 co-IP results in BEAS-2B cells suggest that, by 6 hours post-infection, microRNAs make direct contact with HRV-1B RNA in bronchial epithelial cells. Therefore, we hypothesised that the microRNAs we validated are actually able to bind to the viral RNA and hamper viral replication. In order to test this hypothesis, BEAS-2B cells were employed again. Oligonucleotides antagonists of microRNAs (antimiRs) were used to silence the validated microRNAs one at a time. The results presented here show that miR-155 and miR-128 are able to reduce HRV-1B replication in BEAS-2B cells. In fact, transfection of

antimiRs specific for either microRNA, increased viral replication compared to negative control (fig. 4-3). The experiment performed cannot exclude the possibility that this is an indirect effect. Reducing the activity of those two microRNAs could have affected for instance the IFN-related antiviral machinery. Measuring the expression of IFNs, or genes induced by IFNs, would clarify this point. However, speculations can be made that exclude the possibility of an indirect effect. For example, since miR-155 targets SOCS1, an inhibitor of type I IFN induction (Wang et al. 2010), it can be assumed that reduction of miR-155 favoured viral replication through increase of SOCS1. However, miR-19b has also been shown to target SOCS1 (Pichiorri et al. 2008) but its reduction did not have any effect on viral replication, at least within 8 hours post-infection. However, the use of a more straightforward approach, such as Ago2 co-IP, would be ideal. Indeed, if miR-155 and -128 hampered viral replication by a direct mechanism, the association of viral RNA with Ago2 would be reduced in cells where those miRs were knocked-down. This could be tested in the future, as mainly time limits prevented me from doing so.

The microRNA deficiency found in asthmatic BECs may also be at the base of the other observations we could make regarding their gene expression. In fact, looking at mRNA expression, we also found that both *SMAD2* and *IL13RA1* are higher in asthmatic BECs (fig. 4-6) which also have less miR-155 (fig. 4-5) and this seems to have consequences on the above mentioned pathways. Asthmatic primary BECs in fact, show a trend to over-express several genes that are downstream TGF-β and IL-13 pathways, in the absence of any treatment, with *COL1A1* and *SOCS1* reaching statistical significance (fig. 4-7). In the same way, BEAS-2B cells with lower miR-155 expression, over-expressed *SMAD2*, *IL13RA1*, *COL1A1* and *SOCS1* (fig. 4-9) and in addition, they were more responsive to TGF-β and IL-13 (fig. 4-10). Not only miR-155 was able to reduce the expression of genes sensitive to TGF-β, but the microRNA also clearly contrasted the increased replication of both HRV-1B and -16 induced by TGF-β (fig. 4-11).

Strikingly, while it was possible to show in BEAS-2B cells that knock-down of miR-155 favours HRV-1B replication by 8 hour p.i. (fig. 4-3), its up-regulation did not have the opposite effect (fig. 4-11). These may seem contrasting results at first, but actually they can be explained by assuming that the amount of miR-155 expressed is already at saturating levels, for the miR to have antiviral activity. In such case in fact, reducing miR-155 below a critical point would be expected to promote viral replication. On the contrary its over-expression, would produce molecules that are in excess and do not have an antiviral role.

Although using only a limited number of donors, it was also observed that TGF-β does not influence the expression of miR-155 in asthmatic BECs. This is an interesting finding. In fact, it has been previously shown that miR-155 is down-regulated by TGF-β in lung fibroblasts

(Martin et al. 2006, Pottier et al. 2009) but such investigation has not been performed on primary BECs. However, in the paper by Pottier et. al. (Pottier et al. 2009) they report that TGF-β had no effect on miR-155 in A549 cells, a human alveolar epithelial cell line. Our results on primary BECs are in agreement with this observation and, if confirmed in a larger population, imply that the asthmatic microRNA deficiency is intrinsic to the epithelium, rather than being the effect of the higher TGF-β activity seen in asthmatics. For the same reasons, it would then be interesting to verify whether any of the other microRNAs identified in this study, are affected by TGF-β or IL-13.

Chapter 5

General discussion and future research.

Asthma is a disease with high prelevance worldwide, counting around 300 million people affected and 250,000 estimated deaths per year (GINA 2010). There is no cure for asthma and it is a lifelong condition, where patients suffer from recurrent airflow reduction. Therefore, management of asthma consists in keeping the symptoms under control. This is mainly achieved by avoiding the triggering factors and using a combination of reliever and controller medications (Bernstein 2008, GINA 2010). Although the current asthma management allows patients to lead a good life style, it is not able to avoid asthma exacerbations (Holgate 2005). The latter are severe worsening of the asthmatic symptoms that still occur in controlled patients, and can be life thretening. Therefore, prevention and treatment of asthmatic exacerbtations represent an unmet clinical need. Most asthma exacerbations are associated with respiratory viral infections. Human Rhinovirus (HRV) has been shown to be the virus most often associated with exacerbations (Johnston 2005). From here comes the need to understand the biology of this virus and in particular, what makes lung cells from asthmatics less apt to deal with Rhinovirus compared to healthy cells.

The aim of this project was to evaluate the contribution of microRNAs in this context. MicroRNAs are small non-coding RNA molecules that have received much attention for their ability to regulate gene expression by inhibiting translation. Besides being key regulators of cellular gene expression, microRNAs are also part of the antiviral “arsenal” of the innate immunity (Pedersen et al. 2007).

Two hypotheses were investigated in this project:

1) Cellular microRNAs have antiviral activity against human Rhinovirus.
2) Differences in the expression of microRNAs between asthmatic and healthy BECs contribute to the higher replication that HRV has in asthmatic cells.

The main findings of this thesis are:

1) Impairing microRNA biogenesis, by the prolonged silencing of *DICER*, favours HRV-1B replication in BEAS-2B cell lines.
2) Ago2-containing miRISCs associated with HRV-1B RNA, during infection of BEAS-2B cells.

3) Asthmatic primary BECs express a pool of microRNAs at lower levels compared to healthy counterparts. They also over-express, at baseline, genes that are downstream IL-13 and TGF-β pathways.
4) MiR-155 and miR-128 are involved in the antiviral defence against HRV-1B in BEAS-2B cells.
5) MiR-155 is able to blunt the expression of genes responsive to IL-13 and TGF-β in BEAS-2B cells.

Impairing microRNA biogenesis, by the prolonged silencing of *DICER*, favours HRV-1B replication in BEAS-2B cell line.

Interestingly, although viral replication was increased by silencing *DICER* for a prolonged period, it can be speculated that the IFN production did compensate the loss of the microRNA-mediated antiviral activity. Although IFN production was not affected, as assessed by measuring IFN-β mRNA, viral replication was significantly higher in the cells with lower *DICER* mRNA. A similar study was performed on Influenza A (Matskevich & Moelling 2007). In this paper they show that *DICER* is protective against Influenza A. This was particularly evident in Vero cells, while it was much more modest when they used A549 cells. They also pointed out that this is due to the IFN produced only by the second cells. In fact, Vero cells did not produce IFN during infection, while the human A549 cells did. However they did not clarify whether microRNAs were directly involved in the antiviral protection. Our results instead, demonstrate that *DICER* and microRNAs are active against HRV-1B replication. In fact their reduction leads to a significant increase in viral replication, and this has been shown both by silencing *DICER* (fig. 3-9), which leads to a global reduction of microRNAs, and by silencing specific microRNAs, miR-155 and miR-128 (fig. 4-3).

In general these microRNAs can be expected to have antiviral activity in any cell infected by Rhinovirus. Moreover, it can be speculated that what has been shown for Influenza A applies also to HRV. Cells that do not produce IFN in response to HRV infection could be expected to depend much more on microRNAs for their antiviral resistance. Among such cells, lung fibroblasts may be of interest. In fact, it has been shown that primary lung fibroblasts, from both asthmatic and healthy subjects are productively infected by Rhinovirus. No difference in replication between the two groups was evident. But strikingly, fibroblasts were shown to not produce IFNs in response to viral infection (Bedke et al. 2009). Therefore, it can be expected that microRNAs constitute the main antiviral effectors in lung fibroblasts, and manipulating their expression could prove an interesting therapeutic possibility. The authors of this paper suggest in fact that in a healthy lung, Rhinoviral infection of fibroblasts would be prevented by the bronchial epithelium. While in asthmatic lungs, a more disrupted epithelium may expose the underlying fibroblasts to the virus. For this reason, fibroblasts may constitute an important

reservoir of viral replication, only available in an asthmatic lung (Bedke et al. 2009). Administration of antiviral microRNAs could reach also the exposed fibroblasts in asthmatic lungs and therefore deny such reservoir to the virus.

Ago2-containing miRISCs associate to HRV-1B RNA, during infection of BEAS-2B cells.

As already discussed, it was not possible to provide causal proof that microRNAs hamper HRV-1B replication by a direct mechanism. For this purpose, lentivirally transduced BEAS-2B cells were generated. Unfortunately, they resulted not to be functional and serve the initial purpose. As a consequence, in the future such a proof may be obtained in a number of different ways. Obviously the same strategy may be used. In particular other *DICER* shRNA sequences can be tested and finally one or two functional shRNAs may be adopted. As already mentioned then, Ago2 co-IP could be performed after silencing miR-155 or miR-128, which have been shown to protect against HRV-1B infection (fig. 4-3). Confirmation that these two microRNAs bind to viral RNA can also be achieved by pull-down of biotinylated miR mimics (pre-miRs). The biotin would in fact allow co-purifying the microRNA together with all its targets (Orom & Lund 2007). Finally, also HITS-CLIP could be used. This is a very complex technique, yet very potent because identifies target sequences of microRNAs. Briefly, fragments of microRNA targets, with the bound microRNAs are purified by Ago co-IP. High throughput sequencing is then adopted in order to obtain the sequence of those fragments that in turn, can be used to determine both the microRNA involved and the target (Chi et al. 2009).

Asthmatic primary BECs express a pool of microRNAs at lower levels compared to healthy counterparts. They also over-express at baseline, genes that are downstream IL-13 and TGF-β pathways.

MicroRNA expression and their possible role in asthma, has been investigated in mouse models of allergic asthma. These papers focus on microRNA expression of immune cells and show that several microRNAs are deregulated in asthmatic mice. Studying the role of some of these microRNAs in relation to inflammatory responses, they suggest that targeting microRNAs in the airways may constitute anti-inflammatory treatments for allergic asthma (Lu et al. 2009, Mattes et al. 2009, Polikepahad et al. 2010).

However, such analysis has not been done in humans. In particular microRNA expression of primary BECs had not been studied. This prompted us to compare the microRNA profiles of healthy and asthmatic BECs. Our array data show that a few microRNAs are less expressed in the asthmatic cells compared to healthy BECs.

Very interestingly, some miRs among the ones identified to be poor in asthmatic BECs, were predicted to target efficiently HRV-1B or HRV-16. We decided to focus our attention only on those that were predicted to target both viruses, because of the idea that conservation should be a mirror of function. But actually this is not an evolutionary conservation. It is possible in fact,

that there is a pool of antiviral miRs, with each one targeting a different viral genotype so that altogether they target a large number of different genomes. This idea could be tested by knocking down other miRs that are predicted to target only one of the two viruses and then verify if the predictions are confirmed.

Identification of a microRNA deficiency in asthmatic primary BECs also triggered to question what are the consequences that this entails in terms of cellular functions, not only in terms of viral replication. From our data, it is clear that the levels of *SMAD2* and *IL13RA1* correlate in primary BECs, and that asthmatic cells tend to express more of both (fig. 4-6). This constitutes a novel and very interesting finding because *IL13RA1* and *SMAD2* are key molecules in two pathways, respectively IL-13 and TGF-β, that play important roles in asthma. IL-13 (Huang et al. 1995, Humbert et al. 1997) and TGF-β2 (Sagara et al. 2002, Torrego et al. 2007) are expressed more in asthmatics than in healthy subjects, both at rest and after acute asthmatic episodes such as allergen challenge. IL-13 has several effects highly relevant to asthma, such as airway-smooth-muscle hyperplasia, eosinophilic recruitment, regulation of IgE production, induction of mucus, to say a few (Wynn 2003). This has boosted the interest in this cytokine as a therapeutic target, and indeed blocking its activity is regarded as a promising therapeutic approach (Holgate & Polosa 2008). Also TGF-β is widely considered to contribute to the pathophysiology of asthma. For instance, TGF-β expression has been shown to correlate with the thickness of the basal membrane in lungs of asthmatics (Vignola et al. 1997) and to be induced by bronchoconstriction (Grainge et al. 2011) which typically occurs during acute asthmatic episodes. Not only TGF-β favours the establishment of airway remodelling in asthma but it has also been suggested to favour virus-induced asthma exacerbations by dampening innate immune responses (Thomas et al. 2009). Strikingly, all the microRNAs that were selected during this study because predicted to target both HRV-1B and -16 and whose expression was further validated, have already been shown or are predicted to affect both IL-13 and TGF-β pathways (see fig. 5-2). Since our group has shown that one of these microRNAs, namely miR-155, affects both pathways, a series of expertise and tools were easily available regarding this microRNA. Therefore, over-expression of the latter microRNA was an easy option to exploit in order to test the consequences of the differential expression of microRNAs targeting IL-13 and TGF-β pathways. Interestingly, modulating the expression of miR-155 in BEAS-2B cells roughly mimicked the differences observed in primary BECs. In fact the cells with less miR-155, expressed more *COL1A1*, *SERPINE1* and *SOCS1*, in the absence of any stimulation. This was shown for *COL1A1* and *SOCS1* by over-expressing miR-155 in BEAS-2B cells (fig. 4-9) while for *SERPINE1* it was shown by silencing miR-155 (fig. 4-12). By measuring *SERPINE1* mRNA also confirmed that miR-18a is able to affect TGF-β pathway in BEAS-2B cells (fig. 4-12).

The latter experiment was only performed once. Therefore in the future it will certainly be repeated and extended to include the other microRNAs identified during this project. This would be of great interested giving the following considerations. One limit of the investigation here presented is that while miR-155 was about 4-fold over-expressed in the lentivirally transduced BEAS-2B cell lines (fig. 4-9), the difference between asthmatic and healthy BECs, is more modest being nearly two-fold (fig. 4-2). We hypothesise that although each microRNA may have a small effect separately, because their activities converge on the same pathway (fig. 5-2) altogether they have a significant global effect. In order to prove this hypothesis more experiments are required where the amount of the identified microRNAs is reduced by only a modest percentage using specific antimiRs, either individually or altogether. If the effects of the microRNAs converge as hypothesised, it would be expected that reducing only one miR at a time had very little or no influence on the cellular response to TGF-β or IL-13. Reducing several miRs altogether would instead have a considerable effect. As a matter of fact, cooperation between different microRNAs targeting the same or related targets has already been documented, e.g. (Mestdagh et al. 2010, Nachmani et al. 2010). This would encourage generating a cell model for asthmatic BECs. BEAS-2B cells could be transduced with lentiviral constructs expressing antimiRs (Scherr et al. 2007) in order to mimic the microRNA profile of asthmatic BECs. Such a cell line would be used to test if it is possible to reproduce characteristics of asthmatic BECs, simply by modulating the expression of the selected microRNAs.

Furthermore, all these observations made on cell lines, could be followed by similar experiments using primary BECs. Transfecting little amounts of artificial microRNA mimics (pre-miRs) in asthmatic BECs, would be expected to make them more similar to healthy BECs, for instance regarding viral replication and IFN production (Uller et al. 2010, Wark et al. 2005) besides responsiveness to TGF-β or IL-13. In fact, our findings suggest that deficiency of the microRNAs identified makes cells hyper-responsive to the two cytokines, and this has effect already at baseline, with higher expression of *SOCS1* which in turn inhibits IFN production. At the same time, transfecting healthy BECs with antimiRs would be expected to give them a more "asthmatic" phenotype. This could ultimately be used also to test how those microRNAs affect lung biology, for example in the role of BECs during the differentiation of dendritic cells (Rate et al. 2009).

In summary, the data presented here suggest that asthmatic BECs present a deficiency in a few microRNAs that make them more sensitive towards TGF-β and IL-13. However, it is not known whether this is the case. Although our data show that asthmatic BECs tend to over-express certain genes responsive to TGF-β and IL-13 already at baseline, it is not known if asthmatic

cells would respond more strongly to the two cytokines compared to healthy cells. Therefore, in the future, exploring this possibility will be an essential part of understanding the role of microRNAs in the biology of bronchial epithelial cells in asthma.

Interestingly, the array data also identified that microRNAs belonging to the miR-17-92 cluster are under-expressed in asthmatic BECs. These microRNAs are all encoded closely together, in a region of genomic DNA, mapping at 13q31 (chromosome 13). MiR-17, 18a, 19a and b, 20a and 92 belong to this cluster and all of them, except from miR-92 are under-expressed in asthmatic BECs according to our array data. This is striking and prompts to ask whether there is a genetic correlation between asthma and this genomic region. Intriguingly, a French study reported correlation between locus 13q31 and the eosinophil count in asthmatics (Dizier et al. 2000). Although such correlation was not replicated in other studies (Bouzigon et al. 2010, Denham et al. 2008), it may reinforce the idea that those microRNAs have a role in the pathology of at least a subset of asthmatic subjects and encourage further investigation.

MiR-155 is able to blunt the expression of genes responsive to IL-13 and TGF-β in BEAS-2B cells.

The data presented clearly shows that the microRNAs identified to be under-expressed in asthmatic BECs, such as miR-155 and miR-18a, can dampen the effects of TGF-β and IL-13, two major determinants of the asthmatic pathophysiology.

Therefore, these microRNAs may constitute interesting targets for therapeutic purposes. Moreover, the variability in microRNA expression among the different donors inspires a personalised approach. MicroRNA profiling could precede the administration of a selected and subject-tailored pool of microRNAs aiming at compensating only the microRNAs that each subject shows unbalance in, compared to a healthy “consensus”. Definitely microRNAs hold the potential to be small but “on-target” effectors in the “next step” of a stratified medicine that seem to suit asthma probably more than other diseases, given its remarkable heterogeneity.

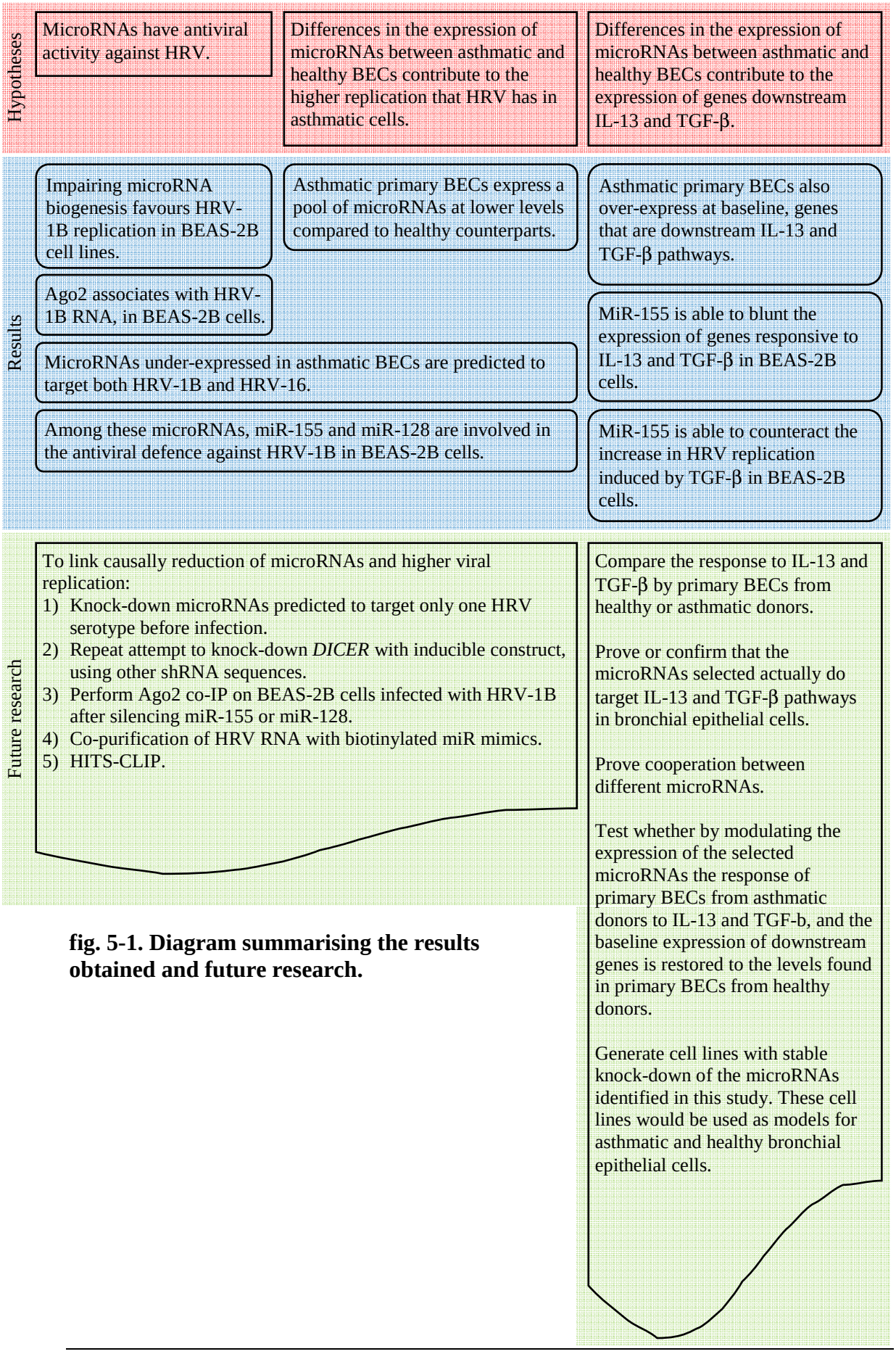

fig. 5-1. Diagram summarising the results obtained and future research.

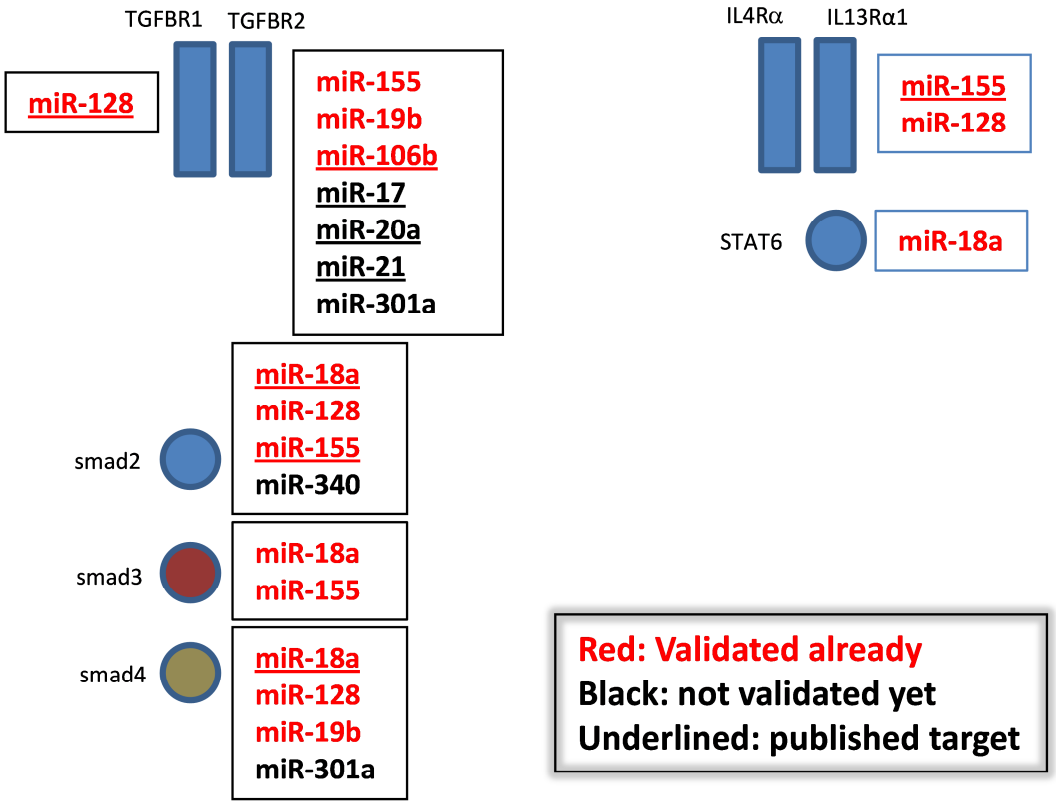

fig. 5-2. MicroRNA deficiency may increase TGF-β and IL-13 signaling in asthmatic BECs.

Schematic representation of the hypothesis presented based on the finding that several microRNAs are less expressed in asthmatic BECs. All the microRNAs reported here can be predicted or have been shown to target the mRNA of the gene they are next to, in this schematic. In this figure "validated" refers to the microRNA expression. Therefore, the microRNAs "not validated yet" are the ones identified by arrays (but not confirmed by single assay RT-qPCR) to be under-expressed in asthmatic BECs. For the predictions obtained from Targetscan 5.2 (Lewis et al. 2005) see appendix (paragraph 6.2).

Published microRNA targets:

- miR-155 / SMAD2 (Louafi et al. 2010).
- miR-18a / SMAD2 and SMAD4 (Mestdagh et al. 2010).
- miR-128 / TGFBR1 (Masri et al. 2010).
- miR-21 / TGFBR2 (Kim et al. 2009).
- miR-106b / TGFBR2 (Wang et al. 2010a).
- miR-17 / TGFBR2 (Mestdagh et al. 2010).
- miR-20a / TGFBR2 (Mestdagh et al. 2010, Volinia et al. 2006).
- miR-155 / IL13RA1 (Martinez-Nunez et al. 2011).

BIBLIOGRAPHY

Amineva, S., Aminev, A., Gern, J. & Palmenberg, A. (2011). **Comparison of Rhinovirus A Infection in Human Primary Epithelial Cells and HeLa Cells.** *J Gen Virol* .

Baraldo, S., Turato, G., Bazzan, E., Ballarin, A., Damin, M., Balestro, E., Oliani, K. L., Calabrese, F., Maestrelli, P., Snijders, D., Barbato, A. & Saetta, M. (2011). **Noneosinophilic asthma in children: relation with airway remodelling.** *Eur Respir J* **38**(3), 575–583.

Barbato, A., Turato, G., Baraldo, S., Bazzan, E., Calabrese, F., Panizzolo, C., Zanin, M., Zuin, R., Maestrelli, P., Fabbri, L. & Saetta, M. (2006). **Epithelial damage and angiogenesis in the airways of children with asthma.** *Am.J.Respir.Crit Care Med.* **174**(9), 975–981.

Bedke, N., Haitchi, H. M., Xatzipsalti, M., Holgate, S. T. & Davies, D. E. (2009). **Contribution of bronchial fibroblasts to the antiviral response in asthma.** *J Immunol* **182**(6), 3660–3667.

Beitzinger, M., Peters, L., Zhu, J., Kremmer, E. & Meister, G. (2007). **Identification of human microRNA targets from isolated argonaute protein complexes.** *RNA.Biol.* **4**(2), 76–84.

Bernstein, D. (2008). **ABCs of Asthma.** *Clin.Cornerstone.* **8**(4), 9–25.

Berry, M. A., Parker, D., Neale, N., Woodman, L., Morgan, A., Monk, P., Bradding, P., Wardlaw, A. J., Pavord, I. D. & Brightling, C. E. (2004). **Sputum and bronchial submucosal IL-13 expression in asthma and eosinophilic bronchitis.** *J Allergy Clin Immunol* **114**(5), 1106–1109.

Bouzigon, E., Forabosco, P., Koppelman, G. H., Cookson, W. O. C. M., Dizier, M.-H., Duffy, D. L., Evans, D. M., Ferreira, M. A. R., Kere, J., Laitinen, T., Malerba, G., Meyers, D. A., Moffatt, M., Martin, N. G., Ng, M. Y., Pignatti, P. F., Wjst, M., Kauffmann, F., Demenais, F. & Lewis, C. M. (2010). **Meta-analysis of 20 genome-wide linkage studies evidenced new regions linked to asthma and atopy.** *Eur J Hum Genet* **18**(6), 700–706.

Brown, B. D., Venneri, M. A., Zingale, A., Sergi, L. S. & Naldini, L. (2006). **Endogenous microRNA regulation suppresses transgene expression in hematopoietic lineages and enables stable gene transfer.** *Nat Med* **12**(5), 585–591.

Burgess, J. K. (2009). **The role of the extracellular matrix and specific growth factors in the regulation of inflammation and remodelling in asthma.** *Pharmacol Ther* **122**(1), 19–29.

Chen, Y., Hamati, E., Lee, P.-K., Lee, W.-M., Wachi, S., Schnurr, D., Yagi, S., Dolganov, G., Boushey, H., Avila, P. & Wu, R. (2006). **Rhinovirus induces airway epithelial gene expression through double-stranded RNA and IFN-dependent pathways.** *Am J Respir Cell Mol Biol* **34**(2), 192–203.

Chi, S., Zang, J., Mele, A. & Darnell, R. (2009). **Argonaute HITS-CLIP decodes microRNA-mRNA interaction maps.** *Nature* **460**(7254), 479–486.

Chiba, Y., Tanabe, M., Goto, K., Sakai, H. & Misawa, M. (2009). **Down-regulation of miR-133a contributes to up-regulation of Rhoa in bronchial smooth muscle cells.** *Am J Respir Crit Care Med* **180**(8), 713–719.

Contoli, M., Message, S. D., Laza-Stanca, V., Edwards, M. R., Wark, P. A. B., Bartlett, N. W., Kebadze, T., Mallia, P., Stanciu, L. A., Parker, H. L., Slater, L., Lewis-Antes, A., Kon, O. M., Holgate, S. T., Davies, D. E., Kotenko, S. V., Papi, A. & Johnston, S. L. (2006). **Role of deficient type III interferon-lambda production in asthma exacerbations.** *Nat Med* **12**(9), 1023–1026.

Cookson, W. (2002). **Asthma genetics.** *Chest* **121**(3 Suppl), 7S–13S.

Corne, J., Marshall, C., Smith, S., Schreiber, J., Sanderson, G., Holgate, S. & Johnston, S. (2002). **Frequency, severity, and duration of rhinovirus infections in asthmatic and non-asthmatic individuals: a longitudinal cohort study.** *Lancet* **359**(9309), 831–834.

Denham, S., Koppelman, G. H., Blakey, J., Wjst, M., Ferreira, M. A., Hall, I. P. & Sayers, I. (2008). **Meta-analysis of genome-wide linkage studies of asthma and related traits.** *Respir Res* **9**, 38.

Dharmage, S. C., Erbas, B., Jarvis, D., Wjst, M., Raherison, C., Norbäck, D., Heinrich, J., Sunyer, J. & Svanes, C. (2009). **Do childhood respiratory infections continue to influence adult respiratory morbidity?** *Eur Respir J* **33**(2), 237–244.

Didcock, L., Young, D. F., Goodbourn, S. & Randall, R. E. (1999). **The V protein of simian virus 5 inhibits interferon signalling by targeting STAT1 for proteasome-mediated degradation.** *J Virol* **73**(12), 9928–9933.

Ding, S., Li, H., Lu, R., Li, F. & Li, W. (2004). **RNA silencing: a conserved antiviral immunity of plants and animals.** *Virus Res.* **102**(1), 109–115.

Dizier, M. H., Besse-Schmittler, C., Guilloud-Bataille, M., Annesi-Maesano, I., Boussaha, M., Bousquet, J., Charpin, D., Degioanni, A., Gormand, F., Grimfeld, A., Hochez, J., Hyne, G., Lockhart, A., Luillier-Lacombe, M., Matran, R., Meunier, F., Neukirch, F., Pacheco, Y., Parent, V., Paty, E., Pin, I., Pison, C., Scheinmann, P., Thobie, N., Vervloet, D., Kauffmann, F., Feingold, J., Lathrop, M. & Demenais, F. (2000). **Genome screen for asthma and related phenotypes in the French EGEA study.** *Am J Respir Crit Care Med* **162**(5), 1812–1818.

Dölken, L., Malterer, G., Erhard, F., Kothe, S., Friedel, C. C., Suffert, G., Marcinowski, L., Motsch, N., Barth, S., Beitzinger, M., Lieber, D., Bailer, S. M., Hoffmann, R., Ruzsics, Z., Kremmer, E., Pfeffer, S., Zimmer, R., Koszinowski, U. H., Grässer, F., Meister, G. & Haas, J. (2010). **Systematic analysis of viral and cellular microRNA targets in cells latently infected with human gamma-herpesviruses by RISC immunoprecipitation assay.** *Cell Host Microbe* **7**(4), 324–334.

Donnelly, R. P. & Kotenko, S. V. (2010). **Interferon-lambda: a new addition to an old family.** *J Interferon Cytokine Res* **30**(8), 555–564.

du Lu, Y., hua Gan, Q., yuan Chi, X. & Qin, S. (2008). **Roles of microRNA in plant defense and virus offense interaction.** *Plant Cell Rep* **27**(10), 1571–1579.

Erjefält, J. S. & Persson, C. G. (1997). **Airway epithelial repair: breathtakingly quick and multipotentially pathogenic.** *Thorax* **52**(11), 1010–1012.

Esslinger, S. & Förstemann, K. (2009). **MicroRNAs repress mainly through mRNA decay.** *Angew Chem Int Ed Engl* **48**(5), 853–855.

Fahy, J. V. (2001). **Remodeling of the airway epithelium in asthma.** *Am J Respir Crit Care Med* **164**(10 Pt 2), S46–S51.

Fiala, M. & Kenny, G. E. (1967). **Effect of magnesium on replication of rhinovirus HGP.** *J Virol* **1**(3), 489–493.

Filipowicz, W., Bhattacharyya, S. N. & Sonenberg, N. (2008). **Mechanisms of post-transcriptional regulation by microRNAs: are the answers in sight?** *Nat.Rev.Genet.* **9**(2), 102–114.

Friedlander, S. & Busse, W. (2005). **The role of rhinovirus in asthma exacerbations.** *J.Allergy Clin.Immunol.* **116**(2), 267–273.

Gantier, M. P., McCoy, C. E., Rusinova, I., Saulep, D., Wang, D., Xu, D., Irving, A. T., Behlke, M. A., Hertzog, P. J., Mackay, F. & Williams, B. R. G. (2011). **Analysis of microRNA turnover in mammalian cells following Dicer1 ablation.** *Nucleic Acids Res* **39**(13), 5692–5703.

García-Sastre, A., Egorov, A., Matassov, D., Brandt, S., Levy, D. E., Durbin, J. E., Palese, P. & Muster, T. (1998). **Influenza A virus lacking the NS1 gene replicates in interferon-deficient systems.** *Virology* **252**(2), 324–330.

Garzon, R., Calin, G. A. & Croce, C. M. (2009). **MicroRNAs in Cancer.** *Annu Rev Med* **60**, 167–179.

Gern, J. (2003). **Mechanisms of virus-induced asthma.** *J.Pediatr.* **142**(2 Suppl), S9–13.

Gern, J. E., Galagan, D. M., Jarjour, N. N., Dick, E. C. & Busse, W. W. (1997). **Detection of rhinovirus RNA in lower airway cells during experimentally induced infection.** *Am J Respir Crit Care Med* **155**(3), 1159–1161.

GINA (2010)'From the Global Strategy for Asthma Management and Prevention, Global Initiative for Asthma (GINA) 2010. Available from: http://www.ginasthma.org/.'.

Grainge, C. L., Lau, L. C. K., Ward, J. A., Dulay, V., Lahiff, G., Wilson, S., Holgate, S., Davies, D. E. & Howarth, P. H. (2011). **Effect of bronchoconstriction on airway remodeling in asthma.** *N Engl J Med* **364**(21), 2006–2015.

Gregory, R., Yan, K., Amuthan, G., Chendrimada, T., Doratotaj, B., Cooch, N. & Shiekhattar, R. (2004). **The Microprocessor complex mediates the genesis of microRNAs.** *Nature* **432**(7014), 235–240.

Grünberg, K., Sharon, R. F., Sont, J. K., 't Veen, J. C. I., Schadewijk, W. A. V., Klerk, E. P. D., Dick, C. R., Krieken, J. H. V. & Sterk, P. J. (2001). **Rhinovirus-induced airway inflammation in asthma: effect of treatment with inhaled corticosteroids before and during experimental infection.** *Am J Respir Crit Care Med* **164**(10 Pt 1), 1816–1822.

Gruber, B. L., Marchese, M. J. & Kew, R. R. (1994). **Transforming growth factor-beta 1 mediates mast cell chemotaxis.** *J Immunol* **152**(12), 5860–5867.

Guo, H., Ingolia, N. T., Weissman, J. S. & Bartel, D. P. (2010). **Mammalian microRNAs predominantly act to decrease target mRNA levels.** *Nature* **466**(7308), 835–840.

Gupta, A., Gartner, J., Sethupathy, P., Hatzigeorgiou, A. & Fraser, N. (2006). **Anti-apoptotic function of a microRNA encoded by the HSV-1 latency-associated transcript.** *Nature* **442**(7098), 82–85.

Hansbro, N., Horvat, J., Wark, P. & Hansbro, P. (2008). **Understanding the mechanisms of viral induced asthma: new therapeutic directions.** *Pharmacol.Ther.* **117**(3), 313–353.

Harfe, B., McManus, M., Mansfield, J., Hornstein, E. & Tabin, C. (2005). **The RNaseIII enzyme Dicer is required for morphogenesis but not patterning of the vertebrate limb.** *Proc.Natl.Acad.Sci.U.S.A* **102**(31), 10898–10903.

Hashimoto, M., Tanaka, H. & Abe, S. (2005). **Quantitative analysis of bronchial wall vascularity in the medium and small airways of patients with asthma and COPD.** *Chest* **127**(3), 965–972.

Hassan, M. Q., Gordon, J. A. R., Lian, J. B., van Wijnen, A. J., Stein, J. L. & Stein, G. S. (2010). **Ribonucleoprotein immunoprecipitation (RNP-IP): a direct in vivo analysis of microRNA-targets.** *J Cell Biochem* **110**(4), 817–822.

Hayden, F. G. (2004). **Rhinovirus and the lower respiratory tract.** *Rev Med Virol* **14**(1), 17–31.

Herold, J. & Andino, R. (2001). **Poliovirus RNA replication requires genome circularization through a protein-protein bridge.** *Mol Cell* **7**(3), 581–591.

Hershey, G. (2003). **IL-13 receptors and signaling pathways: an evolving web.** *J.Allergy Clin.Immunol.* **111**(4), 677–690.

Hewson, C. A., Jardine, A., Edwards, M. R., Laza-Stanca, V. & Johnston, S. L. (2005). **Toll-like receptor 3 is induced by and mediates antiviral activity against rhinovirus infection of human bronchial epithelial cells.** *J Virol* **79**(19), 12273–12279.

Heymann, P., Carper, H., Murphy, D., Platts-Mills, T., Patrie, J., McLaughlin, A., Erwin, E., Shaker, M., Hellems, M., Peerzada, J., Hayden, F., Hatley, T. & Chamberlain, R. (2004). **Viral infections in relation to age, atopy, and season of admission among children hospitalized for wheezing.** *J.Allergy Clin.Immunol.* **114**(2), 239–247.

Holgate, S. (2008). **Pathogenesis of asthma.** *Clin Exp Allergy* **38**(6), 872–897.

Holgate, S. (2010*a*). **A brief history of asthma and its mechanisms to modern concepts of disease pathogenesis.** *Allergy Asthma Immunol.Res.* **2**(3), 165–171.

Holgate, S., Davies, D., Lackie, P., Wilson, S., Puddicombe, S. & Lordan, J. (2000). **Epithelial-mesenchymal interactions in the pathogenesis of asthma.** *J.Allergy Clin.Immunol.* **105**(2 Pt 1), 193–204.

Holgate, S., Roberts, G., Arshad, H., Howarth, P. & Davies, D. (2009). **The role of the airway epithelium and its interaction with environmental factors in asthma pathogenesis.** *Proc.Am.Thorac.Soc.* **6**(8), 655–659.

Holgate, S. T. (2005). **Exacerbations: the asthma paradox.** *Am J Respir Crit Care Med* **172**(8), 941–943.

Holgate, S. T. (2007). **Epithelium dysfunction in asthma.** *J Allergy Clin Immunol* **120**(6), 1233–44; quiz 1245–6.

Holgate, S. T. (2010*b*). **ADAM metallopeptidase domain 33 (ADAM33): identification and role in airways disease.** *Drug News Perspect* **23**(6), 381–387.

Holgate, S. T. & Polosa, R. (2008). **Treatment strategies for allergy and asthma.** *Nat Rev Immunol* **8**(3), 218–230.

Hou, J., Wang, P., Lin, L., Liu, X., Ma, F., An, H., Wang, Z. & Cao, X. (2009). **MicroRNA-146a feedback inhibits RIG-I-dependent Type I IFN production in macrophages by targeting TRAF6, IRAK1, and IRAK2.** *J Immunol* **183**(3), 2150–2158.

Huang, S. K., Xiao, H. Q., Kleine-Tebbe, J., Paciotti, G., Marsh, D. G., Lichtenstein, L. M. & Liu, M. C. (1995). **IL-13 expression at the sites of allergen challenge in patients with asthma.** *J Immunol* **155**(5), 2688–2694.

Humbert, M., Durham, S. R., Kimmitt, P., Powell, N., Assoufi, B., Pfister, R., Menz, G., Kay, A. B. & Corrigan, C. J. (1997). **Elevated expression of messenger ribonucleic acid encoding IL-13 in the bronchial mucosa of atopic and nonatopic subjects with asthma.** *J Allergy Clin Immunol* **99**(5), 657–665.

Humbert, M., Menz, G., Ying, S., Corrigan, C., Robinson, D., Durham, S. & Kay, A. (1999). **The immunopathology of extrinsic (atopic) and intrinsic (non-atopic) asthma: more similarities than differences.** *Immunol.Today* **20**(11), 528–533.

Huntzinger, E. & Izaurralde, E. (2011). **Gene silencing by microRNAs: contributions of translational repression and mRNA decay.** *Nat Rev Genet* **12**(2), 99–110.

Ikeda, K., Satoh, M., Pauley, K., Fritzler, M., Reeves, W. & Chan, E. (2006). **Detection of the argonaute protein Ago2 and microRNAs in the RNA induced silencing complex (RISC) using a monoclonal antibody.** *J.Immunol.Methods* **317**(1-2), 38–44.

Jiang, H., Harris, M. B. & Rothman, P. (2000). **IL-4/IL-13 signaling beyond JAK/STAT.** *J Allergy Clin Immunol* **105**(6 Pt 1), 1063–1070.

Johnston, S. L. (2005). **Overview of virus-induced airway disease.** *Proc Am Thorac Soc* **2**(2), 150–156.

Johnston, S., Pattemore, P., Sanderson, G., Smith, S., Campbell, M., Josephs, L., Cunningham, A., Robinson, B., Myint, S., Ward, M., Tyrrell, D. & Holgate, S. (1996). **The relationship between upper respiratory infections and hospital admissions for asthma: a time-trend analysis.** *Am.J.Respir.Crit Care Med.* **154**(3 Pt 1), 654–660.

Jopling, C. L., Yi, M., Lancaster, A. M., Lemon, S. M. & Sarnow, P. (2005). **Modulation of Hepatitis C Virus RNA Abundance by a Liver-Specific MicroRNA.** *Science* **309**(5740), 1577–1581.

Kallal, L. E. & Lukacs, N. W. (2008). **The role of chemokines in virus-associated asthma exacerbations.** *Curr Allergy Asthma Rep* **8**(5), 443–450.

Keene, J. D., Komisarow, J. M. & Friedersdorf, M. B. (2006). **RIP-Chip: the isolation and identification of mRNAs, microRNAs and protein components of ribonucleoprotein complexes from cell extracts.** *Nat Protoc* **1**(1), 302–307.

Kelly, E. J., Hadac, E. M., Greiner, S. & Russell, S. J. (2008). **Engineering microRNA responsiveness to decrease virus pathogenicity.** *Nat Med* **14**(11), 1278–1283.

Kertesz, M., Iovino, N., Unnerstall, U., Gaul, U. & Segal, E. (2007). **The role of site accessibility in microRNA target recognition.** *Nat.Genet.* **39**(10), 1278–1284.

Khalil, N. (1999). **TGF-beta: from latent to active.** *Microbes Infect* **1**(15), 1255–1263.

Kim, E., Kim, S., Kim, K., Park, J., Kim, Y., Sohn, M. & Kim, K. (2007). **Basement membrane thickening and clinical features of children with asthma.** *Allergy* **62**(6), 635–640.

Kim, Y. J., Hwang, S. J., Bae, Y. C. & Jung, J. S. (2009). **MiR-21 regulates adipogenic differentiation through the modulation of TGF-beta signaling in mesenchymal stem cells derived from human adipose tissue.** *Stem Cells* **27**(12), 3093–3102.

Knight, D. A., Lane, C. L. & Stick, S. M. (2004). **Does aberrant activation of the epithelial-mesenchymal trophic unit play a key role in asthma or is it an unimportant sideshow?** *Curr Opin Pharmacol* **4**(3), 251–256.

Kong, W., Yang, H., He, L., jun Zhao, J., Coppola, D., Dalton, W. S. & Cheng, J. Q. (2008). **MicroRNA-155 is regulated by the transforming growth factor beta/Smad pathway and contributes to epithelial cell plasticity by targeting RhoA.** *Mol Cell Biol* **28**(22), 6773–6784.

Kuehbacher, A., Urbich, C., Zeiher, A. & Dimmeler, S. (2007). **Role of Dicer and Drosha for endothelial microRNA expression and angiogenesis.** *Circ.Res.* **101**(1), 59–68.

Lachowicz-Scroggins, M. E., Boushey, H. A., Finkbeiner, W. E. & Widdicombe, J. H. (2010). **Interleukin-13-induced mucous metaplasia increases susceptibility of human airway epithelium to rhinovirus infection.** *Am J Respir Cell Mol Biol* **43**(6), 652–661.

Landthaler, M., Gaidatzis, D., Rothballer, A., Chen, P., Soll, S., Dinic, L., Ojo, T., Hafner, M., Zavolan, M. & Tuschl, T. (2008). **Molecular characterization of human Argonaute-containing ribonucleoprotein complexes and their bound target mRNAs.** *RNA.* **14**(12), 2580–2596.

Laza-Stanca, V., Stanciu, L., Message, S., Edwards, M., Gern, J. & Johnston, S. (2006). **Rhinovirus replication in human macrophages induces NF-kappaB-dependent tumor necrosis factor alpha production.** *J.Virol.* **80**(16), 8248–8258.

Lecellier, C., Dunoyer, P., Arar, K., Lehmann-Che, J., Eyquem, S., Himber, C., Saib, A. & Voinnet, O. (2005). **A cellular microRNA mediates antiviral defense in human cells.** *Science* **308**(5721), 557–560.

Lee, Y., Ahn, C., Han, J., Choi, H., Kim, J., Yim, J., Lee, J., Provost, P., Radmark, O., Kim, S. & Kim, V. (2003). **The nuclear RNase III Drosha initiates microRNA processing.** *Nature* **425**(6956), 415–419.

Lewis, B. P., Burge, C. B. & Bartel, D. P. (2005). **Conserved seed pairing, often flanked by adenosines, indicates that thousands of human genes are microRNA targets.** *Cell* **120**(1), 15–20.

Li, F. & Ding, S.-W. (2006). **Virus counterdefense: diverse strategies for evading the RNA-silencing immunity.** *Annu Rev Microbiol* **60**, 503–531.

Li, X.-D., Sun, L., Seth, R. B., Pineda, G. & Chen, Z. J. (2005). **Hepatitis C virus protease NS3/4A cleaves mitochondrial antiviral signaling protein off the mitochondria to evade innate immunity.** *Proc Natl Acad Sci U S A* **102**(49), 17717–17722.

Livak, K. J. & Schmittgen, T. D. (2001). **Analysis of Relative Gene Expression Data Using Real-Time Quantitative PCR and the 2-[Delta][Delta]CT Method.** *Methods* **25**(4), 402–408.

Louafi, F., Martinez-Nunez, R. & Sanchez-Elsner, T. (2010). **Microrna-155 (miR-155) targets SMAD2 and modulates the response of macrophages to transforming growth factor-beta(TGF-beta).** *J.Biol.Chem.* pp. –.

Lu, S. & Cullen, B. R. (2004). **Adenovirus VA1 noncoding RNA can inhibit small interfering RNA and MicroRNA biogenesis.** *J Virol* **78**(23), 12868–12876.

Lu, T. X., Munitz, A. & Rothenberg, M. E. (2009). **MicroRNA-21 is up-regulated in allergic airway inflammation and regulates IL-12p35 expression.** *J Immunol* **182**(8), 4994–5002.

Luttmann, W., Franz, P., Matthys, H. & Virchow, J. C. (1998). **Effects of TGF-beta on eosinophil chemotaxis.** *Scand J Immunol* **47**(2), 127–130.

Malmstrom, K., Pelkonen, A., Malmberg, L., Sarna, S., Lindahl, H., Kajosaari, M., Turpeinen, M., Saglani, S., Bush, A., Haahtela, T., Jeffery, P. & Makela, M. (2011). **Lung function, airway remodelling and inflammation in symptomatic infants: outcome at 3 years.** *Thorax* **66**(2), 157–162.

Martin, M. M., Lee, E. J., Buckenberger, J. A., Schmittgen, T. D. & Elton, T. S. (2006). **MicroRNA-155 regulates human angiotensin II type 1 receptor expression in fibroblasts.** *J Biol Chem* **281**(27), 18277–18284.

Martinez-Nunez, R. T., Louafi, F., Friedmann, P. S. & Sanchez-Elsner, T. (2009). **MicroRNA-155 modulates the pathogen binding ability of dendritic cells (DCs) by down-regulation of DC-specific intercellular adhesion molecule-3 grabbing non-integrin (DC-SIGN).** *J Biol Chem* **284**(24), 16334–16342.

Martinez-Nunez, R. T., Louafi, F. & Sanchez-Elsner, T. (2011). **The interleukin 13 (IL-13) pathway in human macrophages is modulated by microRNA-155 via direct targeting of interleukin 13 receptor alpha1 (IL13Ralpha1).** *J Biol Chem* **286**(3), 1786–1794.

Masri, S., Liu, Z., Phung, S., Wang, E., Yuan, Y.-C. & Chen, S. (2010). **The role of microRNA-128a in regulating TGFbeta signaling in letrozole-resistant breast cancer cells.** *Breast Cancer Res Treat* **124**(1), 89–99.

Matskevich, A. & Moelling, K. (2007). **Dicer is involved in protection against influenza A virus infection.** *J.Gen.Virol.* **88**(Pt 10), 2627–2635.

Mattes, J., Collison, A., Plank, M., Phipps, S. & Foster, P. S. (2009). **Antagonism of microRNA-126 suppresses the effector function of TH2 cells and the development of allergic airways disease.** *Proc Natl Acad Sci U S A* **106**(44), 18704–18709.

Maziere, P. & Enright, A. (2007). **Prediction of microRNA targets.** *Drug Discov.Today* **12**(11-12), 452–458.

McCann, K. L. & Imani, F. (2007). **Transforming growth factor beta enhances respiratory syncytial virus replication and tumor necrosis factor alpha induction in human epithelial cells.** *J Virol* **81**(6), 2880–2886.

Meister, G., Landthaler, M., Patkaniowska, A., Dorsett, Y., Teng, G. & Tuschl, T. (2004). **Human Argonaute2 mediates RNA cleavage targeted by miRNAs and siRNAs.** *Mol.Cell* **15**(2), 185–197.

Mestdagh, P., Boström, A.-K., Impens, F., Fredlund, E., Peer, G. V., Antonellis, P. D., von Stedingk, K., Ghesquière, B., Schulte, S., Dews, M., Thomas-Tikhonenko, A., Schulte, J. H., Zollo, M., Schramm, A., Gevaert, K., Axelson, H., Speleman, F. & Vandesompele, J. (2010). **The miR-17-92 microRNA cluster regulates multiple components of the TGF-β pathway in neuroblastoma.** *Mol Cell* **40**(5), 762–773.

Miller, J. E. & Samuel, C. E. (1992). **Proteolytic cleavage of the reovirus sigma 3 protein results in enhanced double-stranded RNA-binding activity: identification of a repeated basic amino acid motif within the C-terminal binding region.** *J Virol* **66**(9), 5347–5356.

Moffatt, M., Kabesch, M., Liang, L., Dixon, A., Strachan, D., Heath, S., Depner, M., von, B. A., Bufe, A., Rietschel, E., Heinzmann, A., Simma, B., Frischer, T., Willis-Owen, S., Wong, K., Illig, T., Vogelberg, C., Weiland, S., von, M. E., Abecasis, G., Farrall, M., Gut, I., Lathrop, G. & Cookson, W. (2007). **Genetic variants regulating ORMDL3 expression contribute to the risk of childhood asthma.** *Nature* **448**(7152), 470–473.

Mogensen, T. & Paludan, S. (2001). **Molecular pathways in virus-induced cytokine production.** *Microbiol.Mol Biol.Rev.* **65**(1), 131–150.

Montuschi, P. & Peters-Golden, M. (2010). **Leukotriene modifiers for asthma treatment.** *Clin.Exp.Allergy* **40**(12), 1732–1741.

Mosser, A. G., Brockman-Schneider, R., Amineva, S., Burchell, L., Sedgwick, J. B., Busse, W. W. & Gern, J. E. (2002). **Similar frequency of rhinovirus-infectible cells in upper and lower airway epithelium.** *J Infect Dis* **185**(6), 734–743.

Nachmani, D., Lankry, D., Wolf, D. G. & Mandelboim, O. (2010). **The human cytomegalovirus microRNA miR-UL112 acts synergistically with a cellular microRNA to escape immune elimination.** *Nat Immunol* **11**(9), 806–813.

Nelson, P., De Planell-Saguer, M., Lamprinaki, S., Kiriakidou, M., Zhang, P., O'Doherty, U. & Mourelatos, Z. (2007). **A novel monoclonal antibody against human Argonaute proteins reveals unexpected characteristics of miRNAs in human blood cells.** *RNA.* **13**(10), 1787–1792.

Neurath, M., Finotto, S. & Glimcher, L. (2002). **The role of Th1/Th2 polarization in mucosal immunity.** *Nat.Med.* **8**(6), 567–573.

O'Connell, R., Taganov, K., Boldin, M., Cheng, G. & Baltimore, D. (2007). **MicroRNA-155 is induced during the macrophage inflammatory response.** *Proc.Natl.Acad.Sci.U.S.A* **104**(5), 1604–1609.

Ogawa, T., Iizuka, M., Sekiya, Y., Yoshizato, K., Ikeda, K. & Kawada, N. (2010). **Suppression of type I collagen production by microRNA-29b in cultured human stellate cells.** *Biochemical and Biophysical Research Communications* **391**(1), 316–321.

Ogawa, Y. & Calhoun, W. (2006). **The role of leukotrienes in airway inflammation.** *J.Allergy Clin.Immunol.* **118**(4), 789–798.

Onoguchi, K., Yoneyama, M., Takemura, A., Akira, S., Taniguchi, T., Namiki, H. & Fujita, T. (2007). **Viral infections activate types I and III interferon genes through a common mechanism.** *J Biol Chem* **282**(10), 7576–7581.

Orom, U. A. & Lund, A. H. (2007). **Isolation of microRNA targets using biotinylated synthetic microRNAs.** *Methods* **43**(2), 162–165.

Otsuka, M., Jing, Q., Georgel, P., New, L., Chen, J., Mols, J., Kang, Y., Jiang, Z., Du, X., Cook, R., Das, S. C., Pattnaik, A. K., Beutler, B. & Han, J. (2007). **Hypersusceptibility to**

Vesicular Stomatitis Virus Infection in Dicer1-Deficient Mice Is Due to Impaired miR24 and miR93 Expression. *Immunity*. **27**(1), 123–134.

Pandit, K. V., Milosevic, J. & Kaminski, N. (2011). **MicroRNAs in idiopathic pulmonary fibrosis.** *Transl Res* **157**(4), 191–199.

Papadopoulos, N., Bates, P., Bardin, P., Papi, A., Leir, S., Fraenkel, D., Meyer, J., Lackie, P., Sanderson, G., Holgate, S. & Johnston, S. (2000). **Rhinoviruses infect the lower airways.** *J.Infect.Dis.* **181**(6), 1875–1884.

Papadopoulos, N., Papi, A., Meyer, J., Stanciu, L., Salvi, S., Holgate, S. & Johnston, S. (2001). **Rhinovirus infection up-regulates eotaxin and eotaxin-2 expression in bronchial epithelial cells.** *Clin.Exp.Allergy* **31**(7), 1060–1066.

Pearce, N., Pekkanen, J. & Beasley, R. (1999). **How much asthma is really attributable to atopy?** *Thorax* **54**(3), 268–272.

Pedersen, I., Cheng, G., Wieland, S., Volinia, S., Croce, C., Chisari, F. & David, M. (2007). **Interferon modulation of cellular microRNAs as an antiviral mechanism.** *Nature* **449**(7164), 919–922.

Perera, R., Daijogo, S., Walter, B. L., Nguyen, J. H. C. & Semler, B. L. (2007). **Cellular protein modification by poliovirus: the two faces of poly(rC)-binding protein.** *J Virol* **81**(17), 8919–8932.

Perez, J. T., Pham, A. M., Lorini, M. H., Chua, M. A., Steel, J. & tenOever, B. R. (2009). **MicroRNA-mediated species-specific attenuation of influenza A virus.** *Nat Biotechnol* **27**(6), 572–576.

Peritz, T., Zeng, F., Kannanayakal, T. J., Kilk, K., Eiríksdóttir, E., Langel, U. & Eberwine, J. (2006). **Immunoprecipitation of mRNA-protein complexes.** *Nat Protoc* **1**(2), 577–580.

Peters, L. & Meister, G. (2007). **Argonaute proteins: mediators of RNA silencing.** *Mol Cell* **26**(5), 611–623.

Phipps, K., Martinez, A., Lu, J., Heinz, B. & Zhao, G. (2004). **Small interfering RNA molecules as potential anti-human rhinovirus agents: in vitro potency, specificity, and mechanism.** *Antiviral Res.* **61**(1), 49–55.

Pichiorri, F., Suh, S.-S., Ladetto, M., Kuehl, M., Palumbo, T., Drandi, D., Taccioli, C., Zanesi, N., Alder, H., Hagan, J. P., Munker, R., Volinia, S., Boccadoro, M., Garzon, R., Palumbo,

A., Aqeilan, R. I. & Croce, C. M. (2008). **MicroRNAs regulate critical genes associated with multiple myeloma pathogenesis.** *Proc Natl Acad Sci U S A* **105**(35), 12885–12890.

Pillai, R. S., Artus, C. G. & Filipowicz, W. (2004). **Tethering of human Ago proteins to mRNA mimics the miRNA-mediated repression of protein synthesis.** *RNA* **10**(10), 1518–1525.

Polikepahad, S., Knight, J. M., Naghavi, A. O., Oplt, T., Creighton, C. J., Shaw, C., Benham, A. L., Kim, J., Soibam, B., Harris, R. A., Coarfa, C., Zariff, A., Milosavljevic, A., Batts, L. M., Kheradmand, F., Gunaratne, P. H. & Corry, D. B. (2010). **Proinflammatory role for let-7 microRNAS in experimental asthma.** *J Biol Chem* **285**(39), 30139–30149.

Pottier, N., Maurin, T., Chevalier, B., Puisségur, M.-P., Lebrigand, K., Robbe-Sermesant, K., Bertero, T., Cardenas, C. L. L., Courcot, E., Rios, G., Fourre, S., Lo-Guidice, J.-M., Marcet, B., Cardinaud, B., Barbry, P. & Mari, B. (2009). **Identification of keratinocyte growth factor as a target of microRNA-155 in lung fibroblasts: implication in epithelial-mesenchymal interactions.** *PLoS One* **4**(8), e6718.

Prchla, E., Kuechler, E., Blaas, D. & Fuchs, R. (1994). **Uncoating of human rhinovirus serotype 2 from late endosomes.** *J Virol* **68**(6), 3713–3723.

Puddicombe, S., Polosa, R., Richter, A., Krishna, M., Howarth, P., Holgate, S. & Davies, D. (2000). **Involvement of the epidermal growth factor receptor in epithelial repair in asthma.** *FASEB J.* **14**(10), 1362–1374.

Rate, A., Upham, J. W., Bosco, A., McKenna, K. L. & Holt, P. G. (2009). **Airway epithelial cells regulate the functional phenotype of locally differentiating dendritic cells: implications for the pathogenesis of infectious and allergic airway disease.** *J Immunol* **182**(1), 72–83.

Reddel, R., Ke, Y., Gerwin, B., McMenamin, M., Lechner, J., Su, R., Brash, D., Park, J., Rhim, J. & Harris, C. (1988). **Transformation of human bronchial epithelial cells by infection with SV40 or adenovirus-12 SV40 hybrid virus, or transfection via strontium phosphate coprecipitation with a plasmid containing SV40 early region genes.** *Cancer Res.* **48**(7), 1904–1909.

Rivas, F. V., Tolia, N. H., Song, J.-J., Aragon, J. P., Liu, J., Hannon, G. J. & Joshua-Tor, L. (2005). **Purified Argonaute2 and an siRNA form recombinant human RISC.** *Nat Struct Mol Biol* **12**(4), 340–349.

Rodriguez, A., Vigorito, E., Clare, S., Warren, M., Couttet, P., Soond, D., van, D. S., Grocock, R., Das, P., Miska, E., Vetrie, D., Okkenhaug, K., Enright, A., Dougan, G., Turner, M. & Bradley, A. (2007). **Requirement of bic/microRNA-155 for normal immune function.** *Science* **316**(5824), 608–611.

Rudel, S., Flatley, A., Weinmann, L., Kremmer, E. & Meister, G. (2008). **A multifunctional human Argonaute2-specific monoclonal antibody.** *RNA.* **14**(6), 1244–1253.

Sagara, H., Okada, T., Okumura, K., Ogawa, H., Ra, C., Fukuda, T. & Nakao, A. (2002). **Activation of TGF-beta/Smad2 signaling is associated with airway remodeling in asthma.** *J Allergy Clin Immunol* **110**(2), 249–254.

Saglani, S., Malmstrom, K., Pelkonen, A., Malmberg, L., Lindahl, H., Kajosaari, M., Turpeinen, M., Rogers, A., Payne, D., Bush, A., Haahtela, T., Makela, M. & Jeffery, P. (2005). **Airway remodeling and inflammation in symptomatic infants with reversible airflow obstruction.** *Am.J.Respir.Crit Care Med.* **171**(7), 722–727.

Saglani, S., Payne, D., Zhu, J., Wang, Z., Nicholson, A., Bush, A. & Jeffery, P. (2007). **Early detection of airway wall remodeling and eosinophilic inflammation in preschool wheezers.** *Am.J.Respir.Crit Care Med.* **176**(9), 858–864.

Saumet, A. & Lecellier, C.-H. (2006). **Anti-viral RNA silencing: do we look like plants?** *Retrovirology* **3**, 3.

Scherr, M., Venturini, L., Battmer, K., Schaller-Schoenitz, M., Schaefer, D., Dallmann, I., Ganser, A. & Eder, M. (2007). **Lentivirus-mediated antagomir expression for specific inhibition of miRNA function.** *Nucleic Acids Res* **35**(22), e149.

Schmitter, D., Filkowski, J., Sewer, A., Pillai, R., Oakeley, E., Zavolan, M., Svoboda, P. & Filipowicz, W. (2006). **Effects of Dicer and Argonaute down-regulation on mRNA levels in human HEK293 cells.** *Nucleic Acids Res.* **34**(17), 4801–4815.

Segal Lab - PITA programme FAQs. **http://genie.weizmann.ac.il/pubs/mir07/mir07_notes.html** .

Shi, Y. & Massagué, J. (2003). **Mechanisms of TGF-beta signaling from cell membrane to the nucleus.** *Cell* **113**(6), 685–700.

Skoner, D., Doyle, W., Seroky, J., Van Deusen, M. & Fireman, P. (1996). **Lower airway responses to rhinovirus 39 in healthy allergic and nonallergic subjects.** *Eur.Respir.J.* **9**(7), 1402–1406.

Slater, L., Bartlett, N. W., Haas, J. J., Zhu, J., Message, S. D., Walton, R. P., Sykes, A., Dahdaleh, S., Clarke, D. L., Belvisi, M. G., Kon, O. M., Fujita, T., Jeffery, P. K., Johnston, S. L. & Edwards, M. R. (2010). **Co-ordinated role of TLR3, RIG-I and MDA5 in the innate response to rhinovirus in bronchial epithelium.** *PLoS Pathog* **6**(11), e1001178.

Stark, G., Kerr, I., Williams, B., Silverman, R. & Schreiber, R. (1998). **How cells respond to interferons. [Review] [319 refs]** *Annual Review of Biochemistry* **67**, 227–264.

Stevens, P., Kicic, A., Sutanto, E., Knight, D. & Stick, S. (2008). **Dysregulated repair in asthmatic paediatric airway epithelial cells: the role of plasminogen activator inhibitor-1.** *Clin.Exp.Allergy* **38**(12), 1901–1910.

Suarez, Y., Fernandez-Hernando, C., Pober, J. & Sessa, W. (2007). **Dicer dependent microRNAs regulate gene expression and functions in human endothelial cells.** *Circ.Res.* **100**(8), 1164–1173.

Subauste, M. C., Jacoby, D. B., Richards, S. M. & Proud, D. (1995). **Infection of a human respiratory epithelial cell line with rhinovirus. Induction of cytokine release and modulation of susceptibility to infection by cytokine exposure.** *J Clin Invest* **96**(1), 549–557.

Subauste, M. C. & Proud, D. (2001). **Effects of tumor necrosis factor-alpha, epidermal growth factor and transforming growth factor-alpha on interleukin-8 production by, and human rhinovirus replication in, bronchial epithelial cells.** *Int Immunopharmacol* **1**(7), 1229–1234.

Sullivan, C. S., Grundhoff, A. T., Tevethia, S., Pipas, J. M. & Ganem, D. (2005). **SV40-encoded microRNAs regulate viral gene expression and reduce susceptibility to cytotoxic T cells.** *Nature* **435**(7042), 682–686.

Swindle, E., Collins, J. & Davies, D. (2009). **Breakdown in epithelial barrier function in patients with asthma: identification of novel therapeutic approaches.** *J.Allergy Clin.Immunol.* **124**(1), 23–34.

Taganov, K., Boldin, M., Chang, K. & Baltimore, D. (2006). **NF-kappaB-dependent induction of microRNA miR-146, an inhibitor targeted to signaling proteins of innate immune responses.** *Proc.Natl.Acad.Sci.U.S.A* **103**(33), 12481–12486.

Taipale, J., Koli, K. & Keski-Oja, J. (1992). **Release of transforming growth factor-beta 1 from the pericellular matrix of cultured fibroblasts and fibrosarcoma cells by plasmin and thrombin.** *J Biol Chem* **267**(35), 25378–25384.

Taipale, J., Lohi, J., Saarinen, J., Kovanen, P. T. & Keski-Oja, J. (1995). **Human mast cell chymase and leukocyte elastase release latent transforming growth factor-beta 1 from the extracellular matrix of cultured human epithelial and endothelial cells.** *J Biol Chem* **270**(9), 4689–4696.

Takeuchi, O. & Akira, S. (2007). **Recognition of viruses by innate immunity.** *Immunol.Rev.* **220**, 214–224.

Tan, L. P., Seinen, E., Duns, G., de Jong, D., Sibon, O. C. M., Poppema, S., Kroesen, B.-J., Kok, K. & van den Berg, A. (2009). **A high throughput experimental approach to identify miRNA targets in human cells.** *Nucleic Acids Res* **37**(20), e137.

Tang, K., Wang, Y., Wang, P., Chen, M., Chen, Y., Hu, H., Hu, P., Wang, B., Yang, W. & Ren, H. (2007). **Upregulation of PHLDA2 in Dicer knockdown HEK293 cells.** *Biochim.Biophys.Acta* **1770**(5), 820–825.

Thelen, M., Uguccioni, M. & Bösiger, J. (1995). **PI 3-kinase-dependent and independent chemotaxis of human neutrophil leukocytes.** *Biochem Biophys Res Commun* **217**(3), 1255–1262.

Thomas, B. J., Lindsay, M., Dagher, H., Freezer, N. J., Li, D., Ghildyal, R. & Bardin, P. G. (2009). **Transforming growth factor-beta enhances rhinovirus infection by diminishing early innate responses.** *Am J Respir Cell Mol Biol* **41**(3), 339–347.

Tili, E., Michaille, J.-J., Cimino, A., Costinean, S., Dumitru, C. D., Adair, B., Fabbri, M., Alder, H., Liu, C. G., Calin, G. A. & Croce, C. M. (2007). **Modulation of miR-155 and miR-125b levels following lipopolysaccharide/TNF-alpha stimulation and their possible roles in regulating the response to endotoxin shock.** *J Immunol* **179**(8), 5082–5089.

Tomankova, T., Petrek, M. & Kriegova, E. (2010). **Involvement of microRNAs in physiological and pathological processes in the lung.** *Respir Res* **11**, 159.

Torrego, A., Hew, M., Oates, T., Sukkar, M. & Chung, K. F. (2007). **Expression and activation of TGF-beta isoforms in acute allergen-induced remodelling in asthma.** *Thorax* **62**(4), 307–313.

Triboulet, R., Mari, B., Lin, Y. L., Chable-Bessia, C., Bennasser, Y., Lebrigand, K., Cardinaud, B., Maurin, T., Barbry, P., Baillat, V., Reynes, J., Corbeau, P., Jeang, K. T. & Benkirane, M. (2007). **Suppression of MicroRNA-Silencing Pathway by HIV-1 During Virus Replication.** *Science* **315**(5818), 1579–1582.

Tschumperlin, D. J., Shively, J. D., Kikuchi, T. & Drazen, J. M. (2003). **Mechanical stress triggers selective release of fibrotic mediators from bronchial epithelium.** *Am J Respir Cell Mol Biol* **28**(2), 142–149.

Tsuchiya, S., Kobayashi, Y., Goto, Y., Okumura, H., Nakae, S., Konno, T. & Tada, K. (1982). **Induction of maturation in cultured human monocytic leukemia cells by a phorbol diester.** *Cancer Res.* **42**(4), 1530–1536.

Turato, G., Barbato, A., Baraldo, S., Zanin, M., Bazzan, E., Lokar-Oliani, K., Calabrese, F., Panizzolo, C., Snijders, D., Maestrelli, P., Zuin, R., Fabbri, L. & Saetta, M. (2008). **Nonatopic children with multitrigger wheezing have airway pathology comparable to atopic asthma.** *Am.J.Respir.Crit Care Med.* **178**(5), 476–482.

Uller, L., Leino, M., Bedke, N., Sammut, D., Green, B., Lau, L., Howarth, P. H., Holgate, S. T. & Davies, D. E. (2010). **Double-stranded RNA induces disproportionate expression of thymic stromal lymphopoietin versus interferon-beta in bronchial epithelial cells from donors with asthma.** *Thorax* **65**(7), 626–632.

Vignola, A. M., Chanez, P., Chiappara, G., Merendino, A., Pace, E., Rizzo, A., la Rocca, A. M., Bellia, V., Bonsignore, G. & Bousquet, J. (1997). **Transforming growth factor-beta expression in mucosal biopsies in asthma and chronic bronchitis.** *Am J Respir Crit Care Med* **156**(2 Pt 1), 591–599.

Volinia, S., Calin, G., Liu, C., Ambs, S., Cimmino, A., Petrocca, F., Visone, R., Iorio, M., Roldo, C., Ferracin, M., Prueitt, R., Yanaihara, N., Lanza, G., Scarpa, A., Vecchione, A., Negrini, M., Harris, C. & Croce, C. (2006). **A microRNA expression signature of human solid tumors defines cancer gene targets.** *Proc.Natl.Acad.Sci.U.S.A* **103**(7), 2257–2261.

Wang, H., Liu, J., Zong, Y., Xu, Y., Deng, W., Zhu, H., Liu, Y., Ma, C., Huang, L., Zhang, L. & Qin, C. (2010a). **miR-106b aberrantly expressed in a double transgenic mouse model for Alzheimer's disease targets TGF-β type II receptor.** *Brain Res* **1357**, 166–174.

Wang, P., Hou, J., Lin, L., Wang, C., Liu, X., Li, D., Ma, F., Wang, Z. & Cao, X. (2010). **Inducible microRNA-155 feedback promotes type I IFN signaling in antiviral innate immunity by targeting suppressor of cytokine signaling 1.** *J Immunol* **185**(10), 6226–6233.

Wang, Q., Nagarkar, D. R., Bowman, E. R., Schneider, D., Gosangi, B., Lei, J., Zhao, Y., McHenry, C. L., Burgens, R. V., Miller, D. J., Sajjan, U. & Hershenson, M. B. (2009). **Role of double-stranded RNA pattern recognition receptors in rhinovirus-induced airway epithelial cell responses.** *J Immunol* **183**(11), 6989–6997.

Wang, X. H., Aliyari, R., Li, W. X., Li, H. W., Kim, K., Carthew, R., Atkinson, P. & Ding, S. W. (2006). **RNA Interference Directs Innate Immunity Against Viruses in Adult Drosophila.** *Science* **312**(5772), 452–454.

Wark, P. A. B., Bucchieri, F., Johnston, S. L., Gibson, P. G., Hamilton, L., Mimica, J., Zummo, G., Holgate, S. T., Attia, J., Thakkinstian, A. & Davies, D. E. (2007). **IFN-gamma-induced protein 10 is a novel biomarker of rhinovirus-induced asthma exacerbations.** *J Allergy Clin Immunol* **120**(3), 586–593.

Wark, P. & Gibson, P. (2006). **Asthma exacerbations . 3: Pathogenesis.** *Thorax* **61**(10), 909–915.

Wark, P., Johnston, S., Bucchieri, F., Powell, R., Puddicombe, S., Laza-Stanca, V., Holgate, S. & Davies, D. (2005). **Asthmatic bronchial epithelial cells have a deficient innate immune response to infection with rhinovirus.** *J.Exp.Med.* **201**(6), 937–947.

Williams, A. E., Larner-Svensson, H., Perry, M. M., Campbell, G. A., Herrick, S. E., Adcock, I. M., Erjefalt, J. S., Chung, K. F. & Lindsay, M. A. (2009). **MicroRNA expression profiling in mild asthmatic human airways and effect of corticosteroid therapy.** *PLoS One* **4**(6), e5889.

Williams, A. E., Moschos, S. A., Perry, M. M., Barnes, P. J. & Lindsay, M. A. (2007). **Maternally imprinted microRNAs are differentially expressed during mouse and human lung development.** *Dev Dyn* **236**(2), 572–580.

Winter, J., Jung, S., Keller, S., Gregory, R. & Diederichs, S. (2009). **Many roads to maturity: microRNA biogenesis pathways and their regulation.** *Nat.Cell Biol.* **11**(3), 228–234.

Wiznerowicz, M. & Trono, D. (2003). **Conditional suppression of cellular genes: lentivirus vector-mediated drug-inducible RNA interference.** *J Virol* **77**(16), 8957–8961.

Wright, R., Rodriguez, M. & Cohen, S. (1998). **Review of psychosocial stress and asthma: an integrated biopsychosocial approach.** *Thorax* **53**(12), 1066–1074.

Wynn, T. A. (2003). **IL-13 effector functions.** *Annu Rev Immunol* **21**, 425–456.

Xiang, W., Paul, A. & Wimmer, E. (1997). **RNA signals in entero- and rhinovirus genome replication.** *Seminars in Virology.8(3)()(pp 256-273), 1997.Date of Publication: 1997.* (3), 256–273.

Xiao, C., Puddicombe, S. M., Field, S., Haywood, J., Broughton-Head, V., Puxeddu, I., Haitchi, H. M., Vernon-Wilson, E., Sammut, D., Bedke, N., Cremin, C., Sones, J., Djukanovic, R., Howarth, P. H., Collins, J. E., Holgate, S. T., Monk, P. & Davies, D. E. (2011). **Defective epithelial barrier function in asthma.** *J Allergy Clin Immunol* .

Yi, R., Qin, Y., Macara, I. G. & Cullen, B. R. (2003). **Exportin-5 mediates the nuclear export of pre-microRNAs and short hairpin RNAs.** *Genes Dev* **17**(24), 3011–3016.

Yoneyama, M. & Fujita, T. (2007). **RIG-I family RNA helicases: cytoplasmic sensor for antiviral innate immunity.** *Cytokine Growth Factor Rev.* **18**(5-6), 545–551.

Chapter 6 Appendix

6.1 Other predictions of miR-155 targeting HRV-1B or -16.

TARGET: HRV-1B
length: 7191
MIRNA: hsa-miR-155
length: 23
minimum free energy (mfe): -25.0 kcal/mol
position 3409

Alignment:

```
target 5' U     A              G   3'
           ACUCC   CAUGAUUGGUAU
           UGGGG   GUGCUAAUCGUA
miRNA  3'       AUA            AUU 5'
```

TARGET: HRV-16
length: 7124
MIRNA: hsa-miR-155
length: 23
mfe: -24.1 kcal/mol
position: 7053

Alignment:

```
target 5' A       AGA     A       G   3'
           ACUCCUA   CAUGA UGGUAU
           UGGGGAU   GUGCU AUCGUA
miRNA  3'         A       A       AUU 5'
```

table 6-1. RNAHybrid predictions for microRNA-155 and HRV-1B or HRV-16.
Programme available on-line at http://bibiserv.techfak.uni-bielefeld.de/rnahybrid/submission.html

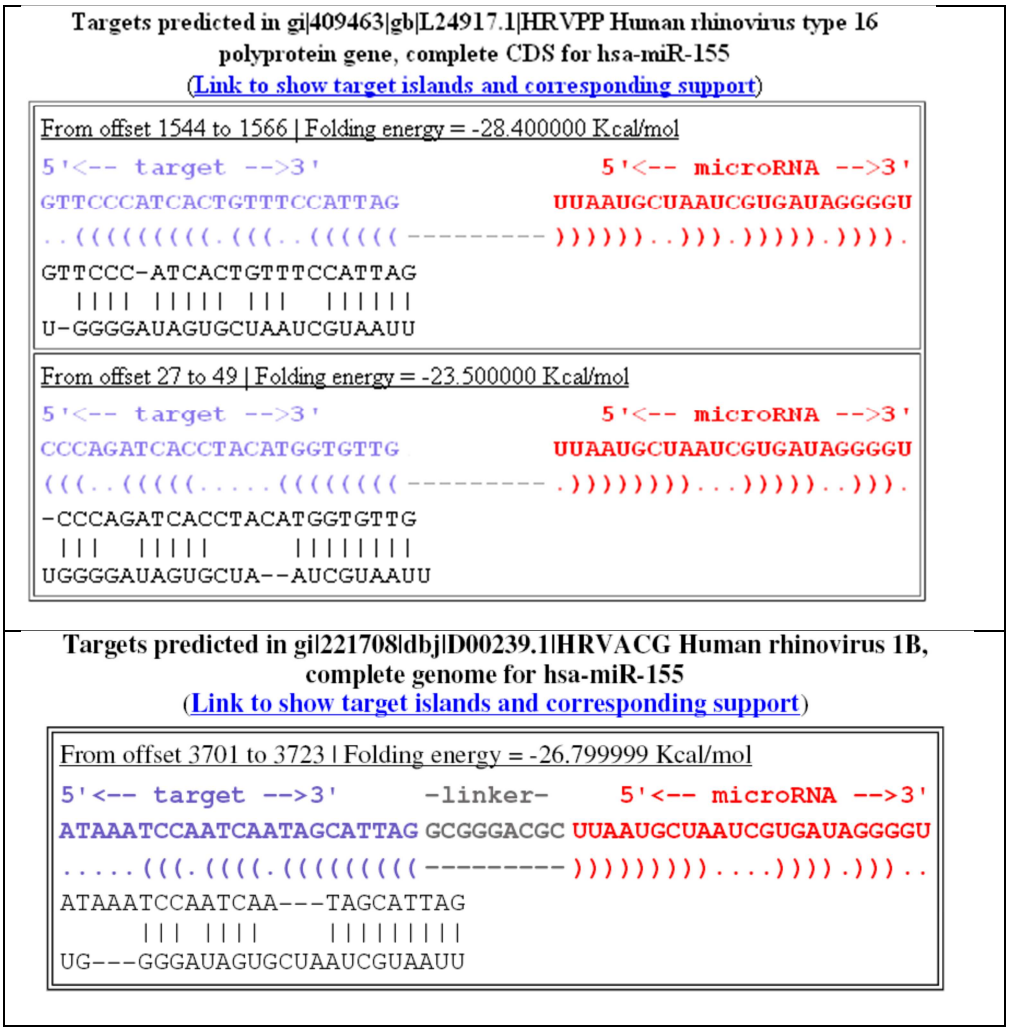

table 6-2. RNA22 predictions for microRNA-155 and HRV-1B or HRV-16.
Programme available on-line at http://cbcsrv.watson.ibm.com/rna22_targets.html

6.2 Other microRNA predictions.

Here are reproduced the predictions mentioned in fig. 5-2 as showed on-line from the database Targetscan 5.2 (Lewis et al. 2005) available on-line at the address: http://www.targetscan.org/vert_50/ .

TargetScan predicts the following site types:

8mer: an exact match to positions 2-8 of the mature miRNA (the seed + position 8) followed by an 'A'

7mer-m8: an exact match to positions 2-8 of the mature miRNA (the seed + position 8)

TGF-β pathway

SMAD2

Position 3359-3365 of SMAD2 3' UTR hsa-miR-128	5' ...UGUUGUUUGCCCAGCCACUGUGA... ||||||| 3' UUUCUCUGGCCAAGUGACACU	8mer
Position 8325-8331 of SMAD2 3' UTR hsa-miR-128	5' ...GCUGCAUCCUUGGUGCACUGUGA... ||||||| 3' UUUCUCUGGCCAAGUGACACU	8mer
Position 412-418 of SMAD2 3' UTR hsa-miR-340	5' ...UUGAUCUAGGCAAACCUUUAUAA... ||||||| 3' UUAGUCAGAGUAACGAAAUAUU	8mer
Position 2095-2101 of SMAD2 3' UTR hsa-miR-340	5' ...GAUUAGGUAUUAAUGCUUUAUAC... ||||||| 3' UUAGUCAGAGUAACGAAAUAUU	7mer-m8
Position 3160-3166 of SMAD2 3' UTR hsa-miR-340	5' ...AGAAGCUCAGAAAGUCUUUAUAA... |||| ||||||| 3' UUAGUCAGAGUAAC---GAAAUAUU	8mer
Position 6205-6211 of SMAD2 3' UTR hsa-miR-340	5' ...AUAUUAAGUUCUAUC--CUUUAUAA... ||| ||||||| 3' UUAGUCAGAGUAACGAAAUAUU	8mer
Position 6450-6456 of SMAD2 3' UTR hsa-miR-340	5' ...UGUGGAAAUCCAUUGCUUUAUAU... |||||||||||| 3' UUAGUCAGAGUAACGAAAUAUU	7mer-m8

SMAD3

Position 1790-1796 of SMAD3 3' UTR hsa-miR-18a	5' ...GAAGAGACGGAAGGAGCACCUUG... ||||||| 3' GAUAGACGUGAUCUACGUGGAAU	7mer-m8
Position 2857-2863 of SMAD3 3' UTR hsa-miR-18a	5' ...AGAUCCUUGUCUUCAGCACCUUC... ||||||| 3' GAUAGACGUGAUCUACGUGGAAU	7mer-m8
Position 4299-4305 of SMAD3 3' UTR hsa-miR-155	5' ...CUUGCUAGGGGUGAAAGCAUUAC... ||||||| 3' UGGGGAUAGUGCUAAUCGUAAUU	7mer-m8

SMAD4

Position 1354-1360 of SMAD4 3' UTR hsa-miR-19b	5' ...AGAUUUUUUUUUUCUUUUGCACU... ||||||| 3' AGUCAAAACGUACCUAAACGUGU	7mer-m8
Position 4024-4030 of SMAD4 3' UTR hsa-miR-128	5' ...UUGUUUAUCUGGAAUCACUGUGG... ||||||| 3' UUUCUCUGGCCAAGUGACACU	7mer-m8
Position 1355-1361 of SMAD4 3' UTR hsa-miR-301a	5' ...GAUUUUUUUUUUCUUUUGCACUU... ||||||| 3' CGAAACUGUUAUGAUAACGUGAC	7mer-m8

TGFR2

Position 265-271 of TGFBR2 3' UTR hsa-miR-19b	5' ...CAAUAGCCAAUAACAUUUGCACU... ||||||| 3' AGUCAAAACGUACCUAAACGUGU	7mer-m8
Position 268-274 of TGFBR2 3' UTR hsa-miR-106b	5' ...UAGCCAAUAACAUUUGCACUUUA... ||||||| 3' UAGACGUGACAGUCGUGAAAU	8mer
Position 461-467 of TGFBR2 3' UTR hsa-miR-155	5' ...GAAGGGACCCAUGACAGCAUUAG... ||||||| 3' UGGGGAUAGUGCUAAUCGUAAUU	7mer-m8
Position 266-272 of TGFBR2 3' UTR hsa-miR-301a	5' ...AAUAGCCAAUAACAUUUGCACUU... ||||| ||||||| 3' CGAAACUGUUAUGAU-AACGUGAC	7mer-m8
Position 566-572 of TGFBR2 3' UTR hsa-miR-301a	5' ...CCAGCUAUGACCACAUUGCACUU... ||||||| 3' CGAAACUGUUAUGAUAACGUGAC	7mer-m8

IL-13 pathway

IL13RA1

Position 24-30 of IL13RA1 3' UTR hsa-miR-128	5' ...AUUUAUUUUUACCUU--CACUGUGA... 3' UUUCUCUGGCCAAGUGACACU	8mer

STAT6

Position 715-721 of STAT6 3' UTR hsa-miR-18a	5' ...UUAAAUGUAUAGCUGGCACCUUA... 3' GAUAGACGUGAUCUACGUGGAAU	8mer